Single-particle energies and wave functions of the Woods–Saxon potential and nonrotational states of odd nuclei in the range $150 < A < 190$

F. A. Gareev, S. P. Ivanova, V. G. Solov'ev, and S. I. Fedotov
Joint Institute for Nuclear Research, Dubna
Fiz. Él. Chast. Atom. Yad., 4, 357-455 (April-June 1973)

Single-particle energies and wave functions for the Woods–Saxon potential are given for deformed nuclei in the range $150 < A < 190$. The energies and wave functions for the nonrotational states of odd nuclei are calculated taking account of the quasiparticle–phonon interaction. The effect of $\Delta N = \pm 2$ mixing is taken into account. A study is made of how the difference between the equilibrium nuclear deformation in the excited state and that in the ground state affects the state energy and structure. A good description is found for the energies of the low-lying nonrotational states in this mass range. The calculated single-particle energies and wave functions for the Woods–Saxon potential can be used to calculate various characteristics of nuclei in this range.

INTRODUCTION

A semimicroscopic approach is widely used in nuclear theory to describe low-lying excited states. This approach involves choosing an effective nuclear interaction; the interaction between nucleons is divided into two parts: the mean nuclear field and the residual interactions. The mean field is the nuclear potential produced by all the nucleons of the nucleus. The large store of experimental information which has been acquired in studies of α, β, and γ spectra and nuclear reactions is used to determine the parameters of this mean-field potential. The residual interactions refer to those forces involved which are not incorporated in the mean field. The residual interactions are extremely important in a nucleus; they change monotonically and slowly from nucleus to nucleus; they are not small, so they cannot be taken into account by means of perturbation theory. The mean field thus determines the specific properties of each nucleus and is responsible for the properties which distinguish some nuclei from others.

In this version of the semimicroscopic description, the nuclear Hamiltonian is written as[1]

$$H = H_{av} + H_{pair} + H_Q + H', \tag{1.1}$$

where H_{pair} represents the interactions leading to pairing correlations of the superconducting type, H_Q represents the multipole–multipole interactions, H' represents other types of residual interactions [e.g., (spin multipole)–(spin multipole) and Gamov–Teller interactions], and H_{av} represents the mean field of the neutron and proton systems. The Nilsson[2,3] and Woods–Saxon[4,5] potentials are used to describe the average field of deformed nuclei.

The potentials used for these calculations give a better description of the mean field of deformed nuclei than that of spherical nuclei. In deformed nuclei the parameters of the average-field potential are chosen such that the nuclear potential contains the corresponding part of the interaction among all nucleons in the nucleus, so the addition of each pair of nucleons is effectively already taken into account. It can be asserted that the mean field is self-consistent for the ground state of each deformed nucleus in the zone of β stability. This circumstance explains the success of Nilsson and Woods–Saxon potentials in describing the low-lying levels of odd deformed nuclei.

The Hamiltonian used to study pairing correlations of the superconducting type is

$$H_0 = H_{av} + H_{pair} = H_0(n) + H_0(p), \tag{1.2}$$

where for the neutron system we have

$$H_0(n) = \sum_{s\sigma} \{E(s) - \lambda_n\} a^+_{s\sigma} a_{s\sigma} - G_N \sum_{s,s'} a^+_{s+} a^+_{s-} a_{s'-} a_{s'+}. \tag{1.3}$$

Here E(s) are the single-particle energies, $a_{s\sigma}$ is the nucleon-annihilation operator, G_N is the pairing-interaction constant, and λ_n is the chemical potential of the neutron system. In the proton system the pairing-interaction constant and the chemical potential are G_Z and λ_p. We denote by $(s\sigma)$ the set of quantum numbers describing a single-particle state of the neutron system, and we denote by $(q\sigma)$ the set describing such a state of the neutron and proton systems; here $\sigma = \pm 1$.

We introduce the canonical Bogolyubov transformation

$$a_{s\sigma} = u_s \alpha_{s-\sigma} + \sigma v_s \alpha^+_{s\sigma}, \tag{1.4}$$

where $\alpha_{s\sigma}$ is the quasiparticle-absorption operator and

$$u_s^2 + v_s^2 = 1. \tag{1.5}$$

The ground-state wave function of the system is found from the condition

$$\alpha_{s\sigma} \Psi_0 = 0. \tag{1.6}$$

Finding the expectation value of $H_0(n)$ in the state Ψ_0 and using a variational principle, we find[1] the following system of equations for the correlation function C_n and chemical potential λ_n:

$$1 = \frac{G_N}{2} \sum_s \frac{1}{\sqrt{C_n^2 + (E(s) - \lambda_n)^2}}; \tag{1.7}$$

$$N = \sum_s \left\{ 1 - \frac{E(s) - \lambda_n}{\sqrt{C_n^2 + (E(s) - \lambda_n)^2}} \right\}, \tag{1.8}$$

where N is the number of neutrons.

The ground-state energy and wave function of the system are

$$\mathcal{E}_0 = \sum_s 2E(s) v_s^2 - \frac{C_n^2}{G_N}; \tag{1.9}$$

$$\Psi_0 = \prod_s (u_s + v_s a^+_{s+} a^+_{s-}) \Psi_{00}, \tag{1.10}$$

where

$$a_{s\sigma}\Psi_{00}=0;\quad \varepsilon(s)=\sqrt{C_n^2+(E(s)-\lambda_n)^2}; \tag{1.11}$$

$$u_s^2=\frac{1}{2}\left\{1+\frac{E(s)-\lambda_n}{\varepsilon(s)}\right\};\quad v_s^2=\frac{1}{2}\left\{1-\frac{E(s)-\lambda_n}{\varepsilon(s)}\right\}. \tag{1.12}$$

In the model of independent quasiparticles the excited states of even–even nuclei are two-quasiparticle states. At higher excitation energies there are four-quasiparticle states, etc. The ground and low-lying states of odd nuclei are single-quasiparticle states. As the excitation energy increases, these states are supplemented by three-quasiparticle states, etc.

The part of Hamiltonian (1.1) corresponding to the multipole–multipole interaction is

$$H_Q=-\sum_{\lambda,\ \mu\geqslant 0}\frac{\varkappa^{(\lambda)}}{2}Q^+_{\lambda\mu}Q_{\lambda\mu}, \tag{1.13}$$

where $Q_{\lambda\mu}$ is the operator corresponding to the multiple moment $\lambda\mu$ (ref. 1). To describe the vibrational states we

$$Q_j(\lambda\mu)=\frac{1}{2}\sum_{q,\ q'}\{\psi^{\lambda\mu j}_{qq'}A(q,\ q')-\varphi^{\lambda\mu j}_{qq'}A^+(q,\ q')\} \tag{1.14}$$

and the operators

$$B(q,\ q')=\sum_\sigma \alpha^+_{q\sigma}\alpha_{q'\sigma}\quad\left(\text{or }\sum_\sigma \sigma\alpha^+_{q-\sigma}\alpha_{q'\sigma}\right); \tag{1.15}$$

$$A(q,\ q')=\frac{1}{\sqrt{2}}\sum_\sigma \sigma\alpha_{q'\sigma}\alpha_{q-\sigma}\quad\left(\text{or }\frac{1}{\sqrt{2}}\sum_\sigma \alpha_{q\sigma}\alpha_{q'\sigma}\right). \tag{1.16}$$

We can write the corresponding part of Hamiltonian (1.1) as

$$\begin{aligned}H_v=&\sum_q \varepsilon(q)B(q,\ q)-\frac{1}{2}\sum_{\lambda,\ \mu\geqslant 0}\varkappa^{(\lambda)}\sum_{qq'}\sum_{q_2q_2'}\sum_{jj'}f^{\lambda\mu}(q,\ q')f^{\lambda\mu}(q_2,\ q_2')\\&\times u_{qq'}u_{q_2q_2'}(\psi^{\lambda\mu j}_{qq'}+\varphi^{\lambda\mu j}_{qq'})(\psi^{\lambda\mu j'}_{q_2q_2'}+\varphi^{\lambda\mu j'}_{q_2q_2'})Q_j^+(\lambda\mu)Q_{j'}(\lambda\mu)\\&-\frac{1}{2\sqrt{2}}\sum_{\lambda,\ \mu\geqslant 0}\varkappa^{(\lambda)}\sum_{qq'}\sum_{q_2q_2'}\sum_j f^{\lambda\mu}(q,\ q')f^{\lambda\mu}(q_2,\ q_2')u_{qq'}v_{q_2q_2'}\\&\times\{(Q_j^+(\lambda\mu)+Q_j(\lambda\mu))B(q_2,\ q_2')+B(q_2,\ q_2')(Q_j^+(\lambda\mu)+Q_j(\lambda\mu))\}.\end{aligned} \tag{1.17}$$

Here $f^{\lambda\mu}(q, q')$ is the matrix element of the operator corresponding to multipole moment $\lambda\mu$, and we set $u_{qq'} = u_qv_{q'} + u_{q'}v_q$ and $v_{qq'} = u_qu_{q'} - v_qv_{q'}$.

The ground-state wave function for an even–even nucleus is defined as a phononless function:

$$Q_j(\lambda\mu)\Psi=0. \tag{1.18}$$

The excited states are treated as single-phonon states and are described by the wave functions

$$Q_j^+(\lambda\mu)\Psi. \tag{1.19}$$

The energies $\omega_j^{\lambda\mu}$ and the wave functions of the single-phonon states are found by a variational principle.[1] For all the single-phonon states (except the 0^+ states) the secular equation is

$$1=2\varkappa^{(\lambda)}\sum_{qq'}\frac{(f^{\lambda\mu}(q,\ q')u_{qq'})^2(\varepsilon(q)+\varepsilon(q'))}{(\varepsilon(q)+\varepsilon(q'))^2-(\omega_j^{\lambda\mu})^2}. \tag{1.20}$$

Using the normalization condition for wave functions (1.19) we easily find

$$\psi^{\lambda\mu j}_{qq'}=\frac{1}{\sqrt{2Y_j(\lambda\mu)}}\cdot\frac{f^{\lambda\mu}(q,\ q')u_{qq'}}{\varepsilon(q)+\varepsilon(q')-\omega_j^{\lambda\mu}}; \tag{1.21}$$

$$\varphi^{\lambda\mu j}_{qq'}=\frac{1}{\sqrt{2Y_j(\lambda\mu)}}\cdot\frac{f^{\lambda\mu}(q,\ q')u_{qq'}}{\varepsilon(q)+\varepsilon(q')+\omega_j^{\lambda\mu}}; \tag{1.21'}$$

$$Y_j(\lambda\mu)=\sum_{q,\ q'}\frac{(f^{\lambda\mu}(q,q')u_{qq'})^2\omega_j^{\lambda\mu}(\varepsilon(q)+\varepsilon(q'))}{[(\varepsilon(q)+\varepsilon(q'))^2-(\omega_j^{\lambda\mu})^2|^2}. \tag{1.22}$$

In this manner we find a quite good description of the single-phonon quadrupole and octupole states in even–even deformed nuclei.[1,6–8]

The single-particle energies and wave functions of the Nilsson potential were used in calculations for the low-lying states of deformed nuclei until 1967 (and, in certain papers, even later).[2,3] To find the correct order of single-particle levels for equilibrium deformations, it is necessary to assume the parameters of the Nilsson potential to differ for different shells, and in certain cases it was also necessary to shift certain subshells. This procedure was successful in obtaining the correct order for the single-particle levels. In the calculations of ref. 9, which took into account pairing correlations of the superconducting type and quasiparticle–phonon interactions, a quite good description was found for the low-lying nonrotational states of several odd deformed nuclei in the rare-earth region.

However, the Nilsson potential has certain serious shortcomings. It has an infinite depth, so its eigenfunctions do not behave correctly at the nuclear boundary or outside the nucleus; the spin–orbit term does not depend on the radius or deformation parameters, etc.

A more realistic potential is required for a good description of the average field. In recent years a finite potential with a diffusing edge – the Woods–Saxon potential – has been used widely. Nemirovskii and Chepurnov[4] reported the first solution for single-particle states for the deformed Woods–Saxon potential. They numerically integrated the system of differential equations, obtaining single-particle energies and wave functions for the neutron and proton systems of rare earth nuclei. However, these calculations are complicated, and practical use of the results is complicated by the fact that the eigenfunctions are given in huge tables. Other methods for solving the Schrödinger equation with the Woods–Saxon potential were proposed later.[10]

An approximate method was worked out[5,11] for solving the Schrödinger equation with the Woods–Saxon potential for spherical and deformed nuclei. This method yields analytic expressions for the wave functions of spherical nuclei. The accuracy of this approximate method for the case of deformed nuclei was evaluated by comparing the results calculated by the method of ref. 11 with those found in ref. 4. It was found[12] that the energies and wave functions calculated by these two methods for single-particle states near the Fermi surface are essentially equal.

The single-particle spectra and wave functions of highly deformed nuclei have been calculated by this ap-

proximate method.[5,13,14] A single-particle basis was given[14] for calculations on the basis of the superfluid model for the ranges $150 \leq A \leq 190$ and $234 \leq A \leq 254$.

Use of the single-particle energies and wave functions of the Woods–Saxon potential leads to a better description of the intensity of transitions (Eλ and Mλ transitions and β decay) between single-quasiparticle states in odd nuclei in the range $150 \leq A \leq 190$ than that found from calculations based on the Nilsson potential.[15]

The single-particle energies and wave functions found for the Woods–Saxon potential[14] led to a better description of those nuclear properties which had previously been described on the basis of the Nilsson potential, and they allowed analysis of experimental results which could not previously be explained, e.g., N-forbidden β decay, for which log ft values in satisfactory agreement with experiment were obtained in ref. 16.

The approximate method proposed in refs. 5 and 11 for the Schrödinger equation with an anisotropic Woods–Saxon potential yields results having the same practical advantages as those found from the Nilsson scheme (the asymptotic quantum numbers $Nn_z\Lambda$ for the single-particle states and representation of the wave functions of deformed nuclei as expansions in bases of analytic functions). In the case in which the projection of the angular momentum on the symmetry axis of the nucleus, K, is a good quantum number, the wave function of the deformed nucleus is

$$\Psi^I_{MK} = \sqrt{\frac{2I+1}{16\pi^2}} \{D^I_{MK}(\theta_e)\,\Psi_i(K^\pi) + (-1)^{I+K} D^I_{M-K}(\theta_e)\,\Psi_i(-K^\pi)\}, \quad (1.23)$$

where θ_e are the Euler angles. Here we will be concerned with the wave functions $\Psi_i(K^\pi)$, which can be used to calculate transition probabilities and properties of nuclei taking rotational motion into account. The functions $\Psi_i(K^\pi)$ serve as a basis for calculating the effects associated with the Coriolis interaction.

Below we describe a method for solving the Schrödinger equation with an axially symmetric Woods–Saxon potential. We give the energies and wave functions for the single-particle states for the Woods–Saxon potential near A = 155, 165, 173, and 181. An analytic procedure is offered for describing the energies and wave functions of the nonrotational states of odd deformed nuclei taking the quasiparticle–phonon interaction into account. The role of hexadecapole deformation and the effect of the particle–phonon interaction on $\Delta N = \pm 2$ mixing are analyzed. The sensitivity of the energy and structure of the nonrotational states to the difference between the equilibrium deformations of the excited and ground states is taken into account. The energies and structures of the low-lying states of many odd nuclei in the range $150 \leq A \leq 190$ are given, and a comparison is made with experiment.

2. METHOD FOR SOLVING THE SCHRÖDINGER EQUATION WITH AN ANISOTROPIC WOODS–SAXON POTENTIAL

We assume the nuclear shape is described by

$$R(\theta, \varphi) = R_0\,(1 + \beta_0 + \sum_\nu \sum_\mu \beta_{\nu\mu} Y_{\nu\mu}(\theta, \varphi)), \quad (2.1)$$

where R_0 is the radius of the spherical nucleus of equal size, β_0 is a constant introduced to satisfy conservation of volume, and $\beta_{\nu\mu}$ are the deformation parameters. The experimental results available show that for nuclei in the ranges $150 < A < 190$ and $226 < A < 256$ we have[17] $\beta_{20} > 0$, $\beta_{40} \neq 0$, and $\beta_{60} \sim 0$. Calculations[18] predict vanishing values for equilibrium deformations of the β_{22} and $\beta_{3\mu}$ types for nuclei in these ranges. We thus assume that ν takes on only even values and we assume $\mu = 0$.

The nuclear potential, which consists of two parts, is

$$V_{nucl}(\mathbf{r}) = V(\mathbf{r}) + V_{s.o}(\mathbf{r}); \quad (2.2)$$

$$V(\mathbf{r}) = -V_0 \{1 + \exp[(r - R(\theta, \varphi))\,\alpha]\}^{-1}; \quad (2.3)$$

$$V_{s.o} = -\varkappa\,[p\sigma]\,\mathrm{grad}\,V(\mathbf{r}), \quad (2.4)$$

where $\varkappa$ is the spin–orbit coupling constant, σ are the Pauli matrices, and $\mathbf{p}$ is the nucleon momentum.

For the proton system we must add the Coulomb interaction:

$$V_c(\mathbf{r}) = \frac{3(Z-1)e^2}{4\pi R_0^3} \int \frac{n(\mathbf{r}')\,d\mathbf{r}'}{|\mathbf{r} - \mathbf{r}'|}, \quad (2.5)$$

where $n(\mathbf{r}') = \{1 + \exp[(r' - R(\theta', \varphi'))\,\alpha]\}^{-1}$ is the density of the charge distribution in the nucleus.

Denoting by $U(\mathbf{r})$ the sum of the nuclear and Coulomb potentials, we write the Schrödinger equation as

$$[(-\hbar^2/2M)\,\Delta + U(\mathbf{r}) - E]\,\varphi(\mathbf{r}) = 0. \quad (2.6)$$

In Eq. (2.6) we use an identity transformation to single out the spherically symmetric part of the potential, finding

$$[(-\hbar^2/2M)\,\Delta + U(r) + \tilde{U}(\mathbf{r}) - E]\,\varphi(\mathbf{r}) = 0, \quad (2.7)$$

where

$$\tilde{U}(\mathbf{r}) = U(\mathbf{r}) - U(r). \quad (2.8)$$

To solve the problem we expand $\tilde{U}(\mathbf{r})$ in a series in spherical harmonics $Y_{\lambda 0}(\theta)$, finding the following expression for $\tilde{V}(\mathbf{r}) = V(\mathbf{r}) - V(r)$:

$$\tilde{V}(\mathbf{r}) = \sum_\lambda A^0_\lambda(\beta_{v0}, r)\,Y_{\lambda 0}(\theta). \quad (2.9)$$

The functions A^0_λ are found numerically.

For the spin–orbit interaction we can write

$$\tilde{V}_{s.o}(\mathbf{r}) = V_{s.o}(\mathbf{r}) - V_{s.o}(r) = W_1 + W_2 + W_3, \quad (2.10)$$

where

$$W_1 = -\frac{\varkappa}{r} \cdot \frac{\partial \tilde{V}}{\partial r} \left(p_0\sigma_\varphi - \frac{1}{\sin\theta}\,p_\varphi\sigma_\theta\right);$$

$$W_2 = -\frac{\varkappa}{r^2 \sin\theta} \cdot \frac{\partial \tilde{V}}{\partial \theta}\,p_\varphi\sigma_r;$$

$$W_3 = \frac{\varkappa}{r} \cdot \frac{\partial \tilde{V}}{\partial \theta}\,p_r\sigma_\varphi, \quad (2.11)$$

σ_θ, σ_φ, σ_r are the Pauli matrices in the spherical coordinate system; p_θ, p_φ, and p_r are the corresponding momentum operators. The contributions of these three terms are different. The operators W_1, W_2, W_3 are non-Hermitian, while $\tilde{V}_{s.o}$ is Hermitian. Accordingly, discarding one term or another may cause the wave functions

to turn out nonorthogonal; this danger is particularly acute for close-lying levels with $\Delta N = \pm 2$.

We turn now to conservation of nuclear volume; for a homogeneous distribution of nuclear matter with a sharp boundary, we have

$$\rho(r) = \begin{cases} \rho_0 = 3/(4\pi R_0^3), & r \leqslant R(\theta, \varphi); \\ 0, & r > R(\theta, \varphi) \end{cases} \qquad (2.12)$$

and with the normalization condition $\int \rho(r)\, dr = 1$, the condition for volume conservation becomes

$$\int d\Omega \int_0^{R(\theta)} r^2\, dr = 4\pi R_0^3/3. \qquad (2.13)$$

Substituting in expression (2.1) for $R(\theta, \varphi)$ with $\mu = 0$ [then we have $R(\theta, \varphi) \equiv R(\theta)$], we find

$$\beta_0 + \beta_0^2 + \frac{1}{3}\beta_0^3 = -\frac{1}{4\pi}\Big[\sum_\nu |\beta_{\nu 0}|^2 (1 + \beta_0/3)$$

$$+ \frac{1}{3}\sum_{\nu'\nu''\nu'''} \beta^*_{\nu' 0}\beta_{\nu'' 0}\beta_{\nu''' 0} \left\{\frac{(2\nu''+1)(2\nu'''+1)}{4\pi(2\nu'+1)}\right\}^{1/2} (\nu''\nu'''00\,|\,\nu' 0)^2\Big]. \qquad (2.14)$$

Retaining terms of up to order $\beta^2_{\nu 0}$ inclusively, we find

$$\beta_0 = -\frac{1}{2} + \sqrt{\frac{1}{4} - \frac{1}{4\pi}\sum_\nu |\beta_{\nu 0}|^2}. \qquad (2.15)$$

If $\sum_\nu |\beta_{\nu 0}|^2 < \pi$, Eq. (2.15) reduces to the familiar equation

$$\beta_0 = -\frac{p}{4\pi}\sum_\nu |\beta_{\nu 0}|^2, \qquad (2.16)$$

where

$$p = 1 + \frac{1}{3}\left(\frac{1}{\pi}\sum_\nu |\beta_{\nu 0}|^2\right) + \frac{3}{12}\left(\frac{1}{\pi}\sum_\nu |\beta_{\nu 0}|^2\right)^2 + \ldots$$

and $p \to 1$ as $\sum_\nu |\beta_{\nu 0}|^2 \to 0$.

In the case of a Woods–Saxon distribution of nuclear matter, condition (2.13) transforms in the following manner:

$$\int d\Omega \int n(r)\, r^2\, dr = 4\pi \int n(r)\, r^2\, dr, \qquad (2.17)$$

where $n(r)$ is of the same form as in (2.5).

We rewrite Eq. (2.17) as

$$\int\int [n(r) - n(r)]\, d\Omega r^2\, dr = \int\int \tilde{n}(r)\, d\Omega r^2\, dr,$$

where $\tilde{n}(r) = n(r) - n(r)$. Expanding $\tilde{n}(r)$ in a series in spherical harmonics $Y_{\lambda 0}(\theta)$, we can reduce volume-conservation condition (2.17) to the simple relation

$$\int\int \tilde{n}(r)\, d\Omega r^2\, dr = \int d\Omega \int \sum_\lambda C^0_\lambda \Big(r, \beta_0, \sum_\nu \beta_{\nu 0}\Big) Y_{\lambda 0}(\theta)\, r^2\, dr$$

$$= \sqrt{4\pi}\int C^0_0 \Big(r, \beta_0, \sum_\nu \beta_{\nu 0}\Big) r^2\, dr = 0. \qquad (2.18)$$

Equation (2.18) is solved by the method of successive approximations; the zeroth approximation has the form (2.16) with $p = 1$. For the equilibrium values of the deformation parameters, $\beta_{\nu 0} \equiv \beta^0_{\nu 0}$, the value of β_0, always negative, is on the order of a few thousandths. The result is an effective decrease in $R(\theta)$, so all the levels of the single-particle spectrum are raised approximately equally. With $\beta_{20} > \beta^0_{20}$ it becomes extremely important to introduce β_0, since the shifts of the various levels are different, and the spectrum of single-particle levels changes significantly. This change cannot be offset by small changes in the potential parameter r_0 (this measure was successful for the equilibrium values).

We seek a solution of Eq. (2.6) as the superposition

$$\varphi = \sum_{nlj} a^\Omega_{nlj}\varphi^\Omega_{nlj}. \qquad (2.19)$$

The functions φ^Ω_{nlj} are the eigenfunctions of the Schrödinger equation with a spherically symmetric potential,

$$[(-\hbar^2/2M)\Delta + V(r) - \varepsilon_{nlj}]\,\varphi^\Omega_{nlj} = 0, \qquad (2.20)$$

where $\varphi^\Omega_{nlj} = R_{nlj}(r)\, Y^\Omega_{lj}$, Y^Ω_{lj} is the spherical spinor, and the radial part of the wave function is approximated highly accurately by the equation[11]

$$R_{nlj} = (1/r)N_n (A/C)^{1/2} H_n[S(r)] \exp[-S^2(r)/2]. \qquad (2.21)$$

Here N_n is a normalization constant, $H_n(x)$ is the Hermite polynomial, A and C are parameters characterizing the wave function of the given state,[11] and $S(r)$ is a correction function, which satisfies the condition

$$\int_{-\sqrt{E}}^{S} (E - \sigma^2)^{1/2}\, d\sigma = \int_{r_1}^{r} p(\xi)\, d\xi, \qquad (2.22)$$

where $p(\xi)$ is the semiclassical momentum, and r_1 is the turning point. Function $S(r)$ is chosen[11] in such a manner that $(E - \sigma^2)^{1/2}$ vanishes simultaneously with $p(\xi)$. Substituting Eq. (2.19) into (2.6), multiplying by $(\varphi^\Omega_{n'l'j'})^*$, and integrating, we find

$$(\varepsilon_{n'l'j'} - E)\, a^\Omega_{n'l'j'} + \sum_{nlj} a^\Omega_{nlj} \langle \varphi^\Omega_{n'l'j'} | \tilde{U} | \varphi_{nlj} \rangle = 0. \qquad (2.23)$$

Since potential $\tilde{U}$ is axially symmetric, Eq. (2.19) contains terms whose l values have the same parity. Solving system (2.23), we find the single-particle energies E and the wave functions [the coefficient a^Ω_{nlj} in expansion (2.19)].

3. SINGLE-PARTICLE LEVEL SCHEMES

In the Nilsson scheme, the relative arrangement of levels is unaffected by changes in A for fixed values of the deformation parameters; the only change is in the energy reference scale, $\hbar\omega_0 \sim A^{-1/3}$. In the case of the Woods–Saxon potential the relative arrangement of subshells is a function of mass number A, since the energies of states having different n, l, j (with $\beta_{\nu 0} = 0$) depend differently on the nuclear radius. Strictly speaking therefore, we must calculate the single-particle states of the Woods–Saxon potential for each value of A; however, the single-particle energies and wave functions vary slowly and monotonically with increasing A. We can therefore divide the range $150 \leq A \leq 190$ into four subranges, with A = 155, 165, 173, and 181.

The single-particle states are calculated by the method described in Sec. 2, where we retain in the sum $\sum_{\nu} \beta_{\nu 0} Y_{\nu 0}(\theta)$ the quadrupole ($\nu = 4$) and hexadecapole ($\nu = 2$) deformations, and where $R(\theta)$ has the form

$$R(\theta) = R_0 \{1 + \beta_0 + \beta_{20} Y_{20}(\theta) + \beta_{40} Y_{40}(\theta)\}. \quad (3.1)$$

The calculated results are shown for the equilibrium values of β_{40}, which are[17] 0.06, 0.02, −0.02, and −0.03 for A near 155, 164, 173, and 181, respectively. Figures 1-8 show parts of the schemes of neutron and proton levels with A = 155, 165, 173, and 181 for approximately equilibrium β_{20} values. The parameters of the Woods–Saxon potential are shown in Table 3.1. We see from this table that the potential parameters change slightly from subrange to subrange. The parameters in Table 3.1 are approximately the same as those for the Woods–Saxon potential for nuclei in the $234 \leq A \leq 260$ range.[19]

Tables of the single-particle energies and wave functions are given in the Appendix. To save space, we show only the states in the energy range between −12 and 0 MeV for these nuclear subranges. The single-particle energies and coefficients of the wave functions are given for the equilibrium values of deformation parameters β_{20} and β_{40}. We see from these tables that the coefficients

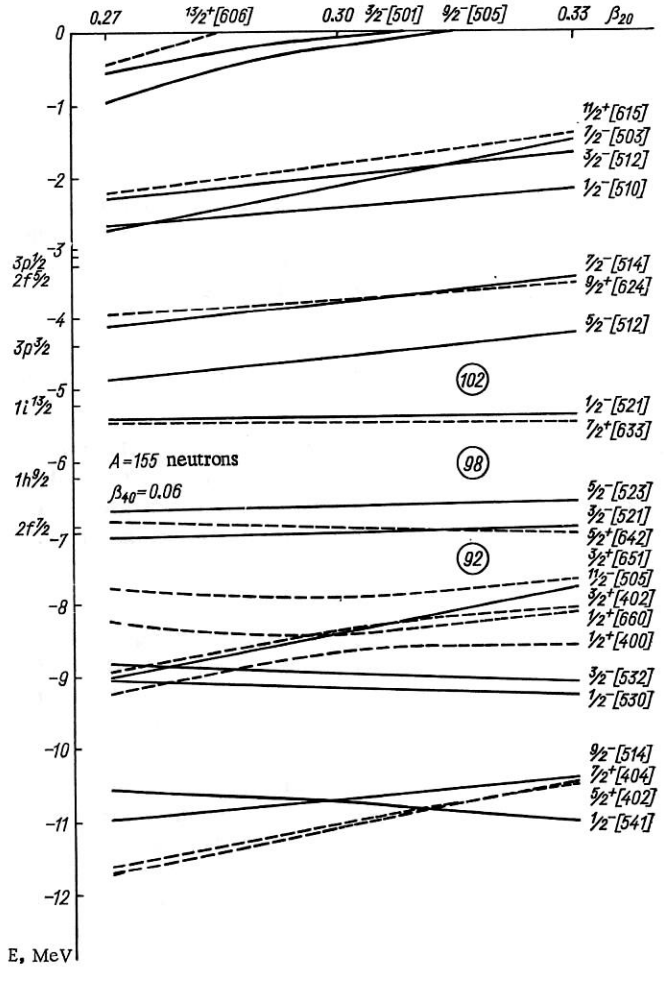

Fig. 1. Scheme of single-particle neutron states for A = 155.

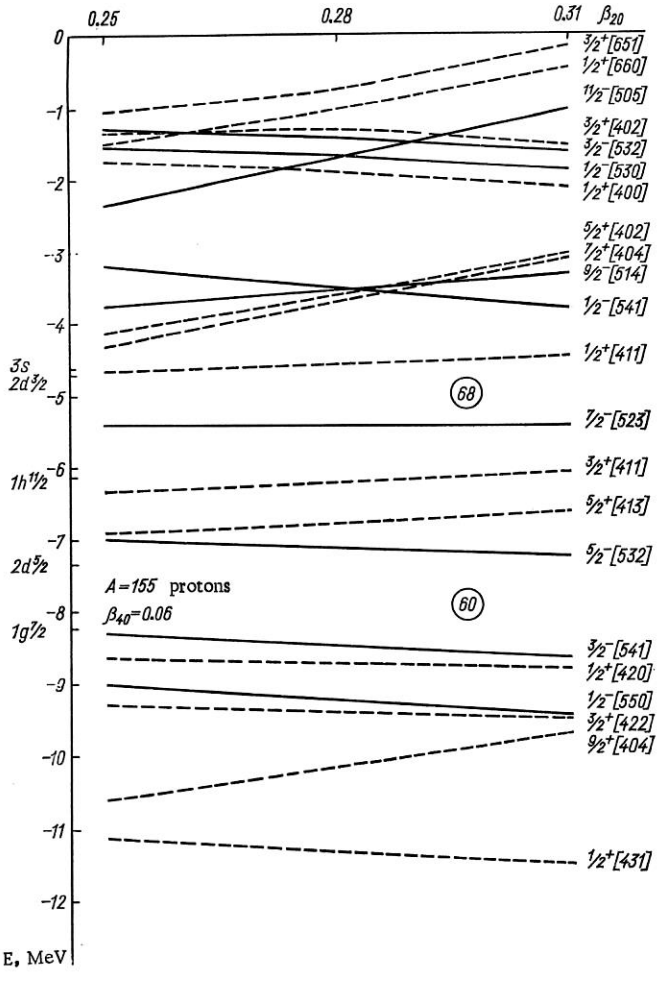

Fig. 2. Scheme of single-particle proton states for A = 155.

for the mixing of the basis wave functions vary slowly from subrange to subrange, while the single-particle energies depend strongly on A. Table 3.2 shows the coefficients a^{Ω}_{nlj} of the 1/2+[411] state for A = 173 and A = 181; we see that the coefficients a^{Ω}_{nlj} depend weakly on A.

To evaluate the various characteristics of deformed nuclei we must know the correlation functions C_n, C_p and the chemical potentials λ_n, λ_p for the neutron and proton systems.

Table 3.3 shows the correlation functions for the ground states of the even–even and odd nuclei. The correlation functions and chemical potentials were calculated from the single-particle schemes in Figs. 1-8 for approximately equilibrium β_{20} and β_{40} values.

4. QUASIPARTICLE–PHONON INTERACTIONS IN ODD DEFORMED NUCLEI

The energies and wave functions of the nonrotational states of odd deformed nuclei are most sensitive to pairing correlations of the superconducting type, quasiparticle–phonon interactions, and the Coriolis interaction.

In this section we consider the effect of the quasiparticle–phonon interaction on the spectra of nonrotational states of deformed nuclei having odd numbers of

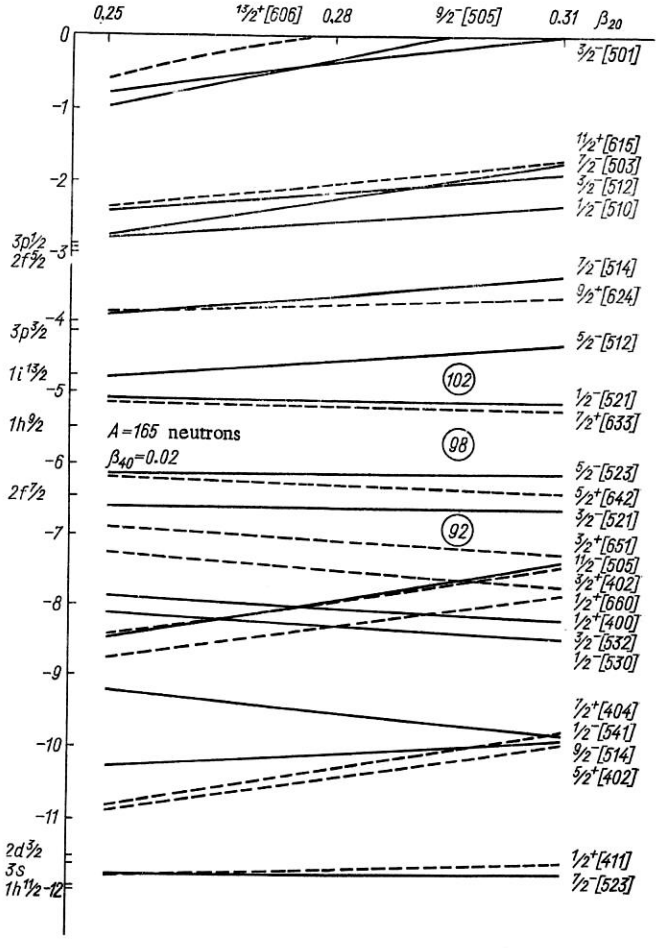

Fig. 3. Scheme of single-particle neutron states for A = 165.

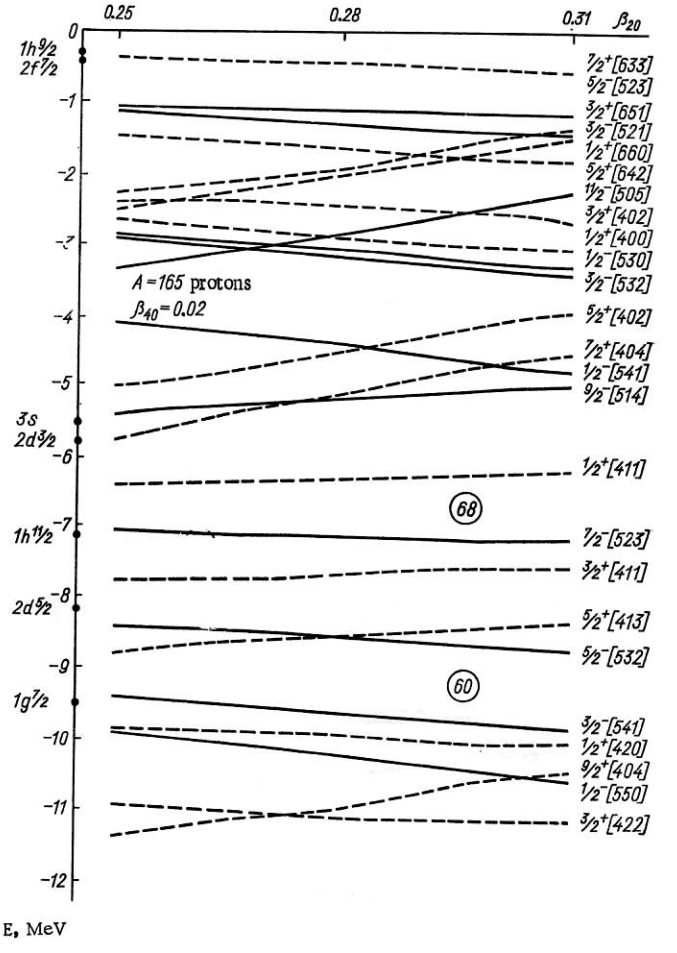

Fig. 4. Scheme of single-particle proton states for A = 165.

neutrons and protons. The Coriolis interaction plays a minor role for most of the rotational bands. According to, e.g., ref. 20, however, the Coriolis interaction may be important for levels deriving from large-j spherical subshells, and it is particularly important for high-spin rotational states. In the mass range of interest here the Coriolis interaction may be most influential on the states of the $i_{13/2}$ subshells (in odd N nuclei) and the $h_{11/2}$ subshells (in odd Z nuclei). It is not difficult to take the Coriolis interaction into account on the basis of the superfluid model, as in ref. 20.

An odd nucleus contains a single quasiparticle in addition to the phonons and quasiparticles of the even–even nucleus with A − 1. This additional quasiparticle causes some change in the phonons, but this change is usually neglected. In studying the quasiparticle–phonon interaction it is assumed that the phonon operators are completely determined, so the constants of the multipole–multipole interaction are fixed.

The quasiparticle–phonon interaction was first taken in the superfluid model in ref. 21; here Hamiltonian (1.1) was used with H' = 0, and the secular equation was found by a variational principle. The roots of the secular equation are the energies of the ground and excited states of the odd deformed nuclei. The mathematical apparatus for this analysis was given in ref. 1. The structures of many nuclei were analyzed in refs. 9, 22, and 23, taking the quasiparticle–phonon interaction into account; it was shown that only the lowest-lying and a few of the higher-lying excited states are approximately single-quasiparticle states. Some of the states are purely collective, i.e., their wave functions are dominated by a single quasiparticle component and a phonon. Most of the states, however, have a complicated structure; their wave functions show contributions from several quasiparticle components and a phonon.

We will now write the basic equations of the theory, taking into account the quasiparticle–phonon interaction in odd deformed nuclei. Using the secular equation (1.20) to determine the phonon energies $\omega_j^{\lambda\mu}$, we can write Hamiltonian (1.17) as

$$H_{vq} = \sum_q \varepsilon(q) B(q, q) - \frac{1}{2} \sum_{\lambda\mu j} \frac{1}{Y_j(\lambda\mu)}$$

$$\times \sum_{q, q'} \frac{(f^{\lambda\mu}(q, q') u_{qq'})^2 (\varepsilon(q) + \varepsilon(q'))}{(\varepsilon(q) + \varepsilon(q'))^2 - (\omega_j^{\lambda\mu})^2} Q_j^+(\lambda\mu) Q_j(\lambda\mu)$$

$$- \frac{1}{4} \sum_{\lambda\mu j} \frac{1}{\sqrt{Y_j(\lambda\mu)}} \sum_{q, q'} v_{qq'} f^{\lambda\mu}(q, q')$$

$$\times \{B(q, q')(Q_j^+(\lambda\mu) + Q_j(\lambda\mu)) + (Q_j^+(\lambda\mu) + Q_j(\lambda\mu)) B(q, q')\}. \quad (4.1)$$

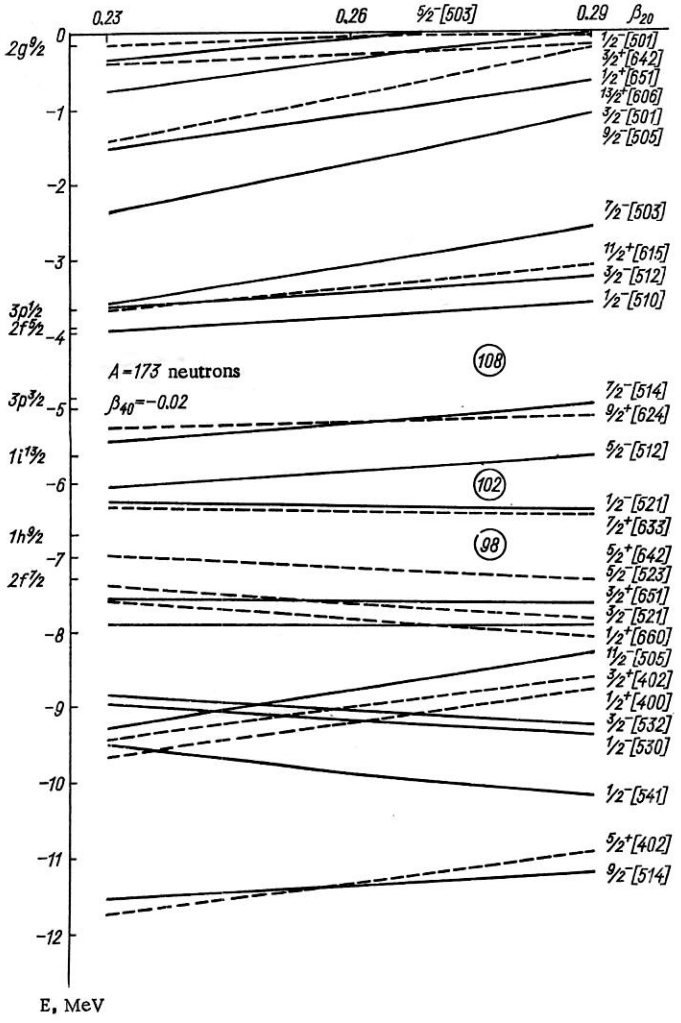

Fig. 5. Scheme of single-particle neutron states for A = 173.

The wave function for an odd nucleus describing a state with a specified K^π is

$$\Psi_i(K^\pi) = \frac{N_i(\rho_1 \dots \rho_n)}{\sqrt{2}} \sum_\sigma \left\{ \sum_{\rho n} C^i_{\rho n} \alpha^+_{\rho n \sigma} + \sum_{\lambda\mu j} \sum_q D^{\lambda\mu ij}_{\nu\sigma}(\rho_1 \dots \rho_n)\, \alpha^+_{q\sigma} Q^+_j(\lambda\mu) \right\} \Psi_0. \quad (4.2)$$

Here the coefficients $[N_i(\rho_1, \dots, \rho_n) C^i_{\rho n}]^2$ and $[N_i(\rho_1, \dots, \rho_n) \cdot D^{\lambda\mu ij}_{q\sigma}(\rho_1, \dots, \rho_n)]^2$ show the contribution to this state of the single-quasiparticle component ρ_n, and the component of the quasiparticle in the state $q\sigma$ plus a phonon $\lambda\mu j$. The summation over ρ_n means that we are taking account of the several states $\rho_1, \dots, \rho_n$ having the same K^π which occur in the Woods–Saxon single-particle scheme. In a study of the low-lying excited states, however, it is not necessary to take into account all the states having the same K^π, since they are generally far apart; it is usually sufficient to take into account two states having the same K^π and approximately equal quasiparticle energies. In this case we write the wave function as

$$\Psi_i(K^\pi; \rho_1, \rho_2) = N_i(\rho_1, \rho_2) \frac{1}{\sqrt{2}} \sum_\sigma \left\{ C^i_{\rho_1} \alpha^+_{\rho_1\sigma} + C^i_{\rho_2} \alpha^+_{\rho_2\sigma} + \sum_{\lambda\mu jq} D^{\lambda\mu ij}_{\rho_1\rho_2 q\sigma} \alpha^+_{q\sigma} Q^+_j(\lambda\mu) \right\} \Psi_0 \quad (4.3)$$

with the normalization condition

$$N_i^2(\rho_1, \rho_2) \left\{ (C^i_{\rho_1})^2 + (C^i_{\rho_2})^2 + \frac{1}{2} \sum_{q\sigma} (D^{\lambda\mu ij}_{\rho_1\rho_2 q\sigma})^2 \right\} = 1. \quad (4.4)$$

Finding the average value of H_{vq} in state (4.3) and using a variational principle, we find the secular equation which gives the energies η_i:

$$P(\eta) = \begin{vmatrix} V_i(\rho_1, \rho_1) - (\varepsilon(\rho_1) - \eta_i) & V_i(\rho_1, \rho_2) \\ V_i(\rho_1, \rho_2) & V_i(\rho_2, \rho_2) - (\varepsilon(\rho_2) - \eta_i) \end{vmatrix} = 0, \quad (4.5)$$

where

$$V_i(\rho, \rho') = \frac{1}{4} \sum_{\lambda\mu jq} \frac{v_{\rho q} v_{\rho' q}}{Y_j(\lambda\mu)} \cdot \frac{f^{(\lambda\mu)}(\rho q)\, f^{(\lambda\mu)}(\rho' q)}{\varepsilon(q) + \omega^{\lambda\mu}_j - \eta_i}; \quad (4.6)$$

and $Y_j(\lambda\mu)$ is given by Eq. (1.22). The quantities $C^i_{\rho 1}$ and $C^i_{\rho 2}$ are

$$C^i_{\rho_1} = 1 - \frac{V_i(\rho_1, \rho_2)}{V_i(\rho_1, \rho_1) - (\varepsilon(\rho_1) - \eta_i)}; \qquad C^i_{\rho_2} = 1 - \frac{V_i(\rho_1, \rho_2)}{V_i(\rho_2, \rho_2) - (\varepsilon(\rho_2) - \eta_i)}. \quad (4.7)$$

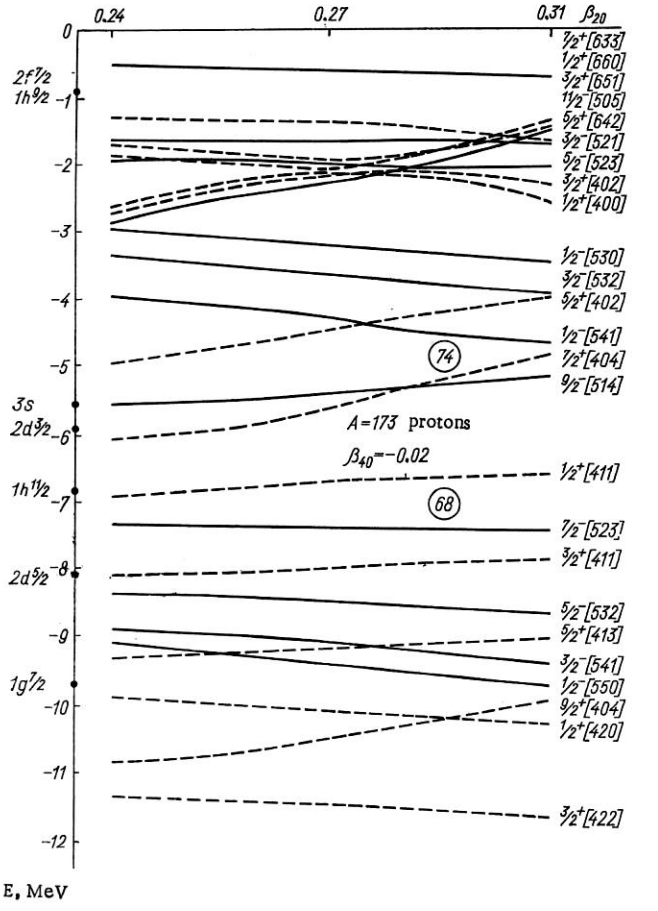

Fig. 6. Scheme of single-particle proton states for A = 173.

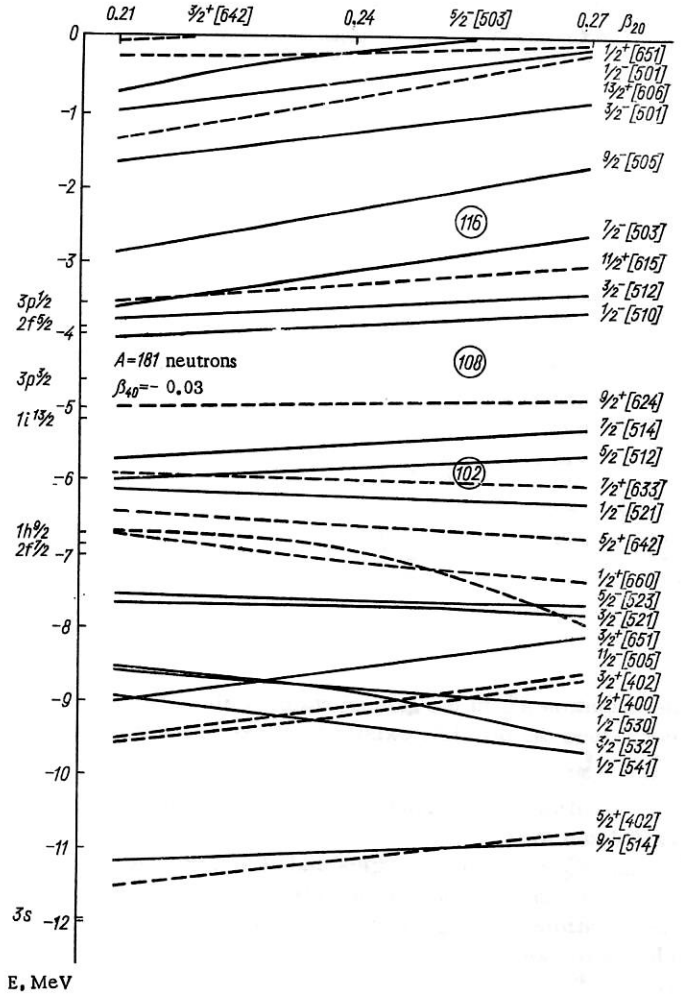

Fig. 7. Scheme of single-particle neutron states for A = 181.

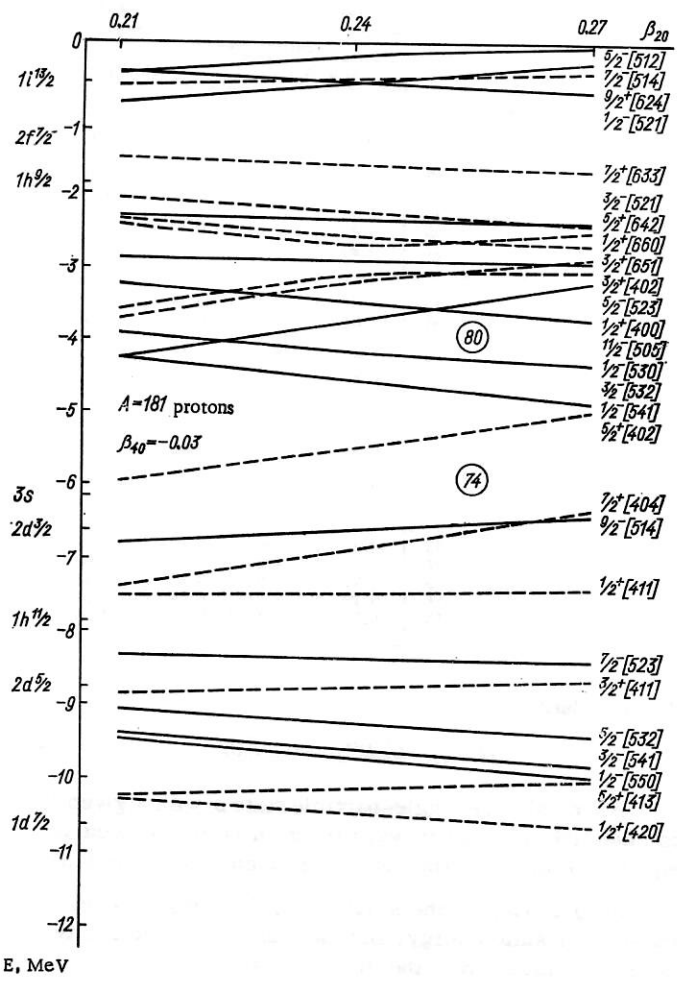

Fig. 8. Scheme of single-particle proton states for A = 181.

TABLE 3.1. Parameters of the Woods–Saxon Potential

A	Neutron system				Proton system			
	V_0, MeV	r_0, F	$\varkappa$, F^2	α, F^{-1}	V_0, MeV	r_0, F	$\varkappa$, F^2	α, F^{-1}
155	47.2	1.26	0.40	1.67	59.2	1.24	0.360	1.63
165	44.8	1.26	0.43	1.67	59.2	1.25	0.355	1.63
173	44.8	1.26	0.42	1.67	59.2	1.25	0.320	1.59
181	43.4	1.26	0.40	1.67	59.8	1.24	0.330	1.67

TABLE 3.2. Coefficients a^{Ω}_{nlj} of the Expansion for the 411 Proton States for $\beta_{20} = 0.24$ and $\beta_{40} = -0.03$ for A = 173 and A = 181

A	173	181	A	173	181
E / nlj	−6.811	−7.544	E / nlj	−6.811	−7.544
$1k_{15/2}$	−0.009	−0.009	$2d_{3/2}$	0.727	0.736
$1k_{17/2}$	−0.009	−0.009	$2d_{5/2}$	0.442	0.428
$2g_{7/2}$	0.074	0.075	$1g_{7/2}$	−0.367	−0.359
$3d_{5/2}$	0.000	−0.003	$1g_{9/2}$	−0.163	−0.160
$1i_{11/2}$	−0.108	−0.113	$2s_{1/2}$	0.021	0.023
$2g_{9/2}$	0.068	0.067	$1d_{3/2}$	0.000	−0.005
$1i_{13/2}$	−0.079	−0.090	$1d_{5/2}$	0.023	0.022
$3s_{1/2}$	−0.292	−0.299	$1s_{1/2}$	0.006	0.007

TABLE 3.3. Correlation Functions and Chemical Potentials for the Ground States of Neutron (N) and Proton (Z) Systems

A range	Neutron system					Proton system					Equilibrium-deformation parameters	
		even $N+1$		odd N			even Z + 1		odd Z			
	N	C_n, MeV	λ_n, MeV	C_n, MeV	λ_n, MeV	Z	C_p, MeV	λ_p, MeV	C_p, MeV	λ_p, MeV	β_{20}^0	β_{40}^0
155	89	1.13	−7.80	0.96	−7.97	59	1.15	−7.85	0.79	−8.04	0.29	0.06
	91	1.08	−7.41	0.87	−7.59	61	1.19	−7.16	0.72	−7.61		
	93	1.03	−7.00	0.81	−7.32	63	1.23	−6.54	0.85	−6.82		
	95	0.96	−6.57	0.72	−6.81	65	1.26	−5.90	0.87	−6.18		
	97	0.90	−6.05	0.50	−6.22	67	1.34	−5.27	0.90	−5.56		
165	93	1.07	−6.50	0.89	−6.68	63	1.12	−8.0			0.28	0.02
	95	1.01	−6.11	0.83	−6.31	65	1.11	−7.36	0.68	−7.86		
	97	0.95	−5.67	0.74	−5.83	67	1.12	−6.70	0.67	−7.15		
	99	0.91	−5.21	0.67	−5.53	69	1.20	−6.05	0.74	−6.53		
	101	0.87	−4.75	0.63	−4.97	71	1.30	−5.50	0.93	−5.99		
173	99	0.89	−6.39	0.71	−6.67	67	1.07	−6.95	0.72	−7.26	0.26	−0.02
	101	0.84	−6.00	0.65	−6.16	69	1.06	−6.28	0.57	−6.55		
	103	0.77	−5.58	0.54	−5.78	71	1.15	−5.65	0.72	−6.11		
	105	0.70	−5.14	0.51	−5.48	73	1.25	−5.09	0.84	−5.32		
181	105	0.84	−5.02	0.66	−5.21	71	0.96	−6.74	0.64	−7.08	0.24	−0.03
	107	0.72	−4.46	0.26	−4.68	73	0.91	−6.07	0.47	−6.27		
	109	0.77	−3.92	0.32	−4.31	75	1.02	−5.37	0.25	−5.74		
	111	0.79	−3.51	0.56	−3.71							
	113	0.73	−3.11	0.55	−3.34							

Then we have

$$D^{\lambda\mu ij}_{\rho_1\rho_2 q\sigma} = C^i_{\rho_1} D^{\lambda\mu ij}_{\rho_1 q\sigma} + C^i_{\rho_2} D^{\lambda\mu ij}_{\rho_2 q\sigma}. \quad (4.8)$$

When only one single-particle state ρ with a given K^π is taken into account in wave function (4.2), the secular equation reduces to the vanishing diagonal term in (4.5).

In each nucleus the smallest of the $\eta_1(K_0^\pi)$ values is the ground-state energy, and the energies of the excited states are found from the differences

$$\eta_i(K^\pi) - \eta_1(K_0^\pi). \quad (4.9)$$

The summation over $\lambda\mu j$ in Eq. (4.5) usually takes into account phonons having $j = 1, 2$; $\lambda = 2$, $\mu = 0.2$, and $\lambda = 3$, $\mu = 0$, 1, and 2. This restriction to the first two groups of Eq. (1.20) and to phonons with $\lambda < 4$ is completely proper, since this procedure takes into account all the ground collective vibrational states of the deformed nuclei. The states which are approximately two-quasiparticle states play a minor role: The associated values of $Y_j(\lambda\mu)$ are extremely large, so the contribution of the corresponding terms to the secular equation is very small.

The blocking effect is taken into account to improve the accuracy of the calculations. For this purpose the $\varepsilon(\rho)$ values are calculated with the $C(\rho)$ and $\lambda(\rho)$ values for the odd system. Where the interaction of quasiparticles with a phonon $\lambda = 2$, $\mu = 0$ is predominant, a more complicated secular equation, including terms used in the absence of a virtual state,[1] must be solved.

The energy and structure of a nonrotational state lying adjacent to a single-quasiparticle state may be quite sensitive to the difference between the equilibrium deformations in the excited and ground states.

It has been pointed out[24] that the equilibrium deformations β_{20}^e of excited single-quasiparticle states, whose single-particle energies vary strongly with increasing deformation parameters, may differ from the equilibrium deformation β_{20}^0 in the ground state. Calculations[18,25] have confirmed the possible existence of excited states having $\beta_{20}^e \neq \beta_{20}^0$.

Equilibrium deformations of the excited states were calculated for this nuclear range in ref. 25. For the states having $\beta_{20}^e \neq \beta_{20}^0$, the energies and structures were calculated by the method outlined above. The equilibrium deformations of the ground and excited states of odd nuclei were calculated by means of the Strutinskii shell correction.[26]

It was shown that there is an appreciable difference $\Delta\beta_{\nu 0} = \beta_{\nu 0}^e - \beta_{\nu 0}^0$ between the equilibrium deformations of the excited and ground states for the single-particle states n505↑, p541↓, p404↓, and several others. Table 4.1 shows the changes in the quadrupole parameters $\Delta\beta_{20}$ and the hexadecapole parameters $\Delta\beta_{40}$ for the deformations of these states in certain nuclei.

Table 4.1 shows that in certain nuclei the $\Delta\beta_{20}$ value will reach 0.04, while the $\Delta\beta_{40}$ value can reach 0.032. Where $\Delta\beta_{20}$ and $\Delta\beta_{40}$ exceed 0.01, the effect of this circumstance $\beta_{\nu 0}^e \neq \beta_{\nu 0}^0$ should be taken into account in calculating the energies and wave functions of the excited states.

The energies and wave functions of the states n505↑, p541↓, p404↓, and p402↑ were calculated with the matrix elements and phonons used in refs. 22 and 23, but the single-particle energies of the Woods–Saxon potential for these states were taken for equilibrium deformations $\beta_{\nu 0}^e$. The energies and wave functions of the single-phonon states were calculated for equilibrium deformations $\beta_{\nu 0}^0$.

As an example, Table 4.2 shows the results calculated for a state approximating the $11/2^-[505]$ state. This table also gives the state energies calculated in ref. 23 for $\beta_{\nu 0}^e = \beta_{\nu 0}^0$. The experimental data are taken from the review by Bunker and Reich.[27] Table 4.2 shows that in all cases taking account that $\beta_{\nu 0}^e \neq \beta_{\nu 0}^0$ leads to a better agreement between the experimental and calculated energies.

TABLE 4.1. Differences between the Equilibrium Deformations $\Delta\beta_{20}$ and $\Delta\beta_{40}$ of Excited States and Ground States

Nucleus	$n\,505\uparrow$		Nucleus	$p\,541\downarrow$	
	$\Delta\beta_{20}$	$\Delta\beta_{40}$		$\Delta\beta_{20}$	$\Delta\beta_{40}$
^{153}Sm	0.027	−0.008	^{171}Tm	0.026	0.017
^{155}Sm	0.019	−0.007	^{169}Lu	0.027	0.003
^{155}Gd	0.033	0.002	^{171}Lu	0.030	0.003
^{157}Gd	0.017	−0.011	^{173}Lu	0.034	0.004
^{159}Gd	0.008	−0.017	^{175}Lu	0.035	0.005
^{161}Gd	0.008	−0.016	^{177}Lu	0.033	0.005
^{157}Dy	0.035	0	^{173}Ta	0.011	0.001
^{159}Dy	0.017	−0.012	^{175}Ta	0.019	0.004
^{161}Dy	0.012	−0.015	^{177}Ta	0.026	0.007
^{163}Dy	0.009	−0.017	^{179}Ta	0.040	0.010
^{165}Dy	0.013	−0.003	^{181}Ta	0.040	0.010
^{161}Er	0.017	−0.018	^{181}Re	0.040	0.010
^{163}Er	0.016	−0.012	^{183}Re	0.030	0.010
^{165}Er	0.007	−0.017			
^{167}Er	0.008	−0.014			
^{169}Er	0.007	−0.013		$p\,404\downarrow$	
	$p\,541\downarrow$		^{161}Ho	−0.010	0.016
			^{163}Ho	−0.009	0.015
			^{163}Tm	−0.007	0.01
^{159}Ho	0.028	0.016	^{165}Tm	−0.006	0.013
^{161}Ho	0.024	0.016	^{167}Tm	−0.008	0.032
^{163}Ho	0.023	0.015	^{169}Tm	−0.008	0.014
^{165}Ho	0.024	0.013	^{171}Tm	−0.009	0.014
^{165}Tm	0.024	0.015	^{181}Re	0.020	0
^{167}Tm	0.023	0.015	^{183}Re	0.020	0
^{169}Tm	0.024	0.016	^{185}Re	0.020	0

TABLE 4.2. Influence of the Conditions $\Delta\beta_{20} \neq 0$ and $\Delta\beta_{40} \neq 0$ on the Energies of the n505↑ States

Nucleus	K^π	Energy, keV			Structure
		experiment	theory		
			$\beta^e_{\nu 0} = \beta^0_{\nu 0}$	$\Delta\beta_{20} \neq 0$ $\Delta\beta_{40} \neq 0$	
^{153}Sm	11/2−	94	470	100	505↑ 97%
^{155}Sm	11/2−	—	800	460	505↑ 98%
^{157}Gd	11/2−	426	830	490	505↑ 98%
^{159}Gd	11/2−	681	1100	820	505↑ 99%
^{161}Gd	11/2−	—	1490	1140	505↑ 99%
^{159}Dy	11/2−	352	820	470	505↑ 99%
^{161}Dy	11/2−	486	1100	760	505↑ 99%

Comparison of the state structure in Table 4.2 with that given in ref. 23 shows that the fact that $\beta^e_{\nu 0} \neq \beta^0_{\nu 0}$ does not have any important influence on the state structure. The occurrence of $\beta^e_{\nu 0} \neq \beta^0_{\nu 0}$ causes only a slight increase in the magnitudes of the single-quasiparticle components.

These results were obtained for well-deformed nuclei, which have high deformation energies and are rigid with respect to β and γ vibrations. In these nuclei inclusion of the effect $\beta^e_{\nu 0} \neq \beta^0_{\nu 0}$ significantly influences the excitation energies of several states near the single-quasiparticle states and improves the agreement with the corresponding experimental results. The effect $\beta^e_{\nu 0} \neq \beta^0_{\nu 0}$ should have a greater influence on the energy and structure of states in transition nuclei.

5. $\Delta N = \pm 2$ MIXING IN ODD DEFORMED NUCLEI

Let us use the results of Sec. 4 to discuss the mixing of two states having identical K^π values in odd deformed nuclei. There is experimental evidence[28,29] that several odd nuclei in the rare-earth region have states whose wave functions contain a significant mixture of components with N = 4 and 6. A pronounced mixing of components having $\Delta N = \pm 2$ should be observed in those odd nuclei for which the pseudocrossing of levels of $\Delta N = \pm 2$ occurs at equilibrium deformations near the energy of the Fermi surfaces.

When the Nilsson potential is used to describe the mean field, the matrix elements with $\Delta N = \pm 2$ are usually neglected, since their magnitudes (on the order of a few keV) are much smaller than the energy spacing between the shells with $\Delta N = \pm 2$. As a result of this approximation, levels having the same K^π but deriving from different N shells cross in the Nilsson scheme.

Use of the Woods–Saxon potential as the mean field leads to a better description of $\Delta N = \pm 2$ mixing, because the Woods–Saxon potential has a radial dependence more realistic than the Nilsson potential. There are small admixtures of components with $\Delta N = \pm 2$ in all the eigenfunctions of the Woods–Saxon potential; they have been used, e.g., to explain[16] N-forbidden β transitions.

The first analysis[4,5] of $\Delta N = \pm 2$ mixing was based on the wave functions of the Woods–Saxon potential. It was shown in ref. 30 that introduction of hexadecapole deforma-

tion β_{40} is important for $\Delta N = \pm 2$ mixing. A study was made[31-33] of the influence of $\Delta N = \pm 2$ mixing on the spectroscopic factors in (d, p) and (d, t) interactions.

It has been shown[34] that the quasiparticle–phonon interaction strongly influences $\Delta N = \pm 2$ mixing in odd deformed nuclei.

Following ref. 35, we will discuss $\Delta N = \pm 2$ mixing in certain deformed nuclei having an odd number of neutrons for two pairs of states: 400↑, 660↑ and 402↓, 651↑. We will study the dependence of the mixing of the N = 4 and 6 components on the deformation parameters β_{30} and β_{40} and on the quasiparticle–phonon interaction.

Let us consider the behavior of the single-particle energies and wave functions of the Woods–Saxon potential near a pseudocrossing of the states 400↑, 660↑ and 402↓, 651↑. When $\Delta N = \pm 2$ coupling is taken into account, it is known that the single-particle levels having identical K^π values do not cross. The region in which two such levels come closest together has been called a pseudocrossing.

In calculations for a neutron system with A = 155 we use the following parameters of the Woods–Saxon potential: $r_0 = 1.24$ F, $V_0 = 48.2$ MeV, $\varkappa = 0.39$ F^2, and $\alpha = 1.8$ F^{-1}. These parameters are better than those given in Table 3.1 because $\Delta N = \pm 2$ mixing is very sensitive to the choice of the mean-field parameters. The accuracy of the calculation is also improved (the rank of the diagonalization matrix is increased). This refinement of parameters in the ground state affects the behavior of pseudocrossing levels. The energies and structures of the ground and excited states of odd deformed nuclei change slightly. We write the eigenfunction (2.19) of the Schrödinger equation with the Woods–Saxon potential for positive-parity states as

$$\varphi_q(\mathbf{r}) = a^q_{001/2}(N=0)\,\varphi^q_{001/2} + \sum_{nlj} a^q_{nlj}(N=2)\,\varphi^q_{nlj} + \sum_{nlj} a^q_{nlj}(N=4)\,\varphi^q_{nlj} + \sum_{nlj} a^q_{nlj}(N=6)\,\varphi^q_{nlj} + \dots . \quad (5.1)$$

The normalization condition is

$$\int \varphi^*_q(\mathbf{r})\,\varphi_q(\mathbf{r})\,d\mathbf{r} = 1 = [a^q_{001/2}(N=0)]^2 + \sum_{nlj}[a^q_{nlj}(N=2)]^2 + \sum_{nlj}[a^q_{nlj}(N=4)]^2 + \sum_{nlj}[a^q_{nlj}(N=6)]^2 + \dots = d^2_0(q) + d^2_2(q) + d^2_4(q) + d^2_6(q) + \dots, \quad (5.2)$$

i.e., the wave functions contain components with N = 0, 2, 4, 6, ..., although one of the components $d^2_N(q)$ usually predominates. For negative-parity states expansion (5.2) contains components with N = 1, 3, 5, ...

We consider a mixture of components with N = 4 and 6 for two pairs of states, 400↑, 660↑ and 402↓, 651↑, near their pseudocrossings. The behavior of the 402↓ and 651↑ levels as functions of β_{20} with $\beta_{40} = 0$ and $\beta_{40} = 0.04$ is shown at the bottom of Fig. 9. Near a pseudocrossing the levels cannot be assigned quantum numbers $Nn_z\Lambda$. The wave function has the same structure before and after a pseudocrossing as it would have if a crossing occurred. Accordingly, the upper curves for $\beta_{20} = 0.30$ are assigned quantum numbers 651↑, and those for $\beta_{20} = 0.33$ are assigned quantum numbers 402↓. The top of the figure shows the d^2_4 and d^2_6 values for the state 402↓ with $\beta_{40} = 0$ and $\beta_{40} = 0.04$. We see that with $\beta_{40} = 0$ these components are mixed over an extremely narrow range $\Delta\beta_{20}$, while with $\beta_{40} = 0.04$ the range is broader.

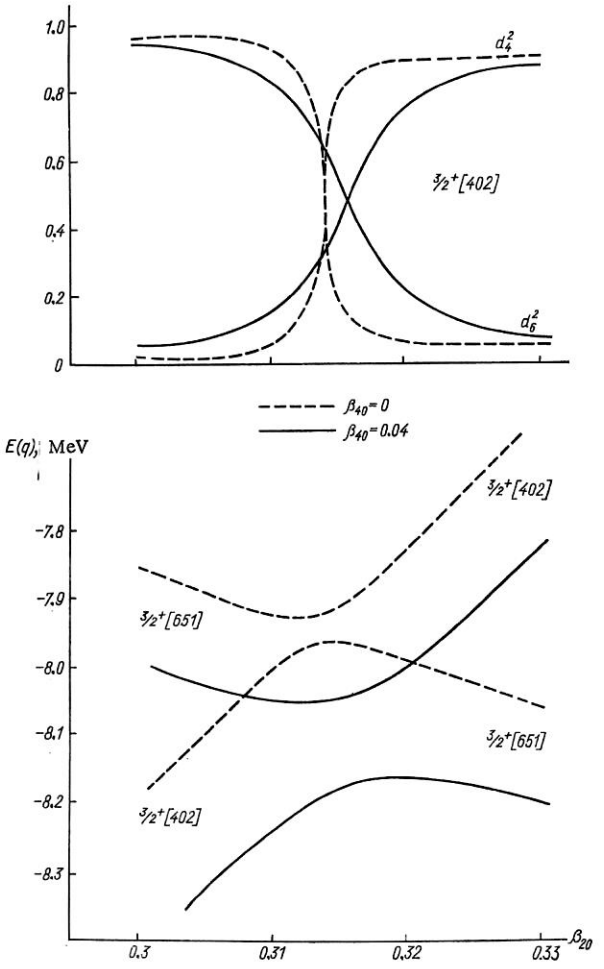

Fig. 9. Dependence of components d^2_4 and d^2_6 for the 402↓ state on β_2. (top); position of the single-particle levels 402↓ and 651↑ near the pseudocrossing with $\beta_{40} = 0$ (dashed curves) and $\beta_{40} = 0.04$ (solid curves) (bottom).

TABLE 5.1. Mixing of Components with N = 4 and N = 6 near a Pseudocrossing of the 660↑ and 400↑ States in the Neutron System with A = 155

β_{20}	$E(q)$, MeV	$d^2_4(q)$	$d^2_6(q)$	$E(q')$, MeV	$d^2_4(q')$	$d^2_6(q')$	$E(q) - E(q')$, MeV
			$\beta_{40} = 0.04$				
0.300	−8.524	0.098	0.856	−8.772	0.937	0.052	0.248
0.305	−8.552	0.190	0.766	−8.695	0.844	0.138	0.143
0.310	−8.549	0.628	0.345	−8.649	0.409	0.558	0.100
0.312	−8.528	0.796	0.184	−8.649	0.240	0.718	0.121
0.315	−8.485	0.903	0.080	−8.661	0.132	0.822	0.176
0.320	−8.403	0.950	0.035	−8.691	0.086	0.866	0.288
0.325	−8.317	0.961	0.024	−8.725	0.074	0.876	0.408
0.330	−8.226	0.965	0.020	−8.751	0.071	0.878	0.525
			$\beta_{40} = 0$				
0.300	−8.228	0.058	0.902	−8.549	0.954	0.027	0.321
0.305	−8.266	0.078	0.880	−8.465	0.934	0.048	0.199
0.310	−8.295	0.220	0.743	−8.389	0.795	0.184	0.094
0.312	−8.295	0.454	0.516	−8.370	0.560	0.412	0.075
0.315	−8.267	0.810	0.172	−8.369	0.206	0.754	0.102
0.320	−8.188	0.927	0.057	−8.399	0.086	0.868	0.211
0.325	−8.103	0.944	0.039	−8.434	0.070	0.885	0.331
0.330	−8.012	0.949	0.034	−8.468	0.065	0.888	0.456

Table 5.1 shows, for a different pair of states 400↑ and 660↑, the single-particle energies E(q) and E(q'), their differences, and the components d_4^2 and d_6^2 as functions of β_{20} with $\beta_{40} = 0$ and $\beta_{40} = 0.04$. From Table 5.1 we see that there is a pronounced mixing of the components with N = 4 and 6 in a range $\Delta\beta_{20} \approx 0.01$ near the pseudocrossing. The mixing range $\Delta\beta_{20}$ increases slightly with increasing β_{40}.

Studies of the solution of the Schrödinger equation for the Woods–Saxon potential have shown that the pseudocrossings of levels having identical K^π values and the extent of the mixing of the components with $\Delta N = \pm 2$ depend strongly on the shape of the potential, the parameters of the potential, and the accuracy of the solution. Study of pseudocrossings thus allows us to refine the shape and parameters of the mean-field potential.

We now turn to the sensitivity of $\Delta N = \pm 2$ mixing to the quasiparticle–phonon interaction in odd deformed nuclei. When two single-particle states ρ_1 and ρ_2 with identical K^π are described simultaneously, wave function (4.2) is written as

$$\Psi_i(K^\pi; \rho_1, \rho_2) = N_i(\rho_1, \rho_2)\frac{1}{\sqrt{2}}\sum_\sigma \left\{C^i_{\rho_1}\alpha^+_{\rho_1\sigma} + C^i_{\rho_2}\alpha^+_{\rho_2\sigma} + \sum_{\lambda\mu j}\sum_q D^{\lambda\mu ji}_{\rho_1\rho_2 q\sigma}\alpha^+_{q\sigma}Q^+_j(\lambda\mu)\right\}\Psi. \quad (5.3)$$

Since asymptotic quantum numbers $Nn_z\Lambda$ cannot be assigned to the single-particle states near a pseudocrossing, we denote the quantum numbers of the wave function of the upper level by ρ_a and those of the lower level by ρ_b. We therefore rewrite wave function (5.3) as

$$\Psi_i(K^\pi; \rho_1, \rho_2) = N_i(\rho_1, \rho_2)\frac{1}{\sqrt{2}}\sum_\sigma \left\{C^i_{\rho_a}\alpha^+_{\rho_a\sigma} + C^i_{\rho_b}\alpha^+_{\rho_b\sigma} + \sum_{\lambda\mu j}\sum_q D^{\lambda\mu ji}_{\rho_1\rho_2 q\sigma}\alpha^+_{q\sigma}Q^+_j(\lambda\mu)\right\}\Psi. \quad (5.4)$$

The normalization condition is

$$N_i^2(\rho_1, \rho_2)\left\{(C^i_{\rho_a})^2 + (C^i_{\rho_b})^2 + \frac{1}{2}\sum_{\lambda\mu j}\sum_{q\sigma}(D^{\lambda\mu ji}_{\rho_1\rho_2 q\sigma})^2\right\} = 1. \quad (5.5)$$

The secular equation giving the energies η_i of the ground and excited states of an odd nucleus has the form of Eq. (4.5).

The contribution to the normalization condition (5.5) of the single-quasiparticle components ρ_a and ρ_b is

$$\left.\begin{aligned}\mathcal{L}^2_{ai} &= (N_i(\rho_1, \rho_2)C^i_{\rho_a})^2;\\ \mathcal{L}^2_{bi} &= (N_i(\rho_1, \rho_2)C^i_{\rho_b})^2.\end{aligned}\right\} \quad (5.6)$$

According to (5.1) the wave function of the single-particle state consists of a sum of terms having different N values. We will take this circumstance into account in determining the contributions of terms having different N to normalization condition (5.5). From (5.2) and (5.6) we find that the contributions of the terms with N = 4 and N = 6 to the normalization of wave function (5.3) are

$$\left.\begin{aligned}P_{4i}(\rho_1, \rho_2) &= \mathcal{L}^2_{ai}d^2_4(\rho_a) + \mathcal{L}^2_{bi}d^2_4(\rho_b);\\ P_{6i}(\rho_1, \rho_2) &= \mathcal{L}^2_{ai}d^2_6(\rho_a) + \mathcal{L}^2_{bi}d^2_6(\rho_b).\end{aligned}\right\} \quad (5.7)$$

Since the quasiparticle–phonon interaction mixes single-particle states, this interaction cannot be responsible for a pronounced change in the distribution of the components with N and N ± 2 in odd nuclei in comparison with the single-particle model.

The quasiparticle–phonon interaction is taken into account in calculation of the energies and wave functions of the first and second nonrotational states in several deformed nuclei having an odd number of neutrons. The calculations are carried out for the A = 155 scheme for $\beta_{40} = 0.04$ and β_{20} in the range from 0.29 to 0.34. The calculated results are shown in Tables 5.2 and 5.3; these

TABLE 5.2. Mixing of the Components with N = 4 and N = 6 near a Pseudocrossing of the States 400↑ and 600↑ with $\beta_{40} = 0.04$

Nucleus	i	$\beta_{20} = 0.30$			$\beta_{20} = 0.31$			$\beta_{20} = 0.32$			$\beta_{20} = 0.33$		
		$\eta_i(1/2^+) - \eta_F$, keV	P_{4i}, %	P_{6i}, %	$\eta_i(1/2^+) - \eta_F$, keV	P_{4i}, %	P_{6i}, %	$\eta_i(1/2^+) - \eta_F$, keV	P_{4i}, %	P_{6i}, %	$\eta_i(1/2^+) - \eta_F$, keV	P_{4i}, %	P_{6i}, %
^{153}Sm	1	54	9	67	58	38	35	45	10	61	98	7	62
	2	736	73	6	325	42	34	338	74	6	432	81	3
^{155}Sm	1	401	8	68	447	41	35	454	15	61	496	5	51
	2	783	72	4	654	41	36	622	70	10	567	62	20
^{155}Gd	1	120	8	64	114	37	34	132	10	60	163	7	62
	2	342	67	4	259	41	33	280	73	6	257	80	3
^{157}Gd	1	480	8	68	498	40	33	436	29	44	437	75	4
	2	634	66	4	586	37	34	493	50	23	619	8	64
^{159}Gd	1	713	7	62	737	40	30	715	41	28	670	68	4
	2	894	63	4	866	33	34	796	32	36	806	8	60
^{161}Gd	1	812	5	38	817	32	18	725	56	4	690	60	2
	2	1052	54	3	922	23	28	878	6	37	844	4	42
^{157}Dy	1	201	15	62	131	35	32	123	9	56	185	7	56
	2	254	61	13	243	40	32	245	71	5	251	77	3
^{159}Dy	1	469	7	65	448	38	30	495	45	25	490	71	2
	2	516	59	5	520	33	32	540	28	39	530	6	61
^{161}Dy	1	624	45	23	539	37	26	453	63	2	365	66	1
	2	780	27	36	736	28	31	753	5	51	781	4	49
^{163}Dy	1	783	5	33	588	29	24	450	11	43	374	16	41
	2	1024	54	3	833	30	27	672	50	8	586	47	12

TABLE 5.3. Mixing of the Components with N = 4 and N = 6 near a Pseudocrossing of the States 402↓ and 651↑ with $\beta_{40} = 0.04$

Nucleus	i	$\beta_{20} = 0.30$			$\beta_{20} = 0.31$			$\beta_{20} = 0.32$			$\beta_{20} = 0.33$		
		$\eta_i(3/2^+) - \eta_F$, keV	P_{4i}, %	P_{6i}, %	$\eta_i(3/2^+) - \eta_F$, keV	P_{4i}, %	P_{6i}, %	$\eta_i(3/2^+) - \eta_F$, keV	P_{4i}, %	P_{6i}, %	$\eta_i(3/2^+) - \eta_F$, keV	P_{4i}, %	P_{6i}, %
^{153}Sm	1	46	6	64	6	22	62	10	35	48	46	15	65
	2	543	84	4	264	66	20	245	58	32	215	79	12
^{155}Sm	1	227	7	77	211	23	60	213	40	44	260	39	45
	2	618	79	4	541	66	20	476	51	36	376	54	34
^{155}Gd	1	31	8	79	0	24	60	0	35	47	8	16	64
	2	225	75	5	220	64	21	212	56	32	157	79	12
^{157}Gd	1	265	9	75	205	26	53	212	43	38	241	60	23
	2	527	72	6	480	58	25	436	45	40	447	29	53
^{159}Gd	1	471	7	67	415	24	50	317	41	33	468	58	28
	2	878	71	5	739	56	23	671	41	40	640	25	52
^{161}Gd	1	772	8	66	638	27	44	521	47	15	438	66	7
	2	981	67	6	934	50	27	900	29	50	747	11	62
^{157}Dy	1	98	11	78	75	29	53	51	40	40	85	23	54
	2	165	74	8	188	57	27	183	50	37	198	70	19
^{159}Dy	1	235	9	65	240	28	46	240	42	33	243	64	17
	2	441	69	8	420	52	27	397	40	40	390	23	56
^{161}Dy	1	556	27	51	491	42	33	422	56	18	343	74	3
	2	657	51	28	648	43	37	628	24	55	627	14	70
^{163}Dy	1	753	10	65	543	22	43	322	31	34	232	24	40
	2	976	64	8	845	50	22	680	40	29	431	47	21

tables show the first two roots (i = 1, 2) of the excitation energy and the contributions of single-quasiparticle components P_{4i} and P_{6i}.

To see how the quasiparticle–phonon interaction influences the mixing of the components with N = 4 and 6, we compare the results in Table 5.1 for $\beta_{40} = 0.04$ with those in Table 5.2, supplementing these results with data for $\beta_{20} = 0.29$ and 0.34. For a deformation parameter $\beta_{20} = 0.29$, the $\Delta N = \pm 2$ mixing is slight both in the single-particle model and in the model taking account of the quasiparticle–phonon interaction. An exceptional case is that of ^{161}Dy, for which with $\beta_{20} = 0.29$, we have $\eta_1(1/2^+) - \eta_F = 754$ keV, $P_{41} = 0.19$, and $P_{61} = 0.41$; $\eta_2(1/2^+) - \eta_F = 852$ keV, $P_{42} = 0.45$, and $P_{62} = 0.15$. For a deformation parameter $\beta_{20} = 0.30$, the $\Delta N = \pm 2$ mixing is slight in the single-particle model, slightly larger in the nuclei studied and large only for ^{161}Dy.

With $\beta_{20} = 0.31$, the $\Delta N = \pm 2$ mixing is pronounced in the single-particle model and in all the nuclei considered. With $\beta_{20} = 0.32$, the $\Delta N = \pm 2$ mixing in the single-particle model and in several of the nuclei is slight, although it is pronounced in ^{157}Gd, ^{159}Gd, and ^{159}Dy. With $\beta_{20} = 0.33$ this mixing is slight in the single-particle model and in most of the nuclei, but in, e.g., ^{163}Dy it remains large.

In those nuclei in which a pseudocrossing occurs near the Fermi surface we find the following features: For the first root with $\beta_{20} = 0.30$ the component P_{61} predominates; with $\beta_{20} = 0.31$ the values of P_{61} and P_{41} become approximately equal; with $\beta_{20} = 0.32$ the value of P_{61} is larger than P_{41}; with $\beta_{20} = 0.33$ component P_{61} predominates; and with $\beta_{20} = 0.34$ component P_{41} predominates. In other words, as β_{20} increases there is a mixing of the components with N = 4 and 6; this mixing eventually starts to fall off, and only then is there an exchange of large components between the two quasiintersecting levels. This behavior is due to the change in the position of the chemical potential with increasing β_{20}. This change occurs in ^{153,155}Sm, ^{155}Gd, and ^{167}Dy. With $\beta_{20} = 0.34$, e.g., in ^{155}Gd, we have $\eta_1(3/2^+) - \eta_F = 105$ keV, $P_{41} = 0.62$, $P_{61} = 0.27$; $\eta_2(3/2^+) - \eta_F = 158$ keV, $P_{42} = 0.34$, $P_{62} = 0.52$. In ^{157}Dy, we have $\eta_1(3/2^+) - \eta_F = 95$ keV, $P_{41} = 0.91$, $P_{61} = 0.03$; $\eta_2(3/2^+) - \eta_F = 208$ keV, $P_{42} = 0.06$, $P_{62} = 0.74$.

With the deformation parameter $\beta_{20} = 0.34$ the single-particle model predicts no strong $\Delta N = \pm 2$ mixing, but this mixing is appreciable in some of the nuclei calculated. In ^{163}Dy, e.g., we have $\eta_1(3/2^+) - \eta_F = 191$ keV, $P_{41} = 0.67$, $P_{61} = 0.04$, $\eta_2(3/2^+) - \eta_F = 420$ keV, $P_{42} = 0.08$, $P_{62} = 0.59$.

The quasiparticle–phonon interaction thus expands the range of β_{20} in which $\Delta N = \pm 2$ mixing occurs. Where the small component exceeds 1/10 the large component, the mixing range in the single-particle model is $\Delta\beta_{20} = 0.01$. When the quasiparticle–phonon interaction is taken into account, this range is $\Delta\beta_{20} = 0.03$, and even broader for some of the nuclei. If the range $\Delta\beta_{20}$ were extremely narrow, as in calculations based on the Nilsson potential neglecting quasiparticle–phonon interactions, the probability for experimentally observing $\Delta N = \pm 2$ mixing would be very low, since it is unlikely that the equilibrium nuclear deformation would fall in this narrow range.

The quasiparticle–phonon interaction complicates the state structure as the excitation energy is increased, reducing the net contribution of the two single-quasiparticle components. At an excitation energy of about 1 MeV, the $\Delta N = \pm 2$ mixing is still appreciable. The calculated relative values of the components with N = 4 and 6 agree satisfactorily with the experimental values for the following deformation parameters: For the $K^\pi = 1/2^+$ and $3/2^+$ states in ^{153}Sm, with $\beta_{20} = 0.310$; for these states in ^{155}Gd, with $\beta_{20} = 0.305$; for the $K^\pi = 1/2^+$ states in ^{159}Gd, with $\beta_{20} = 0.305$; for these states in ^{161}Dy, with $\beta_{20} = 0.305$; for these states in ^{163}Dy, with $\beta_{20} = 0.300$; for the $K^\pi = 3/2^+$ states in ^{157}Dy with $\beta_{20} = 0.315$; for these states in ^{159}Dy, with $\beta_{20} = 0.320$; for the states in ^{161}Dy, with $\beta_{20} = 0.315$; and for these states in ^{163}Dy, with $\beta_{20} = 0.335$. We thus find a correct description of the relative values of

the components P_{4i} and P_{6i} as deformation parameters β_{20} slightly larger than the equilibrium parameters for the neighboring even–even nuclei. With $\beta_{20} = 0.30$ for the $K^\pi = 3/2^+$ states in $^{159-161}$Dy, the calculated P_{41} and P_{61} values for the lower state give a good description of the observed components of the upper state, and vice versa.

The calculated energies of the first and second states $K^\pi = 1/2^+$ and $3/2^+$ are slightly lower than the experimental values. In some nuclei the difference is slight, while in others, e.g., ^{157}Gd and ^{159}Dy, it is appreciable. The calculated energy differences between the first and second $K^\pi = 3/2^+$ or $1/2^+$ describe quite well (within 10–40 keV) the corresponding experimental data. An exceptional case is found with the splitting energies in ^{153}Sm.

From this discussion we can draw the following conclusions regarding the mixing of 400↑, 660↑, and 402↑, 651↓ states in samarium, gadolinium, and dysprosium isotopes having an odd number of neutrons:

a) The N = 4 and 6 components of the wave functions of the Woods–Saxon potential are strongly mixed in a range $\Delta\beta_{20} = 0.01$ near a level pseudocrossing; this range is much broader than the range in which the Nilsson wave functions are mixed.

b) The mixing range $\Delta\beta_{20}$ increases slightly with increasing β_{40}.

c) By analyzing the behavior of the single-particle levels near their pseudocrossing we can refine the shape and parameters of the mean-field potential.

d) The quasiparticle–phonon interaction broadens the range of $\Delta N = \pm 2$ mixing to $\Delta\beta_{20} = 0.03$. This circumstance makes it possible to observe experimentally $\Delta N = \pm 2$ mixing.

e) The quasiparticle–phonon interaction results in values for the N = 4 and 6 components different from those of the single-particle model; in several nuclei the difference is large.

6. NONROTATIONAL STATES OF ODD-A DEFORMED NUCLEI

The behavior of the approximately single-quasiparticle nonrotational states of odd deformed nuclei is a direct reflection of the behavior of the energies of the single-particle states. We cannot directly compare the single-particle energies with experimental values, since the energies of the low-lying states are strongly influenced by pairing correlations of the superconducting type and by the quasiparticle–phonon interaction. This latter interaction causes a fragmentation of the single-particle states over many nuclear levels. The fragmentation becomes more pronounced with increasing excitation energy. The ground states are approximately single-quasiparticle

TABLE 6.1. ^{153}Sm

K^π	Energy, keV		Structure
	expt.	theor.	
3/2+	0	0	651↑ 62%; 402↓ 22%; 660↑ + Q_1(22) 2%
3/2−	35.8	57	521↑ 88%; 521↓ + Q_1(22) 5%; 633↑ + Q_1(32) 3%
1/2+	—	60	660↑ 40%; 400↑ 40%; 550↑ + Q_1(30) 2%
3/2+	320	260	402↓ 66%; 651↑ 20%; 400↑ + Q_1(22) 10%; 404↓ + Q_1(22) 3%
5/2+	195	290	642↑ 92%; 521↑ + Q_1(31) 2%
1/2+	412	330	400↑ 42%; 660↑ 34%; 402↓ + Q_1(22) 20%; 402↑ + Q_1(22) 3%
11/2−	94	100	505↑ 97%;
3/2−	127	540	532↓ 80%; 521↑ 3%; 530↑ + Q_1(22) 7%; 660↑ + Q_1(32) 2%
1/2−	—	560	530↑ 72%; 521↓ 3%; 532↓ + Q_1(22) 10%; 660↑ + Q_1(30) 5%
5/2−	322	570	523↓ 89%; 521↓ + Q_1(22) 6%; 642↑ + Q_1(30) 3%
1/2−	698	780	521↓ 52%; 530↑ 4%; 521↑ + Q_1(22) 25%; 523↓ + Q_1(22) 12%
7/2+	—	1040	633↑ 61%; 651↑ + Q_1(22) 18%; 521↑ + Q_1(32) 18%
5/2+	—	1250	402↑ 31%
1/2+	—	1280	660↑ + Q_1(20) 100%
3/2−	—	1300	521↑ + Q_1(20) 99%
5/2−	—	1350	512↑ 54%; 642↑ + Q_1(30) 21%; 523↓ + Q_1(20) 10%
7/2+	—	1390	404↓ 18%; 402↓ + Q_1(22) 78%; 651↑ + Q_1(22) 3%
11/2+	—	1440	615↑ 2%; 505↑ + Q_1(30) 97%
7/2−	—	1540	503↑ 4%; 505↑ + Q_1(22) 94%
1/2−	—	1560	660↑ + Q_1(30) 95%

TABLE 6.2. ^{155}Sm

K^π	Energy, keV		Structure
	exptl.	theor.	
3/2−	0	0	521↑ 93%; 521↓ + Q_1(22) 2%
5/2+	25	90	642↑ 94%; 523↓ + Q_1(30) 1%
3/2+	—	230	651↑ 77%; 402↓ 7%; 660↑ + Q_1(22) 2%
5/2−	338	310	523↓ 90%; 512↑ 2%; 521↓ + Q_1(22) 3%; 642↑ + Q_1(30) 2%
1/2+	—	400	660↑ 68%; 400↑ 8%; 651↑ + Q_1(22) 4%; 550↑ + Q_1(30) 2%
3/2+	—	620	402↓ 79%; 651↑ 4%; 400↑ + Q_1(22) 13%; 404↓ + Q_1(22) 3%
1/2+	—	780	400↑ 72%; 660↑ 4%; 402↓ + Q_1(22) 19%; 402↑ + Q_1(22) 4%
11/2−	—	460	505↑ 98%
1/2−	824	810	521↓ 66%; 530↑ 5%; 521↑ + Q_1(22) 15%; 523↓ + Q_1(22) 10%
7/2+	—	980	633↑ 81%; 521↑ + Q_1(32) 12%; 651↑ + Q_1(22) 2%
3/2−	—	990	532↓ 75%; 651↑ + Q_1(30) 13%; 530↑ + Q_1(22) 4%
1/2−	—	1000	530↑ 65%; 521↓ 5.5%; 660↑ + Q_1(30) 11%; 532↓ + Q_1(22) 5%
5/2−	—	1220	512↑ 45%; 523↓ 5%; 642↑ + Q_1(30) 42%; 510↑ + Q_1(22) 2%
5/2+	—	1500	523↓ + Q_1(30) 98%
11/2+	—	1560	615↑ 2%; 505↑ + Q_1(30) 98%

TABLE 6.3. ^{155}Gd

K^π	Energy, keV exptl.	Energy, keV theor.	Structure
3/2⁻	0	0	521 ↑ 89%; 521 ↓ + Q_1(22) 6%; 633 ↑ + Q_1(32) 2%
3/2⁺	105	30	651 ↑ 79%; 402 ↓ 8%; 660 ↑ + Q_1(22) 2%
11/2⁻	121	40	505 ↑ 98%
1/2⁺		120	660 ↑ 64%; 400 ↑ 8%; 651 ↑ + Q_1(22) 6%; 550 ↑ + Q_1(30) 5%
3/2⁺	269	225	402 ↓ 75%; 651 ↑ 5%; 400 ↑ + Q_1(22) 10%; 404 ↓ + Q_1(22) 3%
5/2⁺	85	250	642 ↑ 94%; 523 ↓ + Q_1(30) 1%
1/2⁺	368	342	400 ↑ 67%; 660 ↑ 4%; 402 ↓ + Q_1(22) 15%; 402 ↑ + Q_1(22) 4%
5/2⁻	321	450	523 ↓ 89%; 521 ↓ + Q_1(22) 7%
1/2⁻	560	620	521 ↓ 52%; 521 ↑ + Q_1(22) 31%; 523 ↓ + Q_1(22) 14%
3/2⁻		640	532 ↓ 84%; 530 ↑ + Q_1(22) 10%
1/2⁻	423	730	530 ↑ 76%; 532 ↓ + Q_1(22) 15%; 660 ↑ + Q_1(30) 3%
7/2⁺		1000	633 ↑ 50%; 651 ↑ + Q_1(22) 38%; 521 ↑ + Q_1(32) 10%
5/2⁺		1050	402 ↑ 29%; 400 ↑ + Q_1(22) 66%; 660 ↑ + Q_1(22) 2%
1/2⁺		1130	660 ↑ + Q_1(20) 100%;
3/2⁻		1170	521 ↑ + Q_1(20) 100%
7/2⁺	1297	1180	404 ↓ 18%; 402 ↓ + Q_1(22) 79%
3/2⁺		1280	402 ↓ + Q_1(20) 100%
5/2⁻		1300	512 ↑ 47%; 523 ↓ + Q_1(20) 33%; 642 ↑ + Q_1(30) 9%
5/2⁺		1310	642 ↑ + Q_1(20) 100%;
1/2⁺		1320	651 ↑ + Q_1(22) 100 %
7/2⁻		1325	504 ↓ 4%; 505 ↑ + Q_1(22) 94%
7/2⁺		1490	633 ↑ 24%; 511 ↑ + Q_1(22) 61%; 521 ↑ + Q_1(32) 13%
1/2⁻		1500	530 ↑ + Q_1(20) 100%

TABLE 6.4. ^{157}Gd

K^π	Energy, keV exptl.	Energy, keV theor.	Structure
3/2⁻	0	0	521 ↑ 92%; 521 ↓ + Q_1(22) 4%
5/2⁺	64	140	642 ↑ 95%
3/2⁺	—	270	651 ↑ 75%; 402 ↓ 9%; 660 ↑ + Q_1(22) 4%
5/2⁻	435	270	523 ↓ 88%; 512 ↑ 1.6%; 521 ↓ + Q_1(22) 6%
3/2⁺	475	530	402 ↓ 72%; 651 ↑ 6%; 400 ↑ + Q_1(22) 10%; 404 ↓ + Q_1(22) 4%
1/2⁺	684	630	400 ↑ 66%; 660 ↑ 4%; 402 ↓ + Q_1(22) 20%; 402 ↑ + Q_1(22) 6%
1/2⁺	—	480	660 ↑ 68%; 400 ↑ 8%; 651 ↑ + Q_1(22) 9%; 550 ↑ + Q_1(30) 1%
1/2⁻	704	570	521 ↓ 60%; 530 ↑ 2.3%; 521 ↑ + Q_1(22) 21%; 523 ↓ + Q_1(22) 14%
1/2⁻	—	720	530 ↑ 63%; 521 ↓ 2.4%; 532 ↓ + Q_1(22) 13%; 651 ↑ + Q_1(31) 6%
11/2⁻	426	490	505 ↑ 98%
3/2⁻	700	1020	532 ↓ 81%; 530 ↑ + Q_1(22) 9%; 651 ↑ + Q_1(30) 6%
7/2⁺	—	1030	633 ↑ 79%; 521 ↑ + Q_1(32) 10%; 651 ↑ + Q_1(22) 6%
5/2⁻	—	1250	512 ↑ 65%; 523 ↓ 1.7%; 523 ↓ + Q_1(20) 13%; 642 ↑ + Q_1(30) 7%
3/2⁻	—	1450	521 ↑ + Q_1(20) 100%
5/2⁺	—	1500	402 ↑ 28%; 400 ↑ + Q_1(22) 56%; 521 ↑ + Q_1(31) 10%
7/2⁻	—	1520	523 ↑ 2%; 521 ↑ + Q_1(22) 97%
9/2⁺	—	1550	624 ↑ 9%; 642 ↑ + Q_1(22) 90%
7/2⁺	1825	1590	404 ↓ 14%; 402 ↓ + Q_1(22) 52%; 651 ↑ + Q_1(22) 32%
7/2⁺	—	1660	404 ↓ 5%; 651 ↑ + Q_1(22) 68%; 402 ↓ + Q_1(22) 26%

states; fragmentation begins to appear at an excitation energy of 0.5 MeV. At higher energies the fragmentation of the individual single-particle states is important. To assess the validity of these schemes of single-particle levels, the energies and structures calculated for the nonrotational states taking account of the quasiparticle–phonon interaction must be compared with the corresponding experimental data. We turn now to this comparison.

The calculated results and the corresponding experimental data, taken from reviews[27,36] and original papers,[37] are shown in Tables 6.1-6.57. The first column of a table shows the K^π value; this is followed by the experimental and calculated energies of the ground rotational bands; the last column shows the state structure calculated from the wave function normalization condition. In Table 6.2, e.g., we see the nonrotational states of ^{155}Sm. The ground state has $K^\pi = 3/2^-$ and a a structure consisting of a single-quasiparticle component 521 ↑ (93%) and a quasiparticle component 521 ↓ plus the first root of the γ-vibrational phonon $Q_1(22)$ (2%); none of the other components contributes more than 1%. We denote the phonons by $Q_j(\lambda\mu)$, where j indicates the root of Eq. (1.20). Two single-quasiparticle components contribute to some of the states; where the magnitude of the smallest component is greater than 1%, it is shown in the table. In Table 6.2, e.g., the $K^\pi = 5/2^-$ state with an energy of 338 keV is calculated to have an energy of 310 keV and a structure consisting of a single-quasiparticle component 523 ↓ (90%), a single-quasiparticle component 512 ↑ (2%), a component 521 ↓ + Q_1(22) (3%), and a component 642 ↑ + Q_1(30) (2%). The tables show all the single-quasiparticle components greater than 1%, as well as all the nonrotational states up to an excitation energy of 1.3-1.5 MeV and several of the higher-lying states. Some of the tables show the three-quasiparticle states with large K^π. The three-quasiparticle states in odd deformed nuclei were analyzed previously.[38]

As was mentioned above, we have classified the nuclei in the range $150 < A < 190$ into four subranges, carrying out calculations within each subrange for fixed values of β_{20} and β_{40}. Exceptional cases are those states for which we have $\beta_{20}^{e} \neq \beta_{20}^{0}$ and $\beta_{40}^{e} \neq \beta_{40}^{0}$; these inequalities are taken into account for the states n505 ↑, n503 ↑, p541 ↓, p404 ↓, and p402 ↑.

The nuclei are classified into subranges in the following manner:

1) The subrange A = 155, with $\beta_{20}^{0} = 0.29$, $\beta_{40}^{0} = 0.06$, including samarium, gadolinium, europium, and terbium isotopes as well as ^{159}Dy, ^{161}Dy, ^{159}Ho, and ^{161}Ho.

2) The subrange A = 165, with $\beta_{20}^{0} = 0.28$, $\beta_{40}^{0} = 0.02$, consisting of the other dysprosium and holmium isotopes, the thallium isotopes and ^{163}Er, ^{165}Er, ^{167}Er, ^{169}Er, and ^{167}Yb.

TABLE 6.5. ^{159}Gd

K^π	Energy, keV exptl.	Energy, keV theor.	Structure
3/2⁻	0	0	521↑ 93%; 521↓+Q_1(22) 3%
5/2+	68	−70	642↑ 95%; 660↑+Q_1(22) 1%
5/2⁻	146	40	523↓ 92%; 512↑ 1.4%; 521↓+Q_1(22) 4%
3/2⁻	—	470	651↑ 67%; 402↓ 7%; 660↑+Q_1(22) 6%; 521↑+Q_1(20) 3%
1/2+	780	710	660↑ 62%; 400↑ 7%; 651↑+Q_1(22) 12%; 642↑+Q_1(22) 6%
1/2⁻	506	490	521↓ 74%; 523↓+Q_1(22) 14%; 521↑+Q_1(22) 10%
3/2+	743	870	402↓ 71%; 651↑ 5%; 400↑+Q_1(22) 21%; 404↓+Q_1(22) 4%
1/2+	973	890	400↑ 63%; 660↑ 4%; 402↓+Q_1(22) 28%; 402↑+Q_1(22) 5%
7/2+	—	740	633↑ 92%; 521↑+Q_1(32) 4%
5/2⁻	875	920	512↑ 73%; 523↓ 2.4%; 642↑+Q_1(30) 9%; 510↑+Q_1(22) 6%
11/2⁻	681	820	505↑ 99%
1/2⁻	—	1150	530↑ 58%; 660↑+Q_1(30) 12%; 532↓+Q_1(22) 10%
3/2⁻	1109	1200	532↓ 60%; 651↑+Q_1(30) 27%; 530↑+Q_1(22) 6%
5/2+	—	1330	523↓+Q_1(30) 98%
9/2+	—	1340	624↑ 9%; 642↑+Q_1(22) 89%
1/2⁻	—	1410	510↑ 2%; 521↑+Q_1(22) 75%; 523↓+Q_1(22) 10%
7/2⁻	—	1420	521↑+Q_1(22) 100%
3/2⁻	—	1430	521↑+Q_1(20) 95%
1/2⁻	—	1440	510↑ 7%; 523↓+Q_1(22) 61%; 521↑+Q_1(22) 15%
9/2⁻	—	1470	523↓+Q_1(22) 100%
7/2+	—	1570	404↓ 1%; 523↓+Q_1(31) 97%
1/2⁻	1602	1640	510↑ 35%; 512↑+Q_1(22) 34%; 523↓+Q_1(22) 10%
11/2+	—	1820	615↑ 2%; 505↑+Q_1(30) 97%
7/2+	—	1840	404↓ 2%; 651↑+Q_1(22) 91%; 402↓+Q_1(22) 6%
7/2+	1960	1850	404↓ 15%; 402↓+Q_1(22) 74%; 651↑+Q_1(22) 9%

TABLE 6.6. ^{161}Gd

K^π	Energy, keV exptl.	Energy, keV theor.	Structure
5/2⁻	0	0	523↓ 94%; 512↑ 1.4%; 521↓+Q_1(22) 3%
5/2+	—	90	642↑ 95% 660↑+Q_1(22) 3%
1/2⁻	356	290	521↓ 89% 523↓+Q_1(22) 8%
3/2⁻	313	300	521↑ 96%
7/2+	—	420	633↑ 98%
3/2+	—	770	651↑ 66%; 402↓ 8%; 660↑+Q_1(22) 12%
5/2⁻	809	610	512↑ 84%; 523↓ 2.5%; 510↑+Q_1(22) 8%; 521↓+Q_1(22) 2%
1/2+	—	810	660↑ 38%; 400↑ 5%; 642↑+Q_1(22) 29%; 651↑+Q_1(22) 12%
3/2+	—	980	402↓ 67%; 651↑ 6%; 400↑+Q_1(22) 25%; 404↓+Q_1(22) 3%
1/2+	—	1050	400↑ 54%; 660↑ 3%; 402↓+Q_1(22) 33%; 402↑+Q_1(22) 5%
1/2⁻	—	1060	510↑ 7%; 523↓+Q_1(22) 85%; 512↑+Q_1(22) 7%
9/2⁻	—	1070	523↓+Q_1(22) 100%
9/2+	—	1090	624↑ 6%; 642↑+Q_1(22) 93%
1/2⁻	1309	1220	510↑ 27%; 512↑+Q_1(22) 38%; 521↑+Q_1(22) 16%
7/2⁻	—	1240	521↑+Q_1(22) 100%
3/2⁻	—	1450	512↓ 3%; 521↓+Q_1(22) 52%; 521↑+Q_1(20) 44%
11/2⁻	—	1140	505↑ 99%
11/2+	—	1530	615↑ 1%; 633↑+Q_1(22) 99%

3) The subrange A = 173 with $\beta_{20}^0 = 0.26$, $\beta_{40}^0 = -0.02$, consisting of ^{169}Yb, ^{171}Yb, ^{173}Yb, ^{175}Yb, ^{173}Hf, ^{175}Hf, ^{169}Lu, ^{171}Lu, ^{173}Lu, and ^{177}Ta.

4) The subrange A = 181 with $\beta_{20}^0 = 0.26$, $\beta_{40}^0 = -0.03$, consisting of ^{177}Yb, ^{177}Hf, ^{179}Hf, ^{177}Lu, ^{179}Ta, and ^{181}Ta; with the parameter values $\beta_{20}^0 = 0.24$, $\beta_{40}^0 = -0.03$, ^{181}Hf, ^{179}W, ^{181}W, ^{183}W, and ^{181}Re; and with the parameter values $\beta_{20}^0 = 0.21$, $\beta_{40}^0 = -0.03$, ^{185}W, ^{183}Os, ^{185}Os, ^{183}Re, and ^{185}Re.

For the nuclei at boundaries of two subranges, e.g., ^{161}Dy, ^{161}Ho, and ^{169}Lu, calculations were carried out on the basis of two level schemes. Comparison of the results showed some differences in the energies and structures of the nonrotational states. Additional subranges should be introduced for a more accurate calculation of the nuclear levels. The results shown in the tables for these nuclei were obtained by the schemes used to calculate most of the isotopes.

The energies and structures of the 400↑, 600↑ and 651↑, 402↓ states were calculated taking account of the influence of $\Delta N = \pm 2$ mixing for the nuclei of subrange A = 155 with $\beta_{20}^0 = 0.29$–0.30 and $\beta_{40}^0 = 0.04$–0.06. We see from Table 5.4 that there is a pronounced mixing of these states in most of the nuclei at slightly larger values of β_{20}.

As was mentioned in Sec. 4, we neglected the Coriolis interaction in these calculations, since it generally has only a slight effect on the energies and structures of the lower parts of the rotational bands. Using the wave functions found, we can take the Coriolis interaction into account; this influence is greatest in states deriving from the $i_{13/2}$ neutron subshell and the $h_{11/2}$ proton subshell.

In several cases it is desirable to improve the description for the energies of nonrotational states. However, slight changes in the parameters of the Woods–Saxon potential do not result in this improvement. For this reason modifications of the mean-field potential are of interest.

Several excited states have an important admixture of a quasiparticle component plus a γ-vibrational phonon.

TABLE 6.7. ^{159}Dy

K^π	Energy, keV exptl.	Energy, keV theor.	Structure
3/2⁻	0	0	521 ↑ 91%; 521 ↓ + Q_1(22) 5%
5/2⁺	178	197	642 ↑ 97%
3/2⁺	549	240	651 ↑ 65%; 660 ↑ + Q_1(22) 7%
5/2⁻	310	290	523 ↓ 91%; 521 ↓ + Q_1(22) 7%
3/2⁺	418	440	402 ↓ 69%; 400 ↑ + Q_1(22) 20%; 404 ↓ + Q_1(22) 1%; 651 ↑ 8%
1/2⁺	560	520	400 ↑ 59%; 402 ↓ + Q_1(22) 29%; 402 ↑ + Q_1(22) 6%; 660 ↑ 5%
1/2⁺	—	500	660 ↑ 65%; 651 ↑ + Q_1(22) 16%; 400 ↑ + Q_1(20) 1%; 400 ↑ 7%
1/2⁻	534	530	521 ↓ 55%; 521 ↑ + Q_1(22) 27%; 523 ↓ + Q_1(22) 17%
11/2⁻	352	470	505 ↑ 99%
7/2⁺	—	1000	633 ↑ 64%; 521 ↑ + Q_1(32) 21%; 651 ↑ + Q_1(22) 13%
3/2⁻	627	1040	532 ↓ 80%; 530 ↑ + Q_1(22) 13%; 660 ↑ + Q_1(32) 3%
1/2⁻	—	1100	530 ↑ 66%; 532 ↓ + Q_1(22) 20%; 651 ↑ + Q_1(32) 4%
5/2⁻	—	1200	512 ↑ 64%; 523 ↓ + Q_1(20) 22%; 510 ↑ + Q_1(22) 7%
7/2⁻	—	1270	523 ↑ 2%; 521 ↑ + Q_1(22) 97%
1/2⁻	—	1315	521 ↑ + Q_1(22) 100%
9/2⁺	—	1320	624 ↑ 5%; 642 ↑ + Q_1(22) 94%
5/2⁺	—	1340	402 ↑ 26%; 400 ↑ + Q_1(22) 68%; 660 ↑ + Q_1(22) 4%
3/2⁻	—	1350	521 ↑ + Q_1(20) 100%
7/2⁺	—	1360	404 ↓ 7%; 651 ↑ + Q_1(22) 63%; 402 ↓ + Q_1(22) 29%
1/2⁻	—	1500	510 ↑ 3%; 523 ↓ + Q_1(22) 93%; 512 ↑ + Q_1(22) 2%
9/2⁻	—	1520	523 ↓ + Q_1(22) 99%

TABLE 6.8. ^{161}Dy

K^π	Energy, keV exptl.	Energy, keV theor.	Structure
5/2⁺	0	0	642 ↑ 96%, 660 ↑ + Q_1(22) 2%
3/2⁻	75	20	521 ↑ 94%, 521 ↓ + Q_1(22) 3%
5/2⁻	27	28	523 ↓ 93%, 521 ↓ + Q_1(22) 5%
3/2⁺	679	560	651 ↑ 51%, 402 ↓ 27%, 660 ↑ + Q_1(22) 10%
1/2⁻	370	400	521 ↓ 66%, 523 ↓ + Q_1(22) 19%, 521 ↑ + Q_1(22) 14%
1/2⁺	608	780	660 ↑ 36%, 400 ↑ 27%, 651 ↑ + Q_1(22) 20%, 642 ↑ + Q_1(22) 14%
3/2⁺	551	660	402 ↓ 51%, 651 ↑ 28%, 400 ↑ + Q_1(22) 14%, 404 ↓ + Q_1(22) 3%
1/2⁺	774	620	400 ↑ 45%, 660 ↑ 23%, 402 ↓ + Q_1(22) 30%, 402 ↑ + Q_1(22) 2%
7/2⁺	—	760	633 ↑ 91%, 521 ↑ + Q_1(32) 5%
5/2⁻	—	950	512 ↑ 80%, 523 ↓ 2%, 510 ↑ + Q_1(22) 9%, 521 ↓ + Q_1(22) 3%
11/2⁻	486	760	505 ↑ 99%,
9/2⁺	—	1120	624 ↑ 5%, 642 ↑ + Q_1(22) 94%
1/2⁻	—	1130	530 ↑ 4%, 521 ↑ + Q_1(22) 92%
7/2⁻	—	1180	521 ↑ + Q_1(22) 99%
1/2⁻	—	1214	510 ↑ 3%, 523 ↓ + Q_1(22) 93%, 512 ↑ + Q_1(22) 2%
9/2⁻	—	1230	523 ↓ + Q_1(22) 100%
3/2⁻	—	1300	532 ↓ 75%, 530 ↑ + Q_1(22) 14%, 642 ↑ + Q_1(31) 3%
5/2⁺	—	1450	402 ↑ 7%, 521 ↑ + Q_1(31) 79%, 400 ↑ + Q_1(22) 12%
1/2⁻	—	1460	510 ↑ 5%, 642 ↑ + Q_1(32) 86%, 512 ↑ + Q_1(22) 6%
3/2⁻	—	1470	512 ↓ 0.4%, 521 ↑ + Q_1(20) 99%
7/2⁺	—	1480	521 ↑ + Q_1(32) 100%
7/2⁺	1416	1490	404 ↓ 2.4%, 651 ↑ + Q_1(22) 82%, 523 ↓ + Q_1(31) 8%
3/2⁻	—	1500	642 ↑ + Q_1(31) 100%
3/2⁻	1977	1840	512 ↓ 4%, 521 ↓ + Q_1(22) 93%

These states are characterized by large values of the reduced probabilities for E2 transitions. The B(E2) values were calculated in refs. 22 and 23 from the equation derived in ref. 1, with an effective charge of $e_{eff} = 0.2$. There is relatively little experimental information available on the B(E2) values in odd nuclei. In certain cases in which experimental values of B(E2) are available, we find quite good agreement with the calculated values. In ^{187}Re, e.g., the experimental value of $B(E2)_{s.p.u}$ for the $9/2^+$ state with an energy of 840 keV is 2.5, that for the $1/2^+$ state at 511 keV is 3.8, that in ^{185}Re for the $9/2^+$ at 966 keV is 2.6, and that for the $1/2^+$ state in this nucleus, at 645 keV, is 3.6. In all four cases theory yields B(E2) values approximately equal to the experimental values.

In conclusion we will summarize the agreement between the calculated and experimental data on the low-lying nonrotational states of odd deformed nuclei. The calculated energies agree quite well with the experimental energies, although in some cases there are differences of 300 keV or more. The theory is thus not completely satisfactory for predicting the positions of excited states.

Taking into account the complexity of solving the nuclear many-body problem through the use of a small number of parameters determined from the large store of experimental information available, we can conclude that important progress has been made in describing the structures of the low-lying states.

It should be noted that in each particular nucleus we can obtain more accurate predictions regarding the behavior of the low-lying states by refining the parameters of the Woods–Saxon potential, the parameters $\varkappa^{(\lambda)}$, etc. However, these results will not be of such fundamental nature.

In conclusion the authors thank A. A. Korneichuk, L. A. Malov, U. M. Fainer, and N. U. Shirikova for assistance in writing the programs and for useful discussions.

TABLE 6.9. ^{163}Dy

K^π	Energy, keV exptl.	Energy, keV theor.	Structure
11/2⁻	495	910	505 ↑ 98%
3/2+	859	980	402 ↓ 64%, 651 ↑ 8%, 400 ↑ + Q_1(22) 20%
9/2⁻		990	523 ↓ + Q_1(22) 100%
1/2+		1020	400 ↑ 54%, 660 ↑ 3%, 402 ↓ + Q_1(22) 30%
1/2⁻		1020	510 ↑ 3% 523 ↓ + Q_1(22) 89%, 512 ↑ + Q_1(22) 7%
1/2⁻		1140	530 ↑ 15%, 521 ↑ + Q_1(22) 51%, 642 ↑ + Q_1(32) 28%
7/2⁻		1160	521 ↑ + Q_1(22) 100%
9/2+		1200	624 ↑ 26%, 523 ↓ + Q_1(32) 42%, ↓ 642 + Q_1(22) 26%
11/2+		1220	615 ↑ 2%, 633 ↑ + Q_1(22) 98%
5/2⁻		1240	523 ↓ + Q_1(20) 100%
7/2⁻	1448	1270	514 ↓ 78%, 633 ↑ + Q_1(30) 11%, 512 ↓ + Q_1(22) 8%
3/2⁻		1275	532 ↓ 58%, 521 ↑ + Q_1(20) 13%, 530 ↑ + Q_1(22) 11%
9/2⁻		1280	642 ↑ + Q_1(32) 100%
3/2⁻	1795	1300	512 ↓ 16%, 521 ↓ + Q_1(22) 67%, 514 ↓ + Q_1(22) 7%
3/2⁻		1400	521 ↑ + Q_1(20) 87%, 521 ↓ + Q_1(22) 10%
5/2⁻		1410	521 ↓ + Q_1(22) 50%, 642 ↑ + Q_1(30) 49%
7/2+		1420	521 ↑ + Q_1(32) 100%
1/2+		1420	521 ↑ + Q_1(32) 100%

TABLE 6.10. ^{165}Dy

K^π	Energy, keV exptl.	Energy, keV theor.	Structure
7/2+	0	0	633 ↑ 96%
5/2⁻	184	50	512 ↑ 84%, 510 ↑ + Q_1(22) 8%, 624 ↑ + Q_1(32) 4%
1/2⁻	108	130	521 ↓ 97%,
5/2+		330	642 ↑ 89%, 660 ↑ + Q_1(22) 7%
5/2⁻	534	400	523 ↓ 97%
1/2⁻	570	520	510 ↑ 38%, 512 ↑ + Q_1(22) 54%, 512 ↓ + Q_1(22) 5%
1/2+		600	660 ↑ 49%, 642 ↑ + Q_1(22) 33%, 651 ↑ + Q_1(22) 14%
3/2⁻	574	630	521 ↑ 82%, 521 ↓ + Q_1(22) 8%, 633 ↑ + Q_1(32) 4%
3/2+		670	651 ↑ 66%, 633 ↑ + Q_1(22) 16%, 660 ↑ + Q_1(22) 13%
9/2+		710	624 ↑ 73%, 512 ↑ + Q_1(32) 21%, 642 ↑ + Q_1(22) 3%
11/2+		970	615 ↑ 2%, 633 ↑ + Q_1(22) 98%
3/2⁻	1258	1000	512 ↓ 19%, 521 ↓ + Q_1(22) 62%, 514 ↓ + Q_1(22) 10%
7/2⁻		1010	514 ↓ 87%, 512 ↓ + Q_1(22) 10%
1/2⁻		1050	523 ↓ + Q_1(22) 100%
9/2⁻		1050	523 ↓ + Q_1(22) 100%
3/2⁻		1070	521 ↓ + Q_1(22) 92%
5/2⁻		1070	521 ↓ + Q_1(22) 100%
1/2+		1120	400 ↑ 46%, 402 ↓ + Q_1(22) 29%, 642 ↑ + Q_1(22) 9%
3/2+		1150	402 ↓ 64%, 400 ↑ + Q_1(22) 28%, 404 ↓ + Q_1(22) 4%
3/2⁻		1170	512 ↓ 12%, 633 ↑ + Q_1(32) 46%, 521 ↓ + Q_1(22) 27%
9/2+		1180	642 ↑ + Q_1(22) 97%
11/2⁻		1200	633 ↑ + Q_1(32) 100%
1/2⁻		1240	530 ↑ 14%, 642 ↑ + Q_1(32) 80%, 532 ↓ + Q_1(22) 2%
5/2+		1290	521 ↓ + Q_1(32) 100%
9/2⁻		1350	642 ↑ + Q_1(32) 50%, 512 ↑ + Q_1(22) 48%
7/2⁻		1390	521 ↑ + Q_1(22) 100%
1/2⁻		1390	521 ↑ + Q_1(22) 100%

TABLE 6.11. ^{163}Er

K^π	Energy, keV		Structure
	exptl.	theor.	
5/2−	0	0	523 ↓ 93%
5/2+	69	−30	642 ↑ 94%
3/2−	104	20	521 ↑ 92%, $521\downarrow+Q_1(22)$ 3%,
3/2+		130	651 ↑ 87%, $660\uparrow+Q_1(22)$ 7%,
1/2+		260	660 ↑ 78%, $651\uparrow+Q_1(22)$ 12%, $642\uparrow+Q_1(22)$ 4%
1/2−	346	400	521 ↓ 68%, 510 ↑ 2%, $523\downarrow+Q_1(22)$ 18%, $521\uparrow+Q_1(22)$ 10%
7/2+		430	633 ↑ 92%, $521\uparrow+Q_1(32)$ 3%
5/2−	609	480	512 ↑ 79%, $510\uparrow+Q_1(22)$ 7%, $624\uparrow+Q_1(32)$ 6%
3/2+	464	490	402 ↓ 70%, $400\uparrow+Q_1(22)$ 25%, $404\downarrow+Q_1(22)$ 4%
1/2+	541	500	400 ↑ 61%, $402\downarrow+Q_1(22)$ 31%, $402\uparrow+Q_1(22)$ 6%
11/2−	444	900	505 ↑ 99%
1/2−		950	530 ↑ 60%, $532\downarrow+Q_1(22)$ 13%, $642\uparrow+Q_1(32)$ 10%
3/2−		960	532 ↓ 73%, $530\uparrow+Q_1(22)$ 11%, $660\uparrow+Q_1(32)$ 5%
9/2+		970	624 ↑ 30%, $642\uparrow+Q_1(22)$ 61%, $512\uparrow+Q_1(32)$ 6%
1/2−	1074	1090	510 ↑ 22%, 521 ↓ 1%, $523\downarrow+Q_1(22)$ 46%, $512\uparrow+Q_1(22)$ 23%
1/2−		1140	541 ↓ 2%, $521\uparrow+Q_1(22)$ 73%, $523\downarrow+Q_1(22)$ 23%
1/2+		1150	$642\uparrow+Q_1(22)$ 100%
7/2−		1170	$521\uparrow+Q_1(22)$ 100%
1/2−		1175	$521\uparrow+Q_1(22)$ 100%
7/2−		1180	$521\uparrow+Q_1(22)$ 100%
9/2−		1185	$523\downarrow+Q_1(22)$ 100%
7/2+		1300	$651\uparrow+Q_1(22)$ 100%
5/2+		1330	$521\uparrow+Q_1(31)$ 41%, $400\uparrow+Q_1(22)$ 34%
3/2−		1340	512 ↓ 1%, $521\uparrow+Q_1(20)$ 98%
5/2−		1380	512 ↑ 1%, $523\downarrow+Q_1(20)$ 98%
9/2+		1390	642 ↑ 34%, $642\uparrow+Q_1(22)$ 37%, $523\downarrow+Q_1(22)$ 16%
7/2−		1510	514 ↓ 22%, $642\uparrow+Q_1(31)$ 73%

TABLE 6.12. ^{165}Er

K^π	Energy, keV		Structure
	exptl.	theor.	
5/2−	0	0	523 ↓ 95%
5/2+	47	10	642 ↑ 92%, $660\uparrow+Q_1(22)$ 5%
7/2+	117	190	633 ↑ 98%
5/2−	477	210	512 ↑ 84%, $510\uparrow+Q_1(22)$ 9%, $624\uparrow+Q_1(32)$ 4%
1/2−	297	270	521 ↓ 86%, 510 ↑ 1%, $523\downarrow+Q_1(22)$ 10%
3/2−	243	280	521 ↑ 95%
3/2+		350	651 ↑ 82%, $660\uparrow+Q_1(22)$ 14%
1/2+	507	360	660 ↑ 60%, 400 ↑ 1%, $642\uparrow+Q_1(22)$ 19%, $651\uparrow+Q_1(22)$ 16%
3/2+	534	670	402 ↓ 68%, $400\uparrow+Q_1(22)$ 27%, $404\downarrow+Q_1(22)$ 4%
1/2+	746	680	400 ↑ 58%, 660 ↑ 1%, $402\downarrow+Q_1(22)$ 34%, $402\uparrow+Q_1(22)$ 5%
1/2−	920	760	510 ↑ 35%, 521 ↓ 3%, $512\uparrow+Q_1(22)$ 47%, $523\downarrow+Q_1(22)$ 8%
9/2+		850	624 ↑ 41%, $642\uparrow+Q_1(22)$ 50%, $512\uparrow+Q_1(32)$ 7%
9/2−		980	$523\downarrow+Q_1(22)$ 100%
1/2−		1000	510 ↑ 2%, 530 ↑ 3%, $523\downarrow+Q_1(22)$ 90%, $512\uparrow+Q_1(22)$ 3%
1/2−		1140	530 ↑ 8%, $521\uparrow+Q_1(22)$ 84%, $642\uparrow+Q_1(32)$ 5%
7/2−		1150	$521\uparrow+Q_1(22)$ 100%
9/2+		1170	624 ↑ 36%, $642\uparrow+Q_1(22)$ 50%, $512\uparrow+Q_1(32)$ 7%
11/2+		1200	615 ↑ 2%, $633\uparrow+Q_1(22)$ 97%
3/2+		1230	$633\uparrow+Q_1(22)$ 100%
11/2−	591	1360	505 ↑ 99%
3/2−		1270	512 ↓ 19%, 532 ↓ 5%, $521\downarrow+Q_1(22)$ 56%, $514\downarrow+Q_1(22)$ 9%
7/2−	1177	1290	514 ↓ 84%, $512\downarrow+Q_1(22)$ 10%, $633\uparrow+Q_1(30)$ 3%
3/2−		1300	532 ↓ 61%, $521\downarrow+Q_1(22)$ 14%, $530\uparrow+Q_1(22)$ 13%
5/2−		1360	$523\downarrow+Q_1(20)$ 60%, $521\downarrow+Q_1(22)$ 39%
7/2+		1370	$633\uparrow+Q_1(20)$ 100%
3/2−	1474	1500	512 ↓ 22%, $521\downarrow+Q_1(22)$ 30%, $521\uparrow+Q_1(20)$ 20%

TABLE 6.13. ^{167}Er

K^π	Energy, keV exptl.	Energy, keV theor.	Structure
7/2+	0	0	633 ↑ 97%
1/2−	208	120	521 ↓ 97%
5/2−	347	150	512 ↑ 66%, 523 ↓ 24%, 510 ↑ + Q_1(22) 7%
5/2+	812	330	642 ↑ 90%, 660 ↑ + Q_1(22) 7%
5/2−	668	340	523 ↓ 72%, 512 ↑ 22%, 642 ↑ + Q_1(30) 1%
1/2−	763	550	510 ↑ 38%, 512 ↑ + Q_1(22) 54%, 512 ↑ + Q_1(22) 5%
1/2+		590	660 ↑ 50%, 642 ↑ + Q_1(22) 33%, 651 ↑ + Q_1(22) 14%
3/2+	532	650	651 ↑ 68%, 633 ↑ + Q_1(22) 15%, 660 ↓ + Q_1(22) 12%
3/2−	753	660	521 ↑ 85%, 521 ↓ + Q_1(22) 9%
9/2+		800	624 ↑ 82%, 512 ↑ + Q_1(32) 11%, 642 ↑ + Q_1(22) 5%
11/2+		970	615 ↑ 1%, 633 ↑ + Q_1(22) 98%
7/2−	1049	990	514 ↓ 86%, 512 ↓ + Q_1(22) 9%
3/2+		1000	633 ↑ + Q_1(22) 100%
3/2−		1010	512 ↓ 16%, 521 ↓ + Q_1(22) 70%, 514 ↓ + Q_1(22) 8%
1/2−		1050	523 ↓ + Q_1(22) 100%
9/2−		1050	523 ↓ + Q_1(22) 100%
3/2+		1055	651 ↑ 11%, 633 ↑ + Q_1(22) 84%, 660 ↑ + Q_1(22) 4%
5/2−		1070	521 ↓ + Q_1(22) 100%
3/2−		1070	521 ↓ + Q_1(22) 100%
1/2+	1135	1150	400 ↑ 28%, 642 ↑ + Q_1(22) 50%, 402 ↓ + Q_1(22) 18%
3/2+	1086	1170	402 ↓ 66%, 400 ↑ + Q_1(22) 29%, 404 ↓ + Q_1(22) 4%
1/2+		1180	400 ↑ 27%, 642 ↑ + Q_1(22) 50%, 402 ↓ + Q_1(22) 18%
9/2+		1185	624 ↑ 3%, 642 ↑ + Q_1(22) 95%
3/2−	1384	1220	512 ↓ 32%, 521 ↓ + Q_1(22) 29%, 514 ↓ + Q_1(22) 25%
9/2−		1370	512 ↑ + Q_1(22) 100%
1/2−		1380	521 ↑ + Q_1(22) 100%
7/2−		1400	521 ↑ + Q_1(22) 100%

TABLE 6.14. ^{169}Er

K^π	Energy, keV exptl.	Energy, keV theor.	Structure
1/2−	0	0	521 ↓ 90%, 523 ↓ + Q_1(22) 4%, 521 ↑ + Q_1(22) 4%
5/2−	92.2	220	512 ↑ 86%, 510 ↑ + Q_1(22) 10%, 624 ↑ + Q_1(32) 2%
7/2+	243.7	250	633 ↑ 94%, 651 ↑ + Q_1(22) 2%
1/2−	565	610	510 ↑ 43%, 521 ↓ 1%, 512 ↑ + Q_1(22) 43%, 512 ↓ + Q_1(22) 7%
5/2+	—	690	642 ↑ 73%, 642 ↑ + Q_1(20) 17%, 660 ↑ + Q_1(22) 4%
5/2−	850	710	523 ↓ 54%, 521 ↓ + Q_1(22) 45%
3/2−	714.5	730	521 ↑ 39%, 512 ↓ 2%, 521 ↓ + Q_1(22) 51%
3/2+	—	780	651 ↑ 44%, 633 ↑ + Q_1(22) 39%, 651 ↑ + Q_1(20) 10%
9/2+	—	830	624 ↑ 94%, 512 ↑ + Q_1(32) 4%, 633 ↓ + Q_1(22) 1%
1/2+	—	960	660 ↑ 55%, 642 ↑ + Q_1(22) 18%, 660 ↑ + Q_1(20) 11%
3/2−	1082	1030	512 ↓ 21%, 521 ↑ 2%, 521 ↓ + Q_1(22) 49%, 514 ↓ + Q_1(22) 10%
7/2−	823	1040	514 ↓ 83%, 512 ↓ + Q_1(22) 13%, 514 ↓ + Q_1(20) 3%
11/2+	—	1090	633 ↑ + Q_1(22) 100%
11/2−	1394	1100	505 ↑ 72%, 505 ↑ + Q_1(20) 23%
3/2+	860	1110	402 ↓ 2%, 633 ↑ + Q_1(22) 97%
1/2+	1644	1340	400 ↑ 54%, 402 ↓ + Q_1(22) 27%, 402 ↑ + Q_1(22) 4%
3/2+	1526	1400	402 ↓ 62%, 400 ↑ + Q_1(22) 29%

TABLE 6.15. ^{171}Er

K^π	Energy, keV exptl.	Energy, keV theor.	Structure
5/2−	0	0	512 ↑ 91%, 510 ↑ + Q_1(22) 4.7%, 624 ↑ + Q_1(32) 1.7%
1/2−	194	280	521 ↓ 89%
7/2−	531	390	514 ↓ 93%, 512 ↓ + Q_1(22) 5%
7/2+	—	400	633 ↑ 92%, 521 ↑ + Q_1(32) 3%, 651 ↑ + Q_1(22) 3%
9/2+	378	420	624 ↑ 93%, 512 ↑ + Q_1(32) 4.5%
1/2−	706	630	510 ↑ 49%, 512 ↑ + Q_1(22) 40%, 512 ↓ + Q_1(22) 8%
3/2−	906	860	512 ↓ 45%, 521 ↑ 1.7%, 514 ↓ + Q_1(22) 34%, 510 ↑ + Q_1(22) 12%
5/2+	—	920	642 ↑ 85%, 660 ↑ + Q_1(22) 8%, 521 ↓ + Q_1(32) 1.5%
3/2−	—	980	521 ↑ 35%, 512 ↓ 2.2%, 521 ↓ + Q_1(22) 50%, 633 ↑ + Q_1(32) 5%
3/2+	—	1000	651 ↑ 53%, 633 ↑ + Q_1(22) 33%, 660 ↑ + Q_1(22) 7%
5/2−	—	1050	523 ↓ 40%, 521 ↓ + Q_1(22) 55%, 512 ↑ + Q_1(20) 2%
1/2+	—	1120	660 ↑ 60%, 642 ↑ + Q_1(22) 21%, 651 ↑ + Q_1(22) 12%
9/2−	—	1330	512 ↑ + Q_1(22) 100%
11/2+	—	1420	615 ↑ 4%, 633 ↑ + Q_1(22) 95%
1/2+	—	1460	400 ↑ 11%, 512 ↑ + Q_1(32) 81%
7/2−	—	1470	503 ↑ 35%, 514 ↓ + Q_1(20) 54%, 501 ↑ + Q_1(22) 4%

TABLE 6.16. ^{167}Yb

K^π	Energy, keV exptl.	Energy, keV theor.	Structure
5/2⁻	0	0	523↓ 98%
5/2⁺	30	40	642↑ 97%
7/2⁺	67	170	633↑ 98%
3/2⁻	188	290	521↑ 97%
1/2⁻	212	300	521↓ 97%
3/2⁺	—	470	651↑ 94%, 660↑ + Q_1(22) 2%
5/2⁻	401	480	512↑ 91%, 624↑ + Q_1(32) 4%, 510↑ + Q_1(22) 2%
1/2⁺	—	680	660↑ 87%, 651↑ + Q_1(22) 4%, 642↑ + Q_1(22) 4%
9/2⁺	—	1100	624↑ 81%, 512↑ + Q_1(32) 13%, 523↓ + Q_1(32) 3%
3/2⁺	—	1260	402↓ 86%, 400↑ + Q_1(22) 10%
3/2⁻	—	1340	531↑ 9%, 521↑ + Q_1(20) 89%
1/2⁻	—	1400	530↑ 40%, 642↑ + Q_1(32) 51%, 651↑ + Q_1(32) 3%
1/2⁺	—	1440	400↑ 73%, 402↓ + Q_1(22) 16%, 523↓ + Q_1(32) 7%
7/2⁻	—	1460	514↓ 83%, 633↑ + Q_1(30) 12%, 512↓ + Q_1(22) 2%
1/2⁻	—	1500	510↑ 12%, 521↓ + Q_1(20) 75%, 512↑ + Q_1(22) 6%

TABLE 6.17. ^{169}Yb

K^π	Energy, keV exptl.	Energy, keV theor.	Structure
7/2⁺	0	0	633↑ 98%
1/2⁻	24	103	521↓ 98%
5/2⁻	191	160	512↑ 75%, 523↓ 15%, 510↑ + Q_1(22) 6%
5/2⁺	591	370	642↑ 93%, 660↑ + Q_1(22) 4%
5/2⁻	570	400	523↓ 85%, 512↑ 13%
3/2⁻	660	720	521↑ 92%, 521↓ + Q_1(22) 4%
3/2⁺	720	800	651↑ 77%, 633↑ + Q_1(22) 11%, 660↑ + Q_1(22) 10%
1/2⁺		820	660↑ 55%, 642↑ + Q_1(22) 31%, 651↑ + Q_1(22) 12%
1/2⁻	813	840	510↑ 37%, 512↑ + Q_1(22) 51%, 521↓ + Q_1(20) 5%
9/2⁺		890	624↑ 89%, 512↑ + Q_1(32) 7%, 642↑ + Q_1(22) 2%
7/2⁻	960	1080	514↓ 91%, 512↓ + Q_1(22) 6%
11/2⁺		1150	633↑ + Q_1(22) 100%
3/2⁺		1160	633↑ + Q_1(22) 100%
3/2⁻		1220	512↓ 6%, 521↓ + Q_1(22) 91%, 514↓ + Q_1(22) 2%
1/2⁻		1230	523↓ + Q_1(22) 100%
9/2⁻		1230	523↓ + Q_1(22) 100%
3/2⁻		1240	521↓ + Q_1(22) 100%
5/2⁻		1250	521↓ + Q_1(22) 100%
9/2⁺		1350	624↑ 2%, 642↑ + Q_1(22) 97%
3/2⁺		1400	402↓ 72%, 400↑ + Q_1(22) 23%, 404↓ + Q_1(22) 3%
1/2⁻		1410	521↓ + Q_1(20) 100%
1/2⁺		1440	400↑ 59%, 402↓ + Q_1(22) 32%, 402↑ + Q_1(22) 4%
3/2⁻		1500	512↓ 43%, 514↓ + Q_1(22) 30%, 510↑ + Q_1(22) 12%
1/2⁺		1510	660↑ 12%, 642↑ + Q_1(22) 63%, 651↑ + Q_1(22) 24%

TABLE 6.18. ^{171}Yb

K^π	Energy, keV exptl.	Energy, keV theor.	Structure
1/2⁻	0	0	521↓ 95%
5/2⁻	122	10	512↑ 91%, 510↑ + Q_1(22) 5%
7/2⁺	95	110	633↑ 97%
9/2⁺	935	650	624↑ 95%
1/2⁻	945	680	510↑ 47%, 512↑ + Q_1(22) 43%, 512↓ + Q_1(22) 5%
5/2⁻		690	523↓ 85%, 521↓ + Q_1(22) 10%, 642↑ + Q_1(30) 3%
5/2⁺		730	642↑ 89%, 660↑ + Q_1(22) 4%, 523↓ + Q_1(30) 4%
7/2⁻	835	750	514↓ 89%, 512↓ + Q_1(22) 6%, 633↑ + Q_1(30) 3%
3/2⁻	902	870	521↑ 62%, 521↓ + Q_1(22) 31%, 651↑ + Q_1(30) 3%
3/2⁺		940	651↑ 60%, 633↑ + Q_1(22) 27%, 660↑ + Q_1(22) 5%
1/2⁺		1050	660↑ 62%, 642↑ + Q_1(22) 20%, 651↑ + Q_1(22) 9%
3/2⁻		1120	512↓ 51%, 514↓ + Q_1(22) 23%, 510↑ + Q_1(22) 12%
1/2⁻		1260	521↓ + Q_1(20) 100%
11/2⁺		1320	615↑ 2%, 633↑ + Q_1(22) 98%
3/2⁻		1330	521↓ + Q_1(22) 100%
3/2⁺		1340	633↑ + Q_1(22) 100%
7/2⁻		1450	503↑ 58%, 633↑ + Q_1(30) 23%, 514↓ + Q_1(20) 8%
9/2⁻		1500	512↑ + Q_1(22) 100%
1/2⁻		1500	512↑ + Q_1(22) 100%

TABLE 6.19. ^{173}Yb

K^π	Energy, keV exptl.	Energy, keV theor.	Structure
5/2⁻		0	512↑ 96%
7/2+	3501	300	633↑ 96%
9/2+		310	624↑ 96%
1/2⁻	399	320	521↓ 97%
7/2⁻	637	400	514↓ 98%
5/2+		900	642↑ 93%, 521↓+Q_1(32) 2%
3/2⁻	1224	1200	521↑ 56%, 633↑+Q_1(32) 35%, 642↑+Q_1(31) 3%
5/2⁻		1250	523↓ 6%, 512↑+Q_1(20) 93%
3/2+		1260	651↑ 79%, 512↑+Q_1(31) 5%, 521↓+Q_1(32) 5%
1/2⁻	1031	1250	510↑ 41%, 521↓+Q_1(20) 52%, 512↑+Q_1(22) 3%
5/2⁻		1370	523↓ 78%, 633↑+Q_1(31) 7%, 512↑+Q_1(20) 7%
1/2⁻		1380	510↑ 42%, 521↓+Q_1(20) 47%, 512↑+Q_1(22) 6%
1/2+		1400	660↑ 57%, 521↓+Q_1(31) 30%
3/2+		1420	651↑ 3%, 512↑+Q_1(31) 93%
3/2+		1490	521↓+Q_1(31) 100%
1/2+		1490	521↓+Q_1(31) 70%, 512↑+Q_1(32) 24%
7/2⁻		1520	503↑ 4%, 514↓+Q_1(20) 95%
9/2⁻		1530	633↑+Q_1(31) 100%
3/2⁻		1550	521↓+Q_1(22) 100%
3/2⁻	1340	1600	512↓ 50%, 633↑+Q_1(32) 37%, 514↓+Q_1(22) 6%

TABLE 6.20. ^{175}Yb

K^π	Energy, keV exptl.	Energy, keV theor.	Structure
7/2⁻	0	0	514↓ 98%
9/2+	265	50	624↑ 99%
5/2⁻	639	250	512↑ 98%
1/2⁻	920	600	521↓ 95%, 521↑+Q_1(22) 2%
7/2+	≈ 995	700	633↑ 98%
1/2⁻	515	800	510↑ 85%, 512↓+Q_1(22) 8%, 512↑+Q_1(22) 7%
3/2⁻	811	990	512↓ 71%, 514↓+Q_1(22) 18%, 510↑+Q_1(22) 10%
5/2+		1340	642↑ 91%, 624↑+Q_1(22) 4%
7/2⁻		1360	503↑ 17%, 514↓+Q_1(20) 81%
11/2+		1390	514↓+Q_1(32) 100%
3/2+		1390	514↓+Q_1(32) 100%
5/2⁻		1400	624↑+Q_1(32) 100%
5/2⁻		1405	523↓ 5%, 512↑+Q_1(20) 93%
9/2+		1410	512↑+Q_1(32) 100%
1/2+		1410	512↑+Q_1(32) 100%
11/2+		1450	615↑ 98%
7/2⁻		1560	503↑ 65%, 514↓+Q_1(20) 18%, 514↓+Q_1(20) 12%
3/2+		1600	651↑ 72%, 633↑+Q_1(22) 23%
3/2⁻	1616	1640	521↑ 46%, 521↓+Q_1(22) 51%

TABLE 6.21. ^{177}Yb

K^π	Energy, keV exptl.	Energy, keV theor.	Structure
9/2+	0	0	624↑ 99%
7/2⁻	104	480	514↓ 99%
1/2⁻	332	640	510↑ 91%, 512↓+Q_1(22) 8%
5/2⁻		690	512↑ 97%, 624↑+Q_1(32) 1%
3/2⁻	709	930	512↓ 87%, 510↑+Q_1(22) 9%, 514↓+Q_1(22) 3%
7/2+		1110	633↑ 97%, 651↑+Q_1(22) 2%
1/2⁻		1200	521↓ 94%, 521↑+Q_1(22) 3%, 523↓+Q_1(22) 2%, 512↑+Q_1(22) 1%
5/2⁻		1360	512↑ 1%, 624↑+Q_1(32) 99%
11/2+		1380	615↑ 95%, 503↑+Q_1(32) 2%, 514↓+Q_1(32) 2%
17/2+		1400	624↑ $p411$↓ $p404$↓
5/2+		1410	642↑ 4%, 624↑+Q_1(22) 96%
13/2+		1420	624↑+Q_1(22) 100%
3/2+		1470	514↓+Q_1(32) 100%
11/2+		1480	615↑1%, 514↓+Q_1(32) 98%
7/2⁻	1226	1540	503↑73%, 514↓+Q_1(20) 19%, 501↑+Q_1(22) 4%
11/2⁻		1550	514↓+Q_1(22) 100%
3/2⁻		1570	512↓ 2%, 514↓+Q_1(22) 96%, 510↑+Q_1(22) 1%
19/2⁻		1600	624↑ $p411$↓ $p514$↑
7/2⁻		1630	503↑ 18%, 514↓+Q_1(20) 81%, 501↑+Q_1(22) 1%
1/2+		1630	400↑ 1%, 512↑+Q_1(32) 99%
9/2+		1660	512↑+Q_1(32) 99%
9/2⁻		1720	512↑+Q_1(22) 100%
1/2⁻		1720	521↓ 1%, 512↑+Q_1(22) 99%
5/2⁻		1770	523↓ 1%, 512↑+Q_1(20) 99%
5/2+		1780	642↑ 89%, 660↑+Q_1(22) 4%, 624↑+Q_1(22) 4%

TABLE 6.22. ^{178}Hf

K^π	Energy, keV exptl.	Energy, keV theor.	Structure
1/2⁻	0	0	521↓ 97%, 521↑+Q_1(22) 1%
5/2⁻	107	−70	512↑ 94%, 510↑+Q_1(22) 2%
7/2+	197	30	633↑ 98%
9/2+	—	480	624↑ 94%, 512↑+Q_1(32) 4%
7/2⁻	—	490	514↓ 97%, 512↓+Q_1(22) 2%
5/2+	—	510	642↑ 95%, 660↑+Q_1(22) 2%
3/2+	—	810	651↑ 88%, 660↑+Q_1(22) 4%, 633↑+Q_1(22) 4%
5/2⁻	—	900	523↓ 89%, 521↓+Q_1(22) 7%
1/2+	—	910	660↑ 82%, 642↑+Q_1(22) 8%, 651↑+Q_1(22) 6%
3/2⁻	—	970	521↑ 75%, 521↓+Q_1(22) 13%, 633↑+Q_1(32) 5%
1/2⁻	—	1000	510↑ 53%, 512↑+Q_1(22) 35%, 512↑+Q_2(22) 6%
3/2+	—	1370	521↓+Q_1(31) 100%
9/2⁻	—	1380	633↑+Q_1(31) 100%
1/2⁻	—	1390	521↓+Q_1(20) 93%, 521↓+Q_2(20) 6%
3/2⁻	—	1400	512↓ 56%, 514↓+Q_1(22) 24%, 510↑+Q_1(22) 7%
11/2+	—	1540	615↑ 3%, 633↑+Q_1(22) 96%
3/2⁻	—	1560	521↓+Q_1(22) 100%
7/2⁻	—	1700	642↑+Q_1(31) 100%
11/2⁻	—	1800	633↑+Q_1(32) 98%

TABLE 6.23. ^{174}Hf

K^π	Energy, keV exptl.	Energy, keV theor.	Structure
5/2⁻	0	0	512↑ 97%, 510↑+Q_2(22) 1%
1/2⁻	125	280	521↓ 97%, 521↑+Q_2(22) 1%
7/2⁻	348	310	514↓ 98%, 512↓+Q_2(22) 1%
9/2+	—	330	624↑ 98%, 512↑+Q_1(32) 1%
7/2+	207	350	633↑ 97%, 521↑+Q_1(32) 1%
5/2+	—	980	642↑ 96%, 660↑+Q_2(22) 2%
5/2⁻	—	1000	523↓ 1%, 512↑+Q_1(20) 98%
1/2⁻	—	1090	510↑ 25%, 521↓ 3%, 521↓+Q_1(20) 63%, 512↑+Q_2(22) 4%
7/2⁻	—	1260	503↑ 3%, 514↓ 1%, 514↓+Q_1(20) 95%
3/2⁻	—	1280	521↑ 56%, 512↓ 1%, 633↑+Q_1(32) 19%, 521↓+Q_1(22) 9%
3/2+	—	1300	651↑ 81%, 633↑+Q_1(22) 6%, 633↑+Q_2(22) 4%
5/2⁻	—	1360	523↓ 74%, 521↓+Q_1(22) 16%, 521↓+Q_2(22) 7%
3/2⁻	—	1400	512↓ 67%, 514↓+Q_1(22) 12%, 514↓+Q_2(22)11%
3/2+	—	1440	512↑+Q_1(31) 100%
7/2+	—	1441	512↑+Q_1(31) 100%
9/2⁻	—	1460	512↑+Q_1(22) 100%
1/2+	—	1470	660↑ 72%, 521↓+Q_1(31) 11%, 521↓+Q_2(31) 4%
3/2⁻	—	1550	521↓+Q_1(22) 100%
9/2⁻	—	1556	633↑+Q_1(31) 100%
9/2+	—	1660	624↑ 1.4%, 512↑+Q_1(32) 98%
7/2⁻	—	1720	503↑ 1%, 624↑+Q_1(31) 99%

TABLE 6.24. ^{177}Hf

K^π	Energy, keV exptl.	Energy, keV theor.	Structure
7/2⁻	0	0	514↓ 98%
9/2+	321	110	624↑ 99%
5/2⁻	509	154	512↑ 97%
7/2+	746	437	633↑ 97%, 651↑+Q_1(22) 1%, 521↑+Q_1(32) 1%
1/2⁻	560	567	521↓ 94%, 521↓+Q_1(22) 3%, 523↓+Q_1(22) 2%
1/2⁻	590	673	510↑ 82%, 512↓+Q_1(22) 9%, 512↑+Q_1(22) 8%
3/2⁻	804	986	512↓ 75%, 514↓+Q_1(22) 15%, 510↑+Q_1(22) 9%
5/2+		1000	642↑ 93%, 660↑+Q_1(22) 4%
23/2+	1315	1200	514↓ $p404$↓ $p514$↑ 100%
3/2+		1242	651↑ 76%, 633↑+Q_1(22) 13%, 660↑+Q_1(22) 5%
7/2⁻	1058	1242	503↑ 2%, 514↓+Q_1(20) 98%
9/2+		1200	514↓+Q_1(31) 100%
5/2+		1200	514↓+Q_1(31) 100%
25/2⁻		1300	624↑ $p404$↓ $p514$↑ 100%
5/2⁻		1313	512↑+Q_1(20) 100%
7/2+		1344	512↑+Q_1(31) 100%
3/2+		1345	651↑ 1%, 512↑+Q_1(31) 99%
11/2+		1352	615↑ 2%, 514↓+Q_1(32) 98%
3/2+		1356	651↑ 1%, 514↓+Q_1(32) 98%
7/2⁻		1300	624↑+Q_1(31) 100%
11/2⁻		1300	624↑+Q_1(31) 100%
21/2+		1400	512↑ $p404$↓ $p514$↑ 100%
1/2+		1408	660↑ 23%, 512↑+Q_1(32) 72%, 642↑+Q_1(22) 2%
1/2+		1437	660↑ 60%, 512↑+Q_1(32) 28%, 642↑+Q_1(22) 4%
11/2⁻		1446	514↓+Q_1(22) 100%
3/2⁻	1502	1453	521↑ 23%, 514↓+Q_1(22) 76%
5/2⁻		1471	624↑+Q_1(32) 100%

TABLE 6.28. ^{181}W

K^π	Energy, keV exptl.	Energy, keV theor.	Structure
9/2+	0	0	624 ↑ 98%
1/2−	458	250	510 ↑ 83%, 512 ↓ + Q_1 (22) 16%
7/2−	662	380	503 ↑ 58%, 514 ↓ 24%, 501 ↑ + Q_1 (22) 10%, 514 ↓ + Q_1 (20) 5%
7/2−	409	480	514 ↓ 74%, 503 ↑ 20%, 501 ↑ + Q_1 (22) 5%
3/2−	726	530	512 ↓ 79%, 510 ↑ + Q_1 (22) 16%, 514 ↓ + Q_1 (22) 3%
5/2−	366	650	512 ↑ 94%, 624 ↑ + Q_1 (32) 3%
1/2−	385	830	521 ↓ 88%, 521 ↑ + Q_1 (22) 5%, 523 ↓ + Q_1 (22) 3%
7/2+	954	850	633 ↑ 93%, 651 ↑ + Q_1 (22) 4%, 521 ↑ + Q_1 (32) 1%
9/2+		900	624 ↑ + Q_1 (20) 100%
11/2+		1010	615 ↑ 93%, 503 ↑ + Q_1 (32) 4%, 624 ↓ + Q_1 (22) 1%
5/2+		1100	642 ↑ 13%, 624 ↑ + Q_1 (22) 85%
13/2+		1150	624 ↑ + Q_1 (22) 100%
5/2−		1170	512 ↑ 3%, 624 ↑ + Q_1 (32) 97%
7/2−		1210	503 ↑ 2%, 514 ↓ + Q_1 (20) 98%
3/2+		1300	651 ↑ 1%, 514 ↓ + Q_1 (32) 98%
11/2−		1290	514 ↓ + Q_1 (22) 100%
11/2+		1300	514 ↓ + Q_1 (32) 100%
3/2−		1310	512 ↓ 1%, 514 ↓ + Q_1 (22) 96%
5/2−		1380	523 ↓ 2%, 512 ↑ + Q_1 (20) 97%, 521 ↓ + Q_1 (22) 1%
3/2+		1380	651 ↑ 44%, 633 ↑ + Q_1 (22) 46%, 660 ↑ + Q_1 (22) 7%
5/2+		1390	642 ↑ 74%, 624 ↑ + Q_1 (22) 15%, 660 ↑ + Q_1 (22) 9%
11/2−		1420	624 ↑ + Q_1 (31) 100%
7/2−		1420	C24 ↑ + Q_1 (31) 100%
9/2−		1490	512 ↑ + Q_1 (22) 100%
23/2−		1500	624 ↑ p514 ↑ p402 ↑ 100%
3/2−		1570	501 ↑ 30%, 503 ↑ + Q_1 (22) 32%, 512 ↓ + Q_1 (20) 31%

TABLE 6.29. ^{183}W

K^π	Energy, keV exptl.	Energy, keV theor.	Structure
1/2−	0	0	510 ↑ 95%, 512 ↓ + Q_1 (22) 4%
3/2−	209	190	512 ↓ 92%, 501 ↑ 0.2%, 510 ↑ + Q_1 (22) 7%
11/2+	310	500	615 ↑ 98%, 503 ↑ + Q_1 (32) 1%
7/2−	453	580	503 ↑ 95%, 501 ↑ + Q_1 (22) 3%
9/2+	623	600	624 ↑ 98%, 512 ↑ + Q_1 (32) 1%
7/2−	1072	1110	514 ↓ 99%
5/2−	905	1160	512 ↑ 67%, 624 ↑ + Q_1 (32) 19%, 510 ↑ + Q_1 (22) 12%
1/2−		1390	521 ↓ 2%, 510 ↑ + Q_1 (20) 97%
5/2+		1420	642 ↑ 2%, 624 ↑ + Q_1 (22) 98%
13/2+		1430	624 ↑ + Q_1 (22) 100%
5/2−		1450	512 ↑ 2%, 510 ↑ + Q_1 (22) 80%, 624 ↑ + Q_1 (32) 18%
9/2−		1490	505 ↓ 98%, 503 ↓ + Q_1 (22) 2%
3/2−		1490	512 ↓ 4%, 510 ↑ + Q_1 (22) 93%
3/2+		1500	510 ↑ + Q_1 (32) 100%
5/2+		1500	510 ↑ + Q_1 (32) 100%
15/2+		1500	n510 ↑ p514 ↑ p402 ↑ 100%
3/2−		1520	501 ↑ 10%, 512 ↓ + Q_1 (20) 80%, 503 ↑ + Q_1 (22) 8%
7/2+		1530	633 ↑ 97%, 651 ↑ + Q_1 (22) 2%
5/2−		1580	512 ↑ 28%, 624 ↑ + Q_1 (32) 63%, 510 ↑ + Q_1 (22) 8%
1/2−		1670	521 ↓ 90%, 510 ↑ + Q_1 (20) 3%, 521 ↑ + Q_1 (22) 2%
1/2−		1700	510 ↑ 4%, 512 ↓ + Q_1 (22) 96%
17/2+		1700	n512 ↓ p514 ↑ p402 ↑ 100%
3/2−		1760	501 ↑ 19%, 503 ↑ + Q_1 (22) 62%, 512 ↓ + Q_1 (20) 18%

TABLE 6.30. ^{185}W

K^π	Energy, keV exptl.	Energy, keV theor.	Structure
3/2−	0	0	512 ↓ 99%
1/2−	24	20	510 ↑ 99%
7/2−	244	110	503 ↑ 99%
11/2+	198	130	615 ↑ 99%
9/2+	716	720	624 ↑ 98%, 512 ↑ + Q_1 (32) 1%
9/2−	789	730	505 ↓ 100%
1/2−		1010	521 ↓ 3%, 510 ↑ + Q_1 (20) 97%
5/2−		1030	510 ↑ + Q_1 (22) 100%
3/2−		1030	510 ↑ + Q_1 (22) 100%
3/2−		1040	501 ↑ 6%, 512 ↓ + Q_1 (20) 92%, 503 ↑ + Q_1 (22) 1%
7/2−		1080	514 ↓ 1%, 512 ↓ + Q_1 (22) 99%
1/2−		1080	512 ↓ + Q_1 (22) 100%
7/2−		1180	514 ↓ 9%, 503 ↑ + Q_1 (20) 91%
3/2−		1190	501 ↑ 1%, 503 ↑ + Q_1 (22) 98%, 512 ↓ + Q_1 (20) 1%
7/2+		1190	615 ↑ + Q_1 (22) 100%
5/2+		1300	510 ↑ + Q_1 (32) 100%
3/2+		1310	510 ↑ + Q_1 (32) 100%
7/2−	1058	1330	514 ↓ 90%, 503 ↑ + Q_1 (20) 9%
1/2+		1360	512 ↓ + Q_1 (32) 100%
7/2+		1370	512 ↓ + Q_1 (32) 100%
5/2−	888	1490	512 ↑ 75%, 624 ↑ + Q_1 (32) 23%
17/2+		1500	n512 ↓ p514 ↑ p402 ↑ 100%
15/2+		1500	510 ↑ p514 ↑ p402 ↑ 100%
1/2−		1510	521 ↓ 1%, 510 ↑ + Q_1 (20) 99%
7/2+		1580	633 ↑ 99%
25/2−		1600	n615 ↑ p514 ↑ p402 ↑ 100%
1/2−		1740	521 ↓ 93%, 510 ↑ + Q_1 (20) 3%, 541 ↓ + Q_1 (20) 2%

TABLE 6.31. ^{183}Os

K^π	Energy, keV exptl.	Energy, keV theor.	Structure
9/2+	0	0	624 ↑ 98%
1/2−	171	140	510 ↑ 85%, 512 ↓ + Q_1 (22) 15%
3/2−		380	512 ↓ 82%, 510 ↑ + Q_1 (22) 15%
7/2−		410	503 ↑ 89%, 501 ↑ + Q_1 (22) 8%, 615 ↑ + Q_1 (32) 2%
7/2−		470	514 ↓ 99%
7/2+		580	633 ↑ 95%, 651 ↑ + Q_1 (22) 4%
1/2−		590	521 ↓ 90%, 521 ↑ + Q_1 (22) 4%, 523 ↓ + Q_1 (22) 3%
5/2−		630	512 ↑ 95%, 521 ↓ + Q_1 (22) 2%, 624 ↑ + Q_1 (32) 1%
11/2+		740	615 ↑ 97%, 503 ↑ + Q_1 (32) 1%, 624 ↑ + Q_1 (22) 1%
5/2+		890	642 ↑ 50%, 624 ↑ + Q_1 (22) 44%, 660 ↑ + Q_1 (22) 5%
13/2+		990	624 ↑ + Q_1 (22) 100%
7/2−		1000	514 ↓ + Q_1 (20) 100%
3/2+		1020	651 ↑ 60%, 633 ↑ + Q_1 (22) 29%, 660 ↑ + Q_1 (22) 10%
5/2+		1100	642 ↑ 38%, 624 ↑ + Q_1 (22) 56%, 660 ↑ + Q_1 (22) 6%
3/2−		1160	501 ↑ 28%, 503 ↑ + Q_1 (22) 41%, 512 ↓ + Q_1 (20) 25%
5/2−		1170	523 ↓ 2%, 512 ↑ + Q_1 (20) 97%
1/2+		1170	660 ↑ 71%, 642 ↑ + Q_1 (22) 18%, 651 ↑ + Q_1 (22) 10%
15/2−		1600	n624 ↑ p402 ↑ p541 ↓ 100%

TABLE 6.25. ^{179}Hf

K^π	Energy, keV exptl.	Energy, keV theor.	Structure
9/2+	0	0	624 ↑ 99%
1/2−	375	405	510 ↑ 90%, 512 ↓ + Q_1 (22) 10%
7/2−	214	463	514 ↓ 98,8%, 503 ↑ 0,2%
3/2−	720	672	512 ↓ 88%, 510 ↑ + Q_1 (22) 10%, 514 ↓ + Q_1 (22) 2%
5/2−	518	700	512 ↑ 98%, 624 ↑ + Q_1 (32) 1%
7/2+	953	872	633 ↑ 97%, 651 ↑ + Q_1 (22) 2%
1/2−	614	995	521 ↓ 93%, 521 ↑ + Q_1 (22) 3%, 523 ↓ + Q_1 (22) 2%
7/2−	870	933	503 ↑ 91,7%, 514 ↓ 0,3%, 501 ↑ + Q_1 (22) 6%
11/2+		1055	615 ↑ 98%, 503 ↑ + Q_1 (32) 1%
25/2−	1106	1200	624 ↑ $p404$ ↓ $p514$ ↑ 100%
5/2+		1254	642 ↑ 18%, 624 ↑ + Q_1 (22) 81%
13/2+		1292	624 ↑ + Q_1 (22) 100%
11/2−		1392	624 ↑ + Q_1 (31) 100%
7/2−		1392	624 ↑ + Q_1 (31) 100%
5/2−		1403	512 ↑ 0,6%, 624 ↑ + Q_1 (32) 100%
5/2+		1452	642 ↑ 24%, 514 ↓ + Q_1 (31) 68%, 624 ↑ + Q_1 (22) 6%
3/2−		1453	512 ↓ 1%, 514 ↓ + Q_1 (22) 98%
9/2+		1455	514 ↓ + Q_1 (31) 100%
11/2−		1439	514 ↓ + Q_1 (22) 100%
5/2+		1460	642 ↑ 52%, 514 ↓ + Q_1 (31) 32%, 624 ↑ + Q_1 (22) 12%
9/2+		1540	514 ↓ + Q_2 (31) 100%
5/2+		1540	514 ↓ + Q_2 (31) 100%
23/2+		1600	514 ↓ $p404$ ↓ $p514$ ↑ 100%

TABLE 6.26. ^{181}Hf

K^π	Energy, keV exptl.	Energy, keV theor.	Structure
1/2−	0	0	510 ↑ 95%, 512 ↓ + Q_1 (22) 5%
3/2−	255	248	512 ↓ 95%, 510 ↑ + Q_1 (22) 4%
11/2+		553	615 ↑ 99%
7/2−	670	577	503 ↑ 95%, 501 ↑ + Q_1 (22) 3%
9/2+		600	624 ↑ 99%
7/2−		1110	514 ↓ 99%
17/2+		1200	$n510$ ↑ $p404$ ↓ $p514$ ↑ 100%
5/2−		1292	512 ↑ 68%, 510 ↑ + Q_1 (22) 29%, 624 ↑ + Q_1 (32) 1%
5/2+		1389	642 ↑ 2%, 624 ↑ + Q_1 (22) 98%
11/2−		1391	624 ↑ + Q_1 (31) 100%
7/2−		1391	624 ↑ + Q_1 (31) 100%
19/2+		1400	$n512$ ↓ $p404$ ↓ $p514$ ↑ 100%
1/2+		1200	510 ↑ + Q_1 (31) 100%
3/2+		1200	510 ↑ + Q_1 (31) 100%
13/2+		1402	624 ↑ + Q_1 (22) 100%
3/2−	1503	1461	501 ↑ 27%, 512 ↓ 1%, 503 ↑ + Q_1 (22) 56%, 512 ↓ + Q_1 (20) 13%
5/2−		1462	512 ↑ 28%, 510 ↑ + Q_1 (22) 71%
3/2−		1464	512 ↓ 4%, 510 ↑ + Q_1 (22) 96%
9/2−		1479	505 ↓ 98%, 503 ↓ + Q_1 (22) 2%
7/2+		1530	633 ↑ 97%, 651 ↑ + Q_1 (22) 2%
1/2+		1588	512 ↓ + Q_1 (31) 100%
5/2+		1588	512 ↓ + Q_1 (31) 100%
27/2−		1600	$n615$ ↑ $p404$ ↓ $p514$ ↑ 100%

TABLE 6.27. ^{179}W

K^π	Energy, keV exptl.	Energy, keV theor.	Structure
7/2−	0	0	514 ↓ 98%, 512 ↓ + Q_1 (22) 1%
9/2+	309	50	624 ↑ 99%
5/2−	430	150	512 ↑ 98%
7/2+	477	290	633 ↑ 96%, 521 ↑ + Q_1 (32) 2%, 651 ↑ + Q_1 (22) 2%
1/2−	222	310	521 ↓ 91%, 521 ↑ + Q_1 (22) 4%, 523 ↓ + Q_1 (22) 3%
1/2−	627	500	510 ↑ 84%, 512 ↓ + Q_1 (22) 10%, 512 ↑ + Q_1 (22) 5%
5/2+		770	642 ↑ 93%, 660 ↑ + Q_1 (22) 4%
3/2−		810	512 ↓ 80%, 510 ↑ + Q_1 (22) 10%, 514 ↓ + Q_1 (22) 8%
3/2+		980	651 ↑ 75%, 514 ↓ + Q_1 (32) 8%, 633 ↑ + Q_1 (22) 8%
11/2+		1030	615 ↑ 1%, 514 ↓ + Q_1 (32) 98%
3/2+		1030	651 ↑ 7%, 514 ↓ + Q_1 (32) 92%
7/2−		1040	503 ↑ 21%, 514 ↓ + Q_1 (20) 77%, 501 ↑ + Q_1 (22) 1%
1/2+		1100	660 ↑ 11%, 512 ↑ + Q_1 (32) 87%
3/2−		1110	521 ↑ 13%, 633 ↑ + Q_1 (32) 83%, 521 ↓ + Q_1 (22) 4%
9/2+		1110	512 ↑ + Q_1 (32) 100%
5/2−		1120	624 ↑ + Q_1 (32) 99%
5/2−		1150	523 ↓ 2%, 512 ↑ + Q_1 (20) 97%
1/2+		1150	660 ↑ 74%, 512 ↑ + Q_1 (32) 13%, 642 ↑ + Q_1 (22) 7%
11/2−		1190	633 ↑ + Q_1 (32) 100%
7/2−		1190	503 ↑ 68%, 514 ↓ + Q_1 (20) 23%, 501 ↑ + Q_1 (22) 5%
11/2+		1230	615 ↑ 89%, 503 ↑ + Q_1 (32) 6%, 633 ↑ + Q_1 (22) 2%
5/2+		1330	642 ↑ 1%, 521 ↓ + Q_1 (32) 99%
3/2+		1330	651 ↑ 1%, 521 ↓ + Q_1 (32) 98%
7/2+	1680	1500	514 ↓ $p514$ ↑ $p402$ ↑ 100%
23/2−		1600	624 ↑ $p514$ ↑ $p402$ ↑ 100%
19/2+		1700	512 ↑ $p514$ ↑ $p402$ ↑ 100%

TABLE 6.32. ^{185}Os

K^π	Energy, keV exptl.	Energy, keV theor.	Structure
1/2⁻	0	0	510 ↑ 92%, 512 ↓ + Q_1(22) 7%
3/2⁻	128	130	512 ↓ 87%, 510 ↑ + Q_1(22) 12%
7/2⁻		210	503 ↑ 93%, 501 ↑ + Q_1(22) 5%
9/2⁺		390	624 ↑ 99%
11/2⁺		420	615 ↑ 99%
3/2⁻		870	501 ↑ 27%, 512 ↓ 1%, 503 ↑ + Q_1(22) 64%, 512 ↓ + Q_1(20) 5%
9/2⁻		960	505 ↓ 97%, 503 ↓ + Q_1(22) 3%
7/2⁻		970	514 ↓ 99%, 512 ↓ + Q_1(22) 1%
5/2⁻		1060	512 ↑ 48%, 510 ↑ + Q_1(22) 50%
5/2⁺		1100	642 ↑ 6%, 624 ↑ + Q_1(22) 94%
7/2⁺		1110	633 ↑ 96%, 651 ↑ + Q_1(22) 4%
13/2⁺		1130	624 ↑ + Q_1(22) 100%
1/2⁻		1160	521 ↓ 85%, 510 ↑ + Q_1(20) 8%, 521 ↑ + Q_1(22) 3%
3/2⁻		1229	512 ↓ 6%, 510 ↑ + Q_1(22) 88%, 503 ↑ + Q_1(22) 2%

TABLE 6.33. ^{153}Eu

K^π	Energy, keV exptl.	Energy, keV theor.	Structure
5/2⁺	0	0	413 ↓ 96%, 411 ↓ + Q_1(22) 2%
3/2⁺	103	−20	411 ↑ 89%, 411 ↓ + Q_1(22) 5%, 523 ↑ + Q_1(32) 3%
5/2⁻	97	20	532 ↑ 94%, 420 ↑ + Q_1(32) 1%
7/2⁻	—	550	523 ↑ 86%, 411 ↑ + Q_1(32) 10%
1/2⁺	—	670	411 ↑ 48%, 411 ↑ + Q_1(22) 26%, 413 ↓ + Q_1(22) 23%
3/2⁻	—	820	541 ↑ 86%, 550 ↑ + Q_1(22) 5%, 420 ↑ + Q_1(31) 2%
5/2⁻	—	860	532 ↑ + Q_1(20) 100%
5/2⁺	—	900	413 ↓ + Q_1(20) 100%
1/2⁺	—	920	420 ↑ 75%, 532 ↑ + Q_1(32) 8%, 550 ↑ + Q_1(30) 5%, 422 ↓ + Q_1(22) 4%
1/2⁻	—	1000	550 ↑ 42%, 532 ↑ + Q_1(22) 39%, 541 ↑ + Q_1(22) 8%, 420 ↑ + Q_1(30) 6%
3/2⁺	—	1150	411 ↑ + Q_1(20) 100%
9/2⁻	—	1230	514 ↑ 3%, 532 ↑ + Q_1(22) 97%
9/2⁺	—	1300	413 ↓ + Q_1(22) 100%
1/2⁺	—	1380	413 ↓ + Q_1(22) 67%, 411 ↑ + Q_1(22) 31%
1/2⁻	—	1400	550 ↑ 19%, 532 ↑ + Q_1(22) 59%, 541 ↑ + Q_1(22) 11%, 420 ↑ + Q_1(30) 9%
3/2⁻	—	1400	411 ↑ + Q_1(30) 100%
3/2⁻	—	1510	422 ↓ 50%, 420 ↑ + Q_1(22) 26%, 541 ↑ + Q_1(30) 16%, 532 ↑ + Q_1(31) 5%
7/2⁺	—	1520	411 ↑ + Q_1(22) 94%, 532 ↑ + Q_1(31) 5%

TABLE 6.34. ^{155}Eu

K^π	Energy, keV exptl.	Energy, keV theor.	Structure
5/2⁺	0	0	413 ↓ 97%, 411 ↓ + Q_1(22) 2%
3/2⁺	246	34	411 ↑ 92%, 411 ↓ + Q_1(22) 3%
5/2⁻	104	36	532 ↑ 96%, 420 ↑ + Q_1(32) 1%
7/2⁻	614	610	523 ↑ 90%, 411 ↑ + Q_1(32) 7%
3/2⁻	1095	880	541 ↑ 88%, 550 ↑ + Q_1(22) 3%
1/2⁺	765	890	411 ↓ 58%, 411 ↑ + Q_1(22) 22%, 413 ↓ + Q_1(22) 17%
1/2⁺		990	420 ↑ 79%, 550 ↑ + Q_1(30) 6%, 532 ↑ + Q_1(32) 5%
5/2⁺		1030	402 ↑ 2%, 532 ↑ + Q_1(30) 98%
5/2⁻		1070	413 ↓ + Q_1(30) 100%
1/2⁻		1160	550 ↑ 56%, 532 ↑ + Q_1(22) 18%, 420 ↑ + Q_1(30) 15
5/2⁻		1230	532 ↑ + Q_1(20) 100%
5/2⁺		1270	413 ↓ + Q_1(20) 100%
3/2⁻		1330	413 ↓ + Q_1(31) 100%
3/2⁻		1340	411 ↑ + Q_1(30) 100%
3/2⁺		1520	411 ↑ + Q_1(20) 100%
1/2⁻		1530	532 ↑ + Q_1(22) 98%
9/2⁻		1540	514 ↑ 4%, 532 ↑ + Q_1(22) 95%

TABLE 6.35. ^{155}Tb

K^π	Energy, keV exptl.	Energy, keV theor.	Structure
3/2+	0	0	411 ↑ 92%, 411 ↓ + Q_1(22) 4%
7/2−	545	341	523 ↑ 94%, 411 ↑ + Q_1(32) 2%
5/2+	271	390	413 ↓ 96%, 411 ↓ + Q_1(22) 2%
5/2−	227	530	532 ↑ 93%, 550 ↑ + Q_1(22) 2%
1/2+	—	610	411 ↓ 60%, 411 ↑ + Q_1(22) 20%, 413 ↓ + Q_1(22) 8%
3/2+	—	1000	411 ↑ + Q_1(20) 100%
5/2+	—	1100	413 ↓ + Q_1(20) 100%
7/2+	—	1280	413 ↑ 1%, 411 ↑ + Q_1(22) 98%
1/2−	—	1300	550 ↑ 18%, 532 ↑ + Q_1(22) 76%, 541 ↑ + Q_1(22) 3%
1/2+	—	1310	420 ↑ 6%, 411 ↑ + Q_1(22) 80%
1/2+	—	1330	413 ↓ + Q_1(22) 100%
9/2+	—	1330	413 ↓ + Q_1(22) 100%
3/2−	—	1350	541 ↑ 52%, 411 ↑ + Q_1(30) 35%, 550 ↑ + Q_1(22) 3%
5/2+	—	1420	402 ↑ 73%, 523 ↑ + Q_1(31) 9%, 660 ↑ + Q_1(22) 6%, 532 ↑ + Q_1(30) 5%
9/2−	—	1460	514 ↑ 7%, 532 ↑ + Q_1(22) 92%
3/2−	—	1650	541 ↑ 6%, 523 ↑ + Q_1(22) 56%, 411 ↑ + Q_1(30) 34%
7/2+	—	1680	404 ↓ 68%, 523 ↑ + Q_1(30) 28%, 651 ↑ + Q_1(22) 3%

TABLE 6.36. ^{157}Tb

K^π	Energy, keV exptl.	Energy, keV theor.	Structure
3/2+	0	0	411 ↑ 93%, 411 ↓ + Q_1(22) 4%
7/2−	572	360	523 ↑ 95%, 411 ↑ + Q_1(32) 2%
5/2+	328	380	413 ↓ 96%, 411 ↓ + Q_1(22) 2%
5/2−	326	530	532 ↑ 94%, 550 ↑ + Q_1(22) 2%
1/2+	598	640	411 ↓ 64%, 411 ↑ + Q_1(22) 26%, 413 ↓ + Q_1(22) 7%
3/2+	993	1300	411 ↑ + Q_1(20) 100%
3/2−		1370	541 ↑ 48%, 411 ↑ + Q_1(30) 39%
5/2+		1390	402 ↑ 49%, 413 ↓ + Q_1(20) 32%, 523 ↑ + Q_1(31) 10%
7/2+		1400	411 ↑ + Q_1(22) 97%
1/2−		1410	550 ↑ 21%, 532 ↑ + Q_1(22) 72%, 541 ↑ + Q_1(22) 3%
1/2+		1425	420 ↑ 14%, 411 ↑ + Q_1(22) 72%, 532 ↑ + Q_1(32) 2%
5/2+		1450	402 ↑ 21%, 413 ↓ + Q_1(20) 68%, 523 ↑ + Q_1(31) 5%
9/2+		1460	413 ↓ + Q_1(22) 100%

TABLE 6.37. ^{159}Tb

K^π	Energy, keV exptl.	Energy, keV theor.	Structure
3/2+	0	0	411 ↑ 93%, 411 ↓ + Q_1(22) 4%
5/2+	348	370	413 ↓ 96%
7/2−		380	523 ↓ 96%, 411 ↑ + Q_1(32) 2%
5/2−	364	570	532 ↑ 93%, 413 ↓ + Q_1(30) 2%, 550 ↑ + Q_1(22) 2%
1/2+	581	650	411 ↓ 64%, 411 ↑ + Q_1(22) 27%, 413 ↓ + Q_1(22) 7%
3/2−		1170	541 ↑ 17%, 411 ↑ + Q_1(30) 80%
1/2+		1350	420 ↑ 12%, 413 ↓ + Q_1(22) 63%, 411 ↑ + Q_1(22) 19%
5/2+		1360	402 ↑ 29%, 532 ↑ + Q_1(30) 64%, 660 ↑ + Q_1(22) 2%
1/2−		1390	550 ↑ 26%, 532 ↑ + Q_1(22) 65%, 541 ↑ + Q_1(22) 4%
7/2+		1420	411 ↑ + Q_1(22) 97%
9/2+		1470	413 ↓ + Q_1(22) 100%
3/2+		1480	411 ↑ + Q_1(20) 100%
3/2−		1580	541 ↑ 35%, 413 ↓ + Q_1(31) 44%, 411 ↑ + Q_1(30) 12%
1/2+		1650	411 ↓ 30%, 411 ↑ + Q_1(22) 52%, 413 ↓ + Q_1(22) 14%
15/2+		1860	p523 ↑ n521 ↑ n642 ↑

TABLE 6.38. ^{161}Tb

K^π	Energy, keV exptl.	Energy, keV theor.	Structure
3/2+	0	0	411 ↑ 93%, 411 ↓ + Q_1(22) 5%
5/2+	315	360	413 ↓ 97%, 411 ↓ + Q_1(22) 2%
7/2−	417	390	523 ↑ 97%, 411 ↑ + Q_1(32) 1%
1/2+	—	590	411 ↓ 54%, 411 ↑ + Q_1(22) 35%, 413 ↓ + Q_1(22) 10%
5/2−	480	600	532 ↑ 96%, 550 ↑ + Q_1(22) 2%
7/2+	—	1180	411 ↑ + Q_1(22) 99%
1/2+	—	1220	413 ↓ + Q_1(22) 58%, 411 ↑ + Q_1(22) 42%
9/2+	—	1230	413 ↓ + Q_1(22) 100%
1/2−	—	1250	550 ↑ 12%, 532 ↑ + Q_1(22) 85%, 541 ↑ + Q_1(22) 2%
9/2−	—	1370	514 ↑ 4%, 532 ↑ + Q_1(22) 96%
3/2−	—	1420	541 ↑ 16%, 411 ↑ + Q_1(30) 78%, 523 ↑ + Q_1(22) 4%
5/2+	—	1530	402 ↑ 65%, 413 ↓ + Q_1(20) 12%, 532 ↑ + Q_1(30) 11%
3/2+	—	1550	411 ↑ + Q_1(20) 100%
5/2+	—	1560	413 ↓ + Q_1(20) 100%
15/2−	—	1680	p412 ↓ n642 ↑ n523 ↓ 100%
17/2+	—	1730	p523 ↑ n642 ↓ n523 ↓ 100%

TABLE 6.39. ^{159}Ho

K^π	Energy, keV exptl.	Energy, keV theor.	Structure
7/2⁻	0	0	523 ↑ 97%
3/2⁺	—	250	411 ↑ 94%
1/2⁺	206	380	411 ↓ 88%, 411 ↑ + Q_1 (22) 9%
5/2⁺	—	700	402 ↑ 56%, 413 ↓ 28%, 660 ↑ + Q_1 (22) 8%, 411 ↑ + Q_1 (22) 3%
5/2⁺	650	730	413 ↓ 69%, 402 ↑ 23%, 532 ↑ + Q_1 (30) 5%
5/2⁻	624	900	532 ↑ 90%, 550 ↑ + Q_1 (22) 3%, 413 ↓ + Q_1 (30) 3%
7/2⁺	—	700	404 ↓ 97%, 651 ↑ + Q_1 (22) 2%
7/2⁺	—	1050	413 ↑ 2%, 411 ↑ + Q_1 (22) 97%
3/2⁻	—	1100	541 ↑ 5%, 523 ↑ + Q_1 (22) 93%
11/2⁻	—	1130	523 ↑ + Q_1 (22) 100%
1/2⁺	—	1140	420 ↑ 1%, 411 ↑ + Q_1 (22) 91%
9/2⁻	—	1145	514 ↑ 92%, 402 ↑ + Q_1 (32) 4%
3/2⁺	—	1190	411 ↑ + Q_1 (20) 100%
1/2⁻	—	980	541 ↓ 96%, 411 ↓ + Q_1 (30) 2%
9/2⁺	—	1390	413 ↓ + Q_1 (22) 100%
3/2⁻	—	1420	541 ↑ 8%, 411 ↑ + Q_1 (30) 87%
1/2⁻	—	1470	550 ↑ 14%, 532 ↑ + Q_1 (22) 81%, 541 ↑ + Q_1 (22) 2%

TABLE 6.40. ^{161}Ho

K^π	Energy, keV exptl.	Energy, keV theor.	Structure
7/2⁻	0	0	523 ↑ 97%
3/2⁺	299	260	411 ↑ 94%, 411 ↓ + Q_1 (22) 3%
1/2⁺	211	380	411 ↓ 88%, 411 ↑ + Q_1 (22) 9%
5/2⁺	—	700	402 ↑ 79%, 413 ↓ 2%, 660 ↑ + Q_1 (22) 8%
5/2⁺	760	740	413 ↓ 96%, 402 ↑ 2%
5/2⁻	827	950	532 ↑ 89%, 411 ↑ + Q_1 (31) 5%, 550 ↑ + Q_1 (22) 3%
7/2⁺	253	800	404 ↓ 98%, 651 ↑ + Q_1 (22) 1%
1/2⁻	424	1000	541 ↓ 90%, 411 ↑ + Q_1 (32) 8%
7/2⁺	—	1070	413 ↑ 2%, 411 ↑ + Q_1 (22) 98%
9/2⁻	—	1110	514 ↑ 89%, 402 ↑ + Q_1 (32) 7%
3/2⁻	—	1140	541 ↑ 3%, 523 ↑ + Q_1 (22) 96%
1/2⁺	—	1150	420 ↑ 2%, 411 ↑ + Q_1 (22) 98%
11/2⁻	—	1160	523 ↑ + Q_1 (22) 100%
1/2⁺	—	1400	660 ↑ 32%, 402 ↑ + Q_1 (22) 58%, 651 ↑ + Q_1 (22) 5%
9/2⁺	—	1415	413 ↓ + Q_1 (22) 100%
3/2⁺	—	1420	402 ↓ 3%, 523 ↑ + Q_1 (32) 96%
1/2⁻	—	1460	550 ↑ 2%, 411 ↑ + Q_1 (32) 82%, 532 ↑ + Q_1 (22) 10%
3/2⁺	—	1465	411 ↑ + Q_1 (20) 100%

TABLE 6.41. ^{163}Ho

K^π	Energy, keV exptl.	Energy, keV theor.	Structure
7/2⁻	0	0	523 ↑ 98%
3/2⁺	—	240	411 ↑ 95%, 411 ↓ + Q_1 (22) 2%
1/2⁺	298	390	411 ↓ 91%, 411 ↑ + Q_1 (22) 8%
5/2⁻	—	950	532 ↑ 91%, 550 ↑ + Q_1 (22) 3%
5/2⁺	—	1000	413 ↓ 97%
7/2⁺	—	1010	413 ↑ 1%, 411 ↑ + Q_1 (22) 99%
3/2⁻	—	1015	541 ↑ 4%, 523 ↑ + Q_1 (22) 95%
11/2⁻	—	1040	523 ↑ + Q_1 (22) 100%
1/2⁺	—	1120	411 ↓ 8%, 411 ↑ + Q_1 (22) 92%
9/2⁻	—	1180	514 ↑ 95%, 402 ↑ + Q_1 (32) 2%
7/2⁺	440	900	404 ↓ 97%, 523 ↑ + Q_1 (30) 2%
3/2⁺	—	1300	411 ↑ + Q_1 (20) 100%
1/2⁻	—	1320	550 ↑ 1%, 411 ↑ + Q_1 (32) 95%
1/2⁻	—	1400	550 ↑ 16%, 532 ↑ + Q_1 (22) 75%, 411 ↑ + Q_1 (32) 4%
5/2⁺	—	1415	402 ↑ 34%, 411 ↓ + Q_1 (22) 58%, 523 ↑ + Q_1 (31) 2%
17/2⁺	—	1570	$p523 \uparrow n642 \uparrow n523 \downarrow$ 100%
3/2⁻	—	1410	541 ↑ 7%, 411 ↑ + Q_1 (30) 90%

TABLE 6.42. ^{165}Ho

K^π	Energy, keV exptl.	Energy, keV theor.	Structure
7/2⁻	0	0	523 ↑ 98%
3/2⁺	360	230	411 ↑ 94%, 411 ↓ + Q_1 (22) 3%
1/2⁺	429	370	411 ↓ 88%, 411 ↑ + Q_1 (22) 10%
7/2⁺	715	890	404 ↓ 97%, 523 ↑ + Q_1 (30) 2%
3/2⁻		900	541 ↑ 4%, 523 ↑ + Q_1 (22) 95%
5/2⁻	1056	910	532 ↑ 90%, 550 ↑ + Q_1 (22) 3%, 420 ↑ + Q_1 (32) 3%
11/2⁻	689	920	523 ↑ + Q_1 (22) 100%
1/2⁺		940	411 ↑ + Q_1 (22) 100%
5/2⁺	995	1000	413 ↓ 96%, 532 ↑ + Q_1 (30) 2%
1/2⁺	(1037)	1010	411 ↓ 10%, 411 ↑ + Q_1 (22) 90%
9/2⁻		1130	514 ↑ 93%, 402 ↑ + Q_1 (32) 4%
3/2⁺		1140	523 ↑ + Q_1 (32) 100%
1/2⁻		1150	411 ↑ + Q_1 (32) 99%
1/2⁻		1280	550 ↑ 16%, 532 ↑ + Q_1 (22) 76%, 411 ↑ + Q_1 (32) 3%
5/2⁺		1310	402 ↑ 27%, 411 ↓ + Q_1 (22) 67%, 514 ↑ + Q_1 (32) 4%
9/2⁺		1400	413 ↓ + Q_1 (22) 100%
3/2⁻		1450	541 ↑ 27%, 411 ↑ + Q_1 (30) 66%, 523 ↑ + Q_1 (22) 3%
5/2⁺		1520	402 ↑ 49%, 411 ↓ + Q_1 (22) 34%, 514 ↑ + Q_1 (32) 10%

TABLE 6.43. ^{165}Tm

K^π	Energy, keV exptl.	Energy, keV theor.	Structure
1/2+	0	0	411 ↓ 96%
7/2−	149	300	523 ↑ 94%, 411 ↑ + Q_1 (32) 3%
9/2−	—	550	514 ↑ 94%, 402 ↑ + Q_1 (32) 3%
7/2+	69	450	404 ↓ 98%
3/2+	—	660	411 ↑ 84%, 523 ↑ + Q_1 (32) 7%, 411 ↓ + Q_1 (22) 6%
5/2+	—	990	402 ↑ 42%, 413 ↓ 2%, 411 ↓ + Q_1 (22) 49%, 514 ↑ + Q_1 (32) 3%
3/2−	—	1010	541 ↑ 3%, 523 ↑ + Q_1 (22) 96%
11/2−	—	1060	523 ↑ + Q_1 (22) 100%
3/2+	—	1100	411 ↑ 4%, 411 ↓ + Q_1 (22) 94%
5/2+	—	1100	402 ↑ 44%, 413 ↓ 3%, 411 ↓ + Q_1 (22) 46%, 514 ↑ + Q_1 (32) 3%
7/2+	—	1250	413 ↑ 1%, 411 ↑ + Q_1 (22) 98%
1/2+	—	1320	411 ↑ + Q_1 (22) 100%
1/2−	—	980	541 ↓ 96%, 411 ↓ + Q_1 (30) 2%
5/2−	—	1400	532 ↑ 75%, 411 ↑ + Q_1 (31) 14%, 411 ↓ + Q_1 (32) 3%
3/2+	—	1470	651 ↑ 11%, 404 ↓ + Q_1 (22) 86%, 523 ↑ + Q_1 (32) 2%
17/2+	—	1960	p523 ↑ n642 ↑ n523 ↓ 100%

TABLE 6.44. ^{167}Tm

K^π	Energy, keV exptl.	Energy, keV theor.	Structure
1/2+	0	0	411 ↓ 97%
7/2−	293	360	523 ↑ 96%, 411 ↑ + Q_1 (32) 2%
9/2−	—	560	514 ↑ 96%, 402 ↑ + Q_1 (32) 2%
7/2+	179	370	404 ↓ 97%, 651 ↑ + Q_1 (22) 2%
3/2+	471	670	411 ↑ 82%, 411 ↓ + Q_1 (22) 11%, 523 ↑ + Q_1 (32) 4%
5/2+	—	820	402 ↑ 12%, 413 ↓ 3%, 411 ↓ + Q_1 (22) 84%
3/2−	—	900	541 ↑ 3%, 523 ↑ + Q_1 (22) 97%
11/2−	—	940	523 ↑ + Q_1 (22) 100%
3/2+	—	990	411 ↑ 10%, 411 ↓ + Q_1 (22) 89%
5/2+	—	1000	402 ↑ 74%, 411 ↓ + Q_1 (22) 13%, 660 ↑ + Q_1 (22) 4%
7/2+	—	1140	413 ↑ 1%, 411 ↑ + Q_1 (22) 98%
1/2+	—	1200	411 ↑ + Q_1 (22) 100%
1/2−	—	950	541 ↓ 96%, 411 ↓ + Q_1 (30) 3%
5/2−	1527	1510	532 ↑ 81%, 514 ↑ + Q_1 (22) 6%, 411 ↓ + Q_1 (32) 5%
5/2+	1581	1620	413 ↓ 94%, 411 ↓ + Q_1 (22) 3%
19/2+	—	2110	p523 ↑ n523 ↓ n633 ↑ 100%

TABLE 6.45. ^{169}Tm

K^π	Energy, keV exptl.	Energy, keV theor.	Structure
1/2+	0	0	411 ↓ 96%
7/2−	379	360	523 ↑ 95%, 411 ↑ + Q_1 (32) 2%
7/2+	316	370	404 ↓ 98%
9/2−		530	514 ↑ 95%, 402 ↑ + Q_1 (32) 3%
3/2+	571	630	411 ↑ 84%, 411 ↓ + Q_1 (22) 8%, 523 ↑ + Q_1 (32) 4%
5/2+		810	402 ↑ 51%, 413 ↓ 2%, 411 ↓ + Q_1 (22) 30%, 660 ↑ + Q_1 (22) 4%
1/2−		900	541 ↓ 90%, 411 ↓ + Q_1 (30) 5%
3/2−		950	541 ↑ 5%, 523 ↑ + Q_1 (22) 94%
5/2+		1000	402 ↑ 33%, 413 ↓ 4%, 411 ↓ + Q_1 (22) 56%, 660 ↑ + Q_1 (22) 2%
11/2−		1020	523 ↑ + Q_1 (22) 100%
3/2+		1080	411 ↑ 7%, 411 ↓ + Q_1 (22) 92%
7/2+		1190	413 ↑ 2%, 411 ↑ + Q_1 (22) 97%
1/2+		1280	411 ↑ + Q_1 (22) 100%
3/2+		1350	651 ↑ 14%, 404 ↓ + Q_1 (22) 83%
1/2+		1400	660 ↑ 19%, 411 ↓ + Q_1 (20) 42%, 402 ↑ + Q_1 (22) 33%
5/2−		1470	532 ↑ 85%, 550 ↑ + Q_1 (22) 5%, 413 ↓ + Q_1 (30) 4%

TABLE 6.46. ^{171}Tm

K^π	Energy, keV		Structure
	exptl.	theor.	
1/2+	0	0	411 ↓ 97%
7/2−	425	360	523 ↑ 97%
9/2−	—	550	514 ↑ 97%
7/2+	635	430	404 ↓ 98%, 651 ↑ + Q_1 (22) 1%
3/2+	676	680	411 ↑ 88%, 411 ↓ + Q_1 (22) 7%
5/2+	913	930	402 ↑ 70%, 411 ↓ + Q_1 (22) 18%, 660 ↑ + Q_1 (22) 4%
3/2−	—	1015	541 ↑ 4%, 523 ↑ + Q_1 (22) 95%
1/2+	—	1040	411 ↓ + Q_1 (20) 100%
11/2−	—	1070	523 ↑ + Q_1 (22) 100%
5/2+	—	1090	402 ↑ 16%, 413 ↓ 6%, 411 ↓ + Q_1 (22) 75%
3/2+	—	1100	411 ↓ + Q_1 (22) 93%
7/2+	—	1250	413 ↑ 2%, 411 ↑ + Q_1 (22) 98%
1/2−	—	940	541 ↓ 94%, 411 ↓ + Q_1 (30) 4%
1/2−	—	1460	411 ↓ + Q_1 (31) 100%
9/2+	—	1440	523 ↑ + Q_1 (31) 100%
5/2+	—	1445	523 ↑ + Q_1 (31) 100%
5/2−	—	1500	53? ↑ 84%, 411 ↑ + Q_1 (31) 8%, 550 ↑ + Q_1 (22) 4%
5/2+	—	1530	413 ↓ 26%, 411 ↓ + Q_2 (22) 70%
5/2+	—	1640	413 ↓ 63%, 411 ↓ + Q_2 (22) 29%

TABLE 6.47. ^{169}Lu

K^π	Energy, keV		Structure
	exptl.	theor.	
7/2+	0	0	404 ↓ 97%, 402 ↓ + Q_1 (22) 2%
9/2−	—	60	514 ↑ 96%, 402 ↑ + Q_1 (32) 1%
1/2+	—	220	411 ↓ 90%, 411 ↓ + Q_1 (22) 6%
5/2+	—	540	402 ↑ 87%, 514 ↑ + Q_1 (32) 4%, 660 ↑ + Q_1 (22) 4%
3/2+	—	730	411 ↑ 39%, 411 ↓ + Q_1 (22) 56%
7/2−	493	740	523 ↑ 93%, 411 ↑ + Q_1 (32) 3%
1/2−	30	700	541 ↓ 97%, 532 ↓ + Q_1 (22) 2%
5/2+	—	1000	413 ↓ 6%, 411 ↓ + Q_1 (22) 93%
3/2+	—	1050	402 ↓ 10%, 404 ↓ + Q_1 (22) 89%
11/2+	—	1130	404 ↓ + Q_1 (22) 100%
1/2+	—	1270	411 ↓ + Q_1 (20) 100%
5/2−	—	1300	532 ↑ 2%, 514 ↑ + Q_1 (22) 97%
7/2+	—	1305	404 ↓ + Q_1 (20) 100%
13/2−	—	1310	514 ↑ + Q_1 (22) 100%
3/2−	—	1340	541 ↑ 12%, 523 ↑ + Q_1 (22) 85%
9/2−	—	1430	514 ↑ + Q_1 (20) 100%
11/2−	—	1450	523 ↑ + Q_1 (22) 100%
1/2+	—	1510	660 ↑ 30%, 402 ↑ + Q_1 (22) 63%, 402 ↓ + Q_1 (22) 2%
3/2−	—	1530	532 ↓ 59%, 411 ↓ + Q_1 (31) 22%, 541 ↓ + Q_1 (22) 9%
1/2−	—	1550	530 ↑ 7%, 411 ↓ + Q_1 (30) 85%, 411 ↓ + Q_1 (31) 7%
19/2−	—	1720	p404 ↓ n523 ↓ n633 ↑ 100%

TABLE 6.48. ^{171}Lu

K^π	Energy, keV		Structure
	exptl.	theor.	
7/2+	0	0	404 ↓ 97%
9/2−	469	55	514 ↑ 95%, 402 ↑ + Q_1 (32) 3%
1/2+	208	230	411 ↓ 91%, 411 ↑ + Q_1 (22) 5%
5/2+	296	470	402 ↑ 83%, 514 ↑ + Q_1 (32) 10%, 400 ↑ + Q_1 (22) 4%
1/2−	71	700	541 ↓ 98%
7/2−	662	760	523 ↑ 90%, 411 ↑ + Q_1 (32) 8%
3/2+		770	411 ↓ 48%, 411 ↓ + Q_1 (22) 41%, 523 ↑ + Q_1 (32) 9%
3/2+		1150	402 ↓ 13%, 404 ↓ + Q_1 (22) 85%
5/2+		1160	413 ↓ 8%, 411 ↓ + Q_1 (22) 91%
1/2+		1210	411 ↓ + Q_1 (20) 100%
3/2+		1280	411 ↓ + Q_1 (22) 100%
3/2+		1370	404 ↓ + Q_1 (22) 100%
1/2+		1440	411 ↓ + Q_2 (20) 100%
5/2−		1470	532 ↑ 10%, 514 ↑ + Q_1 (22) 63%, 411 ↓ + Q_1 (32) 26%
3/2−		1480	541 ↑ 14%, 523 ↑ + Q_1 (22) 44%, 411 ↓ + Q_1 (32) 39%
1/2−		1490	411 ↓ + Q_1 (30) 100%

TABLE 6.49. ^{173}Lu

K^π	Energy, keV exptl.	Energy, keV theor.	Structure
7/2+	0	0	404↓ 99%
9/2−	—	40	514↑ 97%, 402↑ + Q_1(32) 2%
1/2+	425	310	411↓ 98%
5/2+	357	600	402↑ 84%, 514↑ + Q_1(32) 14%
7/2−	—	720	523↑ 93%, 411↑ + Q_1(32) 6%
1/2−	128	680	541↓ 99%, 411↓ + Q_1(31) 1%
1/2+	—	1070	411↓ + Q_1(20) 100%
3/2+	—	1080	411↑ 67%, 523↑ + Q_1(32) 27%, 411↓ + Q_1(22) 2%
1/2−	—	1160	530↑ 1%, 411↓ + Q_1(31) 98%
3/2−	—	1170	532↓ 2%, 411↓ + Q_1(31) 98%
7/2+	—	1180	404↓ + Q_1(20) 100%
3/2−	—	1270	411↓ + Q_1(32) 100%
5/2−	—	1280	532↑ 3%, 411↓ + Q_1(32) 92%, 404↓ + Q_1(31) 4%
5/2−	—	1290	404↓ + Q_1(31) 95%, 411↓ + Q_1(32) 4%
5/2+	—	1330	642↑ 2%, 411↓ + Q_1(22) 97%
3/2+	—	1330	411↓ + Q_1(22) 100%
7/2+	—	1390	514↑ + Q_1(31) 100%
3/2−	—	1395	532↓ 5%, 404↓ + Q_1(32) 95%
11/2−	—	1400	404↓ + Q_1(32) 100%
3/2+	—	1450	404↓ + Q_1(22) 100%
11/2+	—	1460	404↓ + Q_2(22) 100%
9/2+	—	1500	404↑ 1%, 523↑ + Q_1(31) 99%
1/2−	—	1620	401↓ + Q_1(30) 100%

TABLE 6.50. ^{175}Lu

K^π	Energy, keV exptl.	Energy, keV theor.	Structure
7/2+	0	0	404↓ 99%
9/2−	396	100	514↑ 99%
1/2+	—	310	411↓ 97%
5/2+	343	700	402↑ 96%, 660↑ + Q_1(22) 2%
7/2−	—	850	523↑ 99%
1/2−	358	640	541↓ 98%
3/2+	—	1180	411↑ 69%, 411↓ + Q_1(22) 29%
3/2−	—	1280	411↓ + Q_1(32) 100%
5/2−	—	1280	411↓ + Q_1(32) 100%
19/2+	1401	1300	p404↓ n512↑ n514↓
1/2+	—	1340	411↓ + Q_1(20) 100%
21/2−	—	1360	p514↑ n512↑ n514↓
7/2+	—	1380	404↓ + Q_1(20) 100%
11/2−	—	1390	404↓ + Q_1(32) 100%
3/2−	—	1400	404↓ + Q_1(32) 100%
9/2−	—	1470	514↑ + Q_1(20) 100%
5/2+	—	1490	514↑ + Q_1(32) 100%
13/2+	—	1490	514↑ + Q_1(32) 100%
1/2−	—	1520	411↓ + Q_1(30) 100%
3/2−	—	1600	532↓ 9%, 411↓ + Q_1(31) 90%
3/2−	—	1680	532↓ 82%, 411↓ + Q_1(31) 10%

TABLE 6.51. ^{177}Lu

K^π	Energy, keV exptl.	Energy, keV theor.	Structure
7/2+	0	0	404↓ 97%, 404↓ + Q_1(20) 2,5%
9/2−	150	20	514↑ 98%
1/2+	570	150	411↓ 96%, 411↑ + Q_1(22) 2%
1/2−	—	480	541↓ 86%, 541↓ + Q_1(20) 10%
5/2+	458	670	402↑ 87%, 514↑ + Q_1(32) 5%, 402↑ + Q_1(20) 3%
7/2−	—	870	523↑ 93%, 411↑ + Q_1(32) 4%, 523↑ + Q_1(20) 1%
3/2+	—	900	411↑ 69%, 411↓ + Q_1(22) 22%, 523↑ + Q_1(32) 6%
7/2+	1148	1100	404↓ + Q_1(20) 100%
1/2+	—	1300	411↓ + Q_1(20) 100%
5/2+	—	1280	413↓ 7%, 411↓ + Q_1(22) 90%
23/2−	970	1350	p404↓ n514↓ n624↑ 100%
3/2+	—	1370	402↓ 6%, 404↓ + Q_1(22) 84%
11/2+	1307	1380	404↓ + Q_1(22) 100%
3/2+	—	1380	411↑ 16%, 411↓ + Q_1(22) 77%, 523↑ + Q_1(32) 5%
1/2−	—	1400	411↓ + Q_1(31) 100%
3/2−	—	1400	411↓ + Q_1(31) 100%
9/2−	—	1410	514↑ 0,5%, 514↑ + Q_1(20) 80%, 402↑ + Q_1(32) 19%
5/2−	—	1490	523↓ 0,4%, 411↓ + Q_1(32) 99%
3/2−	—	1500	411↓ + Q_1(32) 100%
11/2+	1230	1510	514↑ + Q_1(31) 100%
7/2+	1240	1510	514↑ + Q_1(31) 100%
25/2+	—	1510	p514↑ n514↓ n624↑ 100%
15/2+	1357	2000	p404↓ n514↓ n510↑ 100%
13/2+	1503	2000	p404↓ n514↓ n510↑ 100%

TABLE 6.52. ^{177}Ta

K^π	Energy, keV exptl.	Energy, keV theor.	Structure
7/2+	0	0	404↓ 99%
9/2−	74	—60	514↑ 99%
5/2+	71	180	402↑ 95%
1/2−	217	300	541↓ 99%, 532↓ + Q_1(22) 1%
1/2+	—	610	411↓ 92%, 411↑ + Q_1(22) 6%
3/2−	—	1020	532↓ 91%, 541↓ + Q_1(22) 6%, 530↑ + Q_1(22) 3%
3/2+	—	1130	402↓ 15%, 404↓ + Q_1(22) 83%
11/2−	—	1200	404↓ + Q_1(32) 100%
3/2−	—	1200	404↓ + Q_1(32) 100%
7/2+	—	1210	404↓ + Q_1(20) 100%
5/2+	—	1220	514↑ + Q_1(32) 100%
13/2+	—	1220	514↑ + Q_1(32) 100%
1/2+	—	1230	660↑ 36%, 402↑ + Q_1(22) 58%, 402↓ + Q_1(22) 3%
3/2+	—	1250	411↑ 43%, 411↓ + Q_1(22) 56%
9/2−	—	1260	514↑ + Q_1(20) 100%
7/2−	—	1270	523↑ 98%
5/2−	—	1300	532↑ 1%, 514↑ + Q_1(22) 99%
1/2−	—	1390	530↑ 90%, 532↓ + Q_1(22) 7%
23/2+	—	1460	p514↑ n512↑ n624↑ 100%
21/2−	—	1470	p514↑ n512↑ n514↓ 100%
1/2+	—	1490	400↑ 37%, 402↑ + Q_1(22) 58%, 402↓ + Q_1(22) 2%
21/2−	—	1510	p404↓ n512↑ n624↑ 100%

TABLE 6.53. ^{179}Ta

K^π	Energy, keV exptl.	Energy, keV theor.	Structure
7/2+	0	0	404↓ 100%
9/2−	31	20	514↑ 100%
5/2+	238	530	402↑ 96%, 660↑ + Q_1(22) 2%, 514↑ + Q_1(32) 1%
1/2+	520	740	411↓ 96%, 411↑ + Q_1(22) 3%
1/2−	750	750	541↓ 98%, 532↓ + Q_1(22) 1%
3/2+		1110	651↑ 1%, 404↓ + Q_1(22) 99%
11/2+		1120	404↓ + Q_1(22) 100%
5/2−		1120	514↑ + Q_1(22) 99%
13/2−		1130	514↑ + Q_1(22) 100%
7/2+		1130	514↑ + Q_1(31) 100%
5/2−		1130	404↓ + Q_1(31) 100%
3/2−		1180	532↓ 88%, 404↓ + Q_1(32) 9%, 541↓ + Q_1(22) 2%
7/2+		1180	404↓ + Q_1(20) 100%
7/2+		1220	514↑ + Q_1(31) 100%
9/2−		1220	514↑ + Q_1(20) 100%
11/2−		1230	404↓ + Q_1(32) 100%
3/2−		1230	532↓ 8%, 404↓ + Q_1(32) 91%
5/2+		1230	402↑ 1%, 514↑ + Q_1(32) 99%
13/2+		1240	514↑ + Q_1(32) 100%
23/2−		1300	p404↓ n514↓ n624↑ 100%
25/2+		1300	p514↑ n514↓ n624↑ 100%
3/2+		1470	411↑ 16%, 411↓ + Q_1(22) 84%
5/2+		1550	413↓ 1%, 411↓ + Q_1(22) 99%
1/2−		1590	411↓ + Q_1(31) 100%
3/2−		1590	411↓ + Q_1(31) 100%
21/2−		1600	p404↓ n512↑ n624↑ 100%

TABLE 6.54. ^{181}Ta

K^π	Energy, keV exptl.	Energy, keV theor.	Structure
7/2+	0	0	404↓ 100%
9/2−	6	10	514↑ 100%
5/2+	482	560	402↑ 98%, 660↑ + Q_1(22) 1%
1/2−		750	541↓ 99%, 532↓ + Q_1(22) 1%
1/2+	615	810	411↓ 97%, 411↑ + Q_1(22) 2%
3/2+		1120	404↓ + Q_1(22) 100%
11/2+		1130	404↓ + Q_1(22) 100%
7/2+		1130	514↑ + Q_1(31) 100%
5/2−		1130	404↓ + Q_1(31) 100%
9/2−		1130	404↓ + Q_1(31) 100%
5/2−		1140	514↑ + Q_1(22) 100%
13/2−		1140	514↑ + Q_1(22) 100%
3/2−		1200	532↓ 98%, 541↓ + Q_1(22) 1%
17/2−		1300	p404↓ n624↑ n510↑ 100%
19/2+		1300	p514↑ n624↑ n510↑ 100%
7/2+		1400	404↓ + Q_1(20) 100%
9/2−		1400	514↑ + Q_1(20) 100%
3/2+		1520	411↑ 12%, 411↓ + Q_1(22) 88%
5/2+		1580	413↓ 1%, 411↓ + Q_1(22) 99%
1/2−		1580	411↓ + Q_1(31) 100%
3/2−		1580	411↓ + Q_1(31) 100%
19/2−		1600	p404↓ n624↑ n512↓ 100%
7/2−		1690	523↑ 98%, 411↑ + Q_1(32) 1%
1/2−		1740	530↑ 96%, 532↓ + Q_1(22) 2%

TABLE 6.55. ^{181}Re

K^π	Energy, keV		Structure
	exptl.	theor.	
5/2+	0	0	402 ↑ 97%, 400 ↑ + Q_1 (22) 1,6%
1/2−	432	150	541 ↓ 92%, 541 ↓ + Q_1 (20) 6,7%
9/2−	262	360	514 ↑ 99%
7/2+	820	630	404 ↓ 95%, 404 ↓ + Q_1 (20) 4%
1/2+	932	930	400 ↑ 38%, 402 ↑ + Q_1 (22) 58%, 402 ↓ + Q_1 (22) 3%
9/2+		1020	404 ↑ 2%, 402 ↑ + Q_1 (22) 98%
1/2+	826	930	411 ↓ 95%, 411 ↑ + Q_1 (22) 2%, 530 ↑ + Q_1 (20) 5%
1/2−	1108	1040	530 ↓ 73%, 402 ↑ + Q_1 (32) 17%
11/2−	—	1130	505 ↑ 9%, 505 ↑ + Q_1 (20) 8%
3/2+	1060	1140	402 ↑ 57%, 400 ↑ + Q_1 (22) 39%, 402 ↓ + Q_1 (20) 3%
5/2+	—	1170	642 ↑ 0,2%, 514 ↑ + Q_1 (32) 99%
13/2+	—	1180	514 ↑ + Q_1 (32) 100%
9/2−	—	1190	402 ↑ + Q_1 (32) 100%
1/2−	—	1210	530 ↑ 15%, 402 ↑ + Q_1 (32) 82%
3/2−	867	1030	532 ↓ 44%, 532 ↓ + Q_1 (20) 6%, 541 ↓ + Q_1 (22) 45%
11/2−	—	1330	404 ↓ + Q_1 (32) 100%
3/2−	—	1340	532 ↓ 3%, 404 ↓ + Q_1 (32) 93%
3/2+	1060	1360	651 ↑ 7%, 541 ↓ + Q_1 (32) 92%
5/2+	—	1390	541 ↓ + Q_1 (32) 100%
1/2+	—	1420	660 ↑ 80%, 660 ↑ + Q_1 (20) 11%
3/2−	—	1490	402 ↑ + Q_1 (31) 100%
21/2−	—	1490	p402 ↑ n624 ↑ n514 ↓ 100%
7/2−	—	1500	402 ↑ + Q_1 (31) 100%
25/2+	—	1800	p514 ↑ n624 ↑ n514 ↓ 100%
25/2+	—	2700	p402 ↑ n624 ↑ n615 ↑ 100%

TABLE 6.56. ^{183}Re

K^π	Energy, keV		Structure
	exptl.	theor.	
5/2+	0	0	402 ↑ 98%, 400 ↑ + Q_1 (22) 2%
9/2−	496	430	514 ↑ 99%
1/2−	702	600	541 ↓ 89%, 541 ↓ + Q_1 (20) 9%
7/2+	851	900	404 ↓ 93%, 404 ↓ + Q_1 (20) 6%
1/2+	1102	970	411 ↓ 93%, 411 ↑ + Q_1 (22) 4%
11/2−	1301	1000	505 ↑ 92%, 505 ↑ + Q_1 (20) 7%
1/2+	889	1060	400 ↑ 28%, 402 ↑ + Q_1 (22) 70%
9/2+		1310	404 ↑ 0,7%, 402 ↑ + Q_1 (22) 99%
1/2−		1370	530 ↑ 0,4%, 402 ↑ + Q_1 (32) 99%
9/2−		1370	402 ↑ + Q_1 (32) 100%
5/2−		1390	532 ↑ 1,3%, 514 ↑ + Q_1 (22) 98%
13/2−		1400	514 ↑ + Q_1 (22) 100%
5/2+		1430	413 ↓ 0.2%, 514 ↑ + Q_1 (32) 99%
3/2+	1035	1500	402 ↓ 71%, 404 ↓ + Q_1 (22) 15%, 400 ↑ + Q_1 (22) 10%
3/2+	1354	1590	411 ↑ 29%, 411 ↓ + Q_1 (22) 68%
3/2−		1670	532 ↓ 69%, 541 ↓ + Q_1 (22) 19%, 532 ↓ + Q_1 (20) 5%
21/2−		2000	p402 ↑ n624 ↑ n514 ↓ 100%
25/2+	1907	2200	p402 ↑ n624 ↑ n615 ↑ 100%
25/2+		2300	p514 ↑ n624 ↑ n514 ↑ 100%

TABLE 6.57. ^{185}Re

K^π	Energy, keV		Structure
	exptl.	theor.	
5/2+	0	0	402 ↑ 96%, 400 ↑ + Q_1 (22) 3%
9/2−	387	460	514 ↑ 99%
1/2−	1045	620	541 ↓ 88%, 541 ↓ + Q_1 (20) 9,6%
1/2+	645	660	400 ↑ 18%, 402 ↑ + Q_1 (22) 80%, 402 ↓ + Q_1 (22) 2%
9/2+	966	860	404 ↑ 0,7%, 402 ↑ + Q_1 (22) 99%
7/2+	—	930	404 ↓ 92%, 404 ↓ + Q_1 (20) 6,7%
5/2−	—	940	532 ↑ 1%, 514 ↑ + Q_1 (22) 99%
1/2+	879	950	411 ↓ 89%, 402 ↑ + Q_1 (22) 5,8%, 411 ↑ + Q_1 (22) 4%
13/2−	—	960	514 ↑ + Q_1 (22) 100%
11/2−	1303	1030	505 ↑ 91%, 505 ↑ + Q_1 (20) 8%
3/2+	931	1210	402 ↓ 15%, 404 ↓ + Q_1 (22) 78%, 400 ↑ + Q_1 (22) 3%
3/2+	—	1210	411 ↑ 16%, 411 ↓ + Q_1 (22) 84%
11/2+	—	1260	404 ↓ + Q_1 (22) 100%
5/2+	—	1340	413 ↓ 3%, 411 ↓ + Q_1 (22) 97%
9/2−	—	1410	402 ↑ + Q_1 (32) 100%
5/2+	—	1410	402 ↑ 0,1%, 402 ↑ + Q_1 (20) 99%
1/2−	—	1410	402 ↑ + Q_1 (32) 100%
3/2−	—	1440	532 ↓ 24%, 541 ↓ + Q_1 (22) 68%
3/2+	—	1480	402 ↓ 61%, 404 ↓ + Q_1 (22) 19%, 400 ↑ + Q_1 (22) 19%
5/2−	—	1540	523 ↓ 3%, 541 ↓ + Q_1 (22) 97%

TABLE A.1. A = 155, Z = 0, RO = 1.24, VO = 48.2, $\varkappa$ = 0.39, α = 1.80. Basis Wave Functions

$+E$	$N+1$	L	J	A	$B1$	C	B	Nn
+11.55	1	8	8.5	6.1804	5.0937	5.1989	4.0103	0.5747
+4.05	1	6	5.5	5.3582	4.1796	4.3492	3.8315	0.5764
+0.86	2	4	4.5	5.3106	3.1596	3.8239	3.5535	0.3530
−5.19	1	6	6.5	5.7956	4.3681	4.6728	4.6309	0.5925
−12.48	2	2	1.5	4.3760	2.3197	2.9751	3.7338	0.3713
−12.53	3	0	0.5	3.5732	1.3184	2.1781	3.2696	0.1750
−14.92	2	2	2.5	4.5283	2.3138	2.9908	3.9003	0.3655
−15.72	1	4	3.5	4.9639	3.4602	3.7592	4.2957	0.5787
−20.36	1	4	4.5	5.3110	3.5065	3.8922	4.6417	0.5643
−30.47	2	0	0.5	3.3555	1.1949	1.8353	3.3090	0.3433
−31.94	1	2	1.5	4.4181	2.4844	2.8457	4.0936	0.5205
−33.47	1	2	2.5	4.6238	2.4841	2.8776	4.2370	0.5046
−43.80	1	0	0.5	3.2328	1.0729	1.4226	3.0329	0.3934

TABLE A.2. A = 155, Z = 0, RO = 1.24, VO = 48.2, $\varkappa$ = 0.39, α = 1.80. Basis Wave Functions

$+E$	$N+1$	L	J	A	$B1$	C	B	Nn
+14.81	1	7	6.5	5.5491	4.4437	4.4830	3.1266	0.5295
+3.02	1	7	7.5	5.9960	4.7491	4.9679	4.4424	0.5923
−3.05	3	1	0.5	4.1368	1.8546	2.7161	3.1158	0.1683
−3.21	2	3	2.5	4.7419	2.7571	3.3915	3.5304	0.3652
−4.36	3	1	1.5	4.1966	1.8517	2.7226	3.2637	0.1699
−6.20	1	5	4.5	5.1692	3.8459	4.0981	4.1765	0.5875
−6.93	2	3	3.5	4.9383	2.7603	3.4445	3.8837	0.3671
−13.01	1	5	5.5	5.5702	3.9564	4.3055	4.6891	0.5822
−21.59	2	1	0.5	3.9405	1.8157	2.4676	3.6462	0.3624
−22.83	2	1	1.5	4.0334	1.8099	2.4729	3.7197	0.3569
−24.34	1	3	2.5	4.7237	2.9954	3.3425	4.2657	0.5553
−27.21	1	3	3.5	5.0062	3.0260	3.4184	4.4994	0.5389
−38.43	1	1	0.5	3.9807	1.8641	2.2293	3.7328	0.4696
−39.04	1	1	1.5	4.1032	1.8627	2.2390	3.8042	0.4586

TABLE A.3. A = 155N

β_{20}	.280		.280	.280	.280	.280
β_{40}	.060		.060	.060	.060	.060
	Ω = 1/2		Ω = 3/2		Ω = 5/2	
Energy	−9.205	−8.476	−8.859	−7.899	−11.527	−6.796
$Nn_z\Lambda$	400	660	402	651	402	642
a	.190	6.521	0	0	0	0
1 8 17/2	−.023	.214	.018	.209	.001	.199
1 6 11/2	−.053	−.019	−.065	−.041	.048	−.075
2 4 9/2	−.085	.405	.072	.386	.081	.339
1 6 13/2	−.091	.846	.076	.866	.002	.902
2 2 3/2	.528	.036	.930	−.086	0	0
3 0 1/2	.770	.097	0	0	0	0
2 2 5/2	−.243	−.143	.219	−.113	.948	−.056
1 4 7/2	−.187	−.006	−.236	.036	.254	.026
1 4 9/2	.078	−.206	−.077	−.185	−.138	−.151
2 0 1/2	.071	.010	0	0	0	0
1 2 3/2	.046	.004	.092	−.010	0	0
1 2 5/2	−.041	−.009	.041	−.008	.096	−.004
1 0 1/2	.016	.002	0	0	0	0
	Ω = 7/2		Ω = 9/2	Ω = 11/2	Ω = 13/2	
Energy	−11.611	−5.287	−3.611	−1.957	−.420	
$Nn_z\Lambda$	404	633	624	615	606	
1 8 17/2	.001	.178	.145	.102	.055	
1 6 11/2	.098	−.096	−.100	−.080	0	
2 4 9/2	−.030	.252	.144	0	0	
1 6 13/2	.005	.940	.972	.992	.998	
1 4 7/2	.985	.027	0	0	0	
1 4 9/2	.136	−.102	−.055	0	0	

TABLE A.4. A = 155N

β_{20}	.280	.280	.280	.280	.280	.280
β_{40}	.060	.060	.060	.060	.060	.060
	$\Omega = 1/2$				$\Omega = 3/2$	
Energy	−10.820	−9.074	−5.230	−2.446	−8.830	−6.837
$Nn_z\Lambda$	541	530	521	510	532	524
a	1.307	−.178	.272	−.315	0	0
1 9 19/2	.017	−.021	.016	.010	.016	−.019
1 7 13/2	.119	.136	.104	−.078	.152	.115
1 7 15/2	.076	−.086	.060	.034	.068	−.077
3 1 1/2	.309	−.091	−.548	.081	0	0
2 3 5/2	.499	.223	−.370	.521	.447	.007
3 1 3/2	−.381	.473	.213	.668	−.199	.337
1 5 9/2	.533	.568	.430	−.298	.734	.480
2 3 7/2	−.260	.509	−.526	−.407	−.309	.749
1 5 11/2	.292	−.302	.189	.088	.278	−.266
2 1 1/2	−.116	.008	.060	−.027	0	0
2 1 3/2	.108	−.090	−.005	.048	.049	−.041
1 3 5/2	−.164	−.104	−.030	.030	−.133	−.050
1 3 7/2	.021	−.012	−.027	−.045	.023	.021
1 1 1/2	−.013	.001	.014	−.009	0	0
1 1 3/2	.016	−.016	−.000	.011	.009	−.010
	$\Omega = 3/2$		$\Omega = 5/2$		$\Omega = 7/2$	
Energy	−2.060	−.476	−6.474	−4.589	−3.869	−2.639
$Nn_z\Lambda$	512	501	523	512	514	503
1 9 19/2	−.009	.001	.012	−.012	.007	−.004
1 7 13/2	−.066	−.062	.149	.093	.118	.077
1 7 15/2	−.030	.002	.051	−.047	.029	−.014
2 3 5/2	.604	.651	.290	−.053	0	0
3 1 3/2	−.596	.691	0	0	0	0
1 5 9/2	−.290	−.252	.835	.429	.850	.484
2 3 7/2	.417	−.133	−.358	.875	−.471	.862
1 5 11/2	−.107	.008	.249	−.179	.202	−.063
2 1 3/2	−.050	.099	0	0	0	0
1 3 5/2	.041	.052	−.070	−.027	0	0
1 3 7/2	.053	−.020	.012	.069	−.022	.113
1 1 3/2	−.004	.024	0	0	0	0
	$\Omega = 9/2$		$\Omega = 11/2$			
Energy	−10.695	−.859	−9.008			
$Nn_z\Lambda$	514	505	505			
1 9 19/2	.018	.001	.009			
1 7 13/2	−.057	.089	−.040			
1 7 15/2	.117	.006	.068			
1 5 9/2	−.105	.990	0			
1 5 11/2	.986	.110	.997			

TABLE A.5. A = 155, Z = 63, RO = 1.24, VO = 59.2, $\varkappa$ = 0.36, α = 1.63.
Basis Wave Functions

$\pm E$	$N+1$	L	J	A	$B1$	C	B	Nn
+18.54	1	8	8.5	6.1289	5.0522	5.1668	4.2330	0.5880
+11.77	1	6	5.5	5.3327	4.1860	4.3412	3.9620	0.5854
+8.50	2	4	4.5	5.2821	3.2091	3.8683	3.7130	0.3642
+1.68	1	6	6.5	5.7487	4.4124	4.6732	4.7115	0.6018
−4.63	3	0	0.5	3.6026	1.3229	2.2035	3.3383	0.1762
−4.69	2	2	1.5	4.3864	2.3492	3.0122	3.8083	0.3760
−7.33	2	2	2.5	4.5420	2.3533	3.0464	3.9752	0.3711
−8.22	1	4	3.5	4.9442	3.4978	3.7829	4.3488	0.5862
−13.44	1	4	4.5	5.2830	3.5932	3.9481	4.6977	0.5763
−22.66	2	0	0.5	3.4244	1.2053	1.8808	3.3960	0.3440
−24.50	1	2	1.5	4.4369	2.5623	2.9281	4.1636	0.5316
−26.32	1	2	2.5	4.6505	2.5941	2.9938	4.3249	0.5194
−36.06	1	0	0.5	3.5079	1.1508	1.5890	3.3209	0.3968

TABLE A.6. A = 155, Z = 63, RO = 1.24, VO = 59.2, $\varkappa$ = 0.36, α = 1.63.
Basis Wave Functions

$+E$	$N+1$	L	J	A	$B1$	C	B	Nn
+22.70	1	7	6.5	5.5230	4.4144	4.4679	3.2466	0.5385
+9.92	1	7	7.5	5.9456	4.7559	4.9484	4.5612	0.6014
+5.18	3	1	0.5	4.1363	1.8685	2.7435	3.2096	0.1717
+4.69	2	3	2.5	4.7327	2.7889	3.4234	3.6426	0.3729
+3.68	3	1	1.5	4.2036	1.8650	2.7573	3.3543	0.1729
+1.38	1	5	4.5	5.1436	3.8722	4.0996	4.2500	0.5946
+0.62	2	3	3.5	4.9317	2.8029	3.4918	3.9746	0.3742
−6.12	1	5	5.5	5.5303	4.0177	4.3339	4.7478	0.5924
−13.79	2	1	0.5	3.9724	1.8374	2.5097	3.7165	0.3655
−15.12	2	1	1.5	4.0702	1.8378	2.5276	3.7945	0.3607
−16.89	1	3	2.5	4.7161	3.0663	3.3965	4.3173	0.5653
−20.21	1	3	3.5	4.9984	3.1230	3.5054	4.5629	0.5524
−30.89	1	1	0.5	4.0623	1.9575	2.3516	3.8569	0.4815
−31.66	1	1	1.5	4.2001	1.9751	2.3884	3.9508	0.4731

TABLE A.7. A = 155P

β_{20}	.280	.280	.280	.280	.280	.280
β_{40}	.060	.060	.060	.060	.060	.060
	Ω = 1/2					Ω = 3/2
Energy	−11.420	−8.799	−4.642	−2.065	−1.049	−9.464
$Nn_z\Lambda$	431	420	411	400	660	422
a	−2.688	1.627	−.519	6.518	.265	0
1 10 21/2	.002	−.003	.002	.058	.007	.002
1 8 17/2	.011	−.014	.008	.246	.031	.011
1 6 11/2	.165	.099	−.099	−.003	−.060	.170
2 4 9/2	−.013	.102	.109	.392	−.002	−.031
1 6 13/2	.049	−.063	.025	.834	.103	.049
3 0 1/2	−.199	.434	−.371	−.068	.780	0
2 2 3/2	.488	−.103	.681	−.104	.510	.306
2 2 5/2	−.156	.689	.458	−.104	−.271	−.199
1 4 7/2	.768	.406	−.363	.044	−.173	.871
1 4 9/2	.214	−.365	−.178	−.243	.029	.258
2 0 1/2	.057	−.063	.009	−.007	.082	0
1 2 3/2	−.169	−.018	.021	−.008	.050	−.089
1 2 5/2	.027	−.022	.043	.001	−.048	.028
1 0 1/2	.010	−.014	.003	−.002	.022	0
	Ω = 3/2			Ω = 5/2		
Energy	−6.275	−1.453	−.755	−6.835	−3.661	−.221
$Nn_z\Lambda$	411	402	651	413	402	642
1 10 21/2	−.001	.055	−.011	.001	.001	.051
1 8 17/2	−.003	.238	−.045	.005	.004	.229
1 6 11/2	.080	−.056	−.058	.151	.050	−.072
2 4 9/2	.134	.375	−.023	−.044	.098	.328
1 6 13/2	−.017	.845	−.157	.026	.014	.893
2 2 3/2	−.153	.165	.918	0	0	0
2 2 5/2	.877	−.066	.244	−.215	.946	−.076
1 4 7/2	.323	−.031	−.232	.937	.245	.025
1 4 9/2	−.277	−.224	−.023	.224	−.143	−.170
1 2 3/2	−.013	.016	.101	0	0	0
1 2 5/2	.040	.004	.046	.016	.108	−.006
	Ω = 7/2		Ω = 9/2			
Energy	−11.931	−3.768	−10.233			
$Nn_z\Lambda$	413	404	404			
1 10 21/2	.003	.000	.001			
1 8 17/2	.020	.001	.009			
1 6 11/2	−.064	.107	−.045			
2 4 9/2	−.052	−.033	−.113			
1 6 13/2	.129	.004	.074			
1 4 7/2	−.133	.984	0			
1 4 9/2	.979	.139	.990			

TABLE A.8. A = 155P

β_{20}	.280	.280	.280	.280	.280	.280
β_{40}	.060	.060	.060	.060	.060	.060
	$\Omega = 1/2$				$\Omega = 3/2$	
Energy	−11.698	−9.393	−3.568	−1.751	−8.614	−1.508
$Nn_z\Lambda$	301	550	541	530	541	532
a	.635	−5.462	1.552	−.401	0	0
1 9 19/2	.000	.046	.020	−.026	.045	.019
1 7 13/2	−.008	−.017	.134	.143	−.045	.167
1 7 15/2	.001	.213	.081	−.102	.214	.076
3 1 1/2	−.056	−.032	.295	−.098	0	0
2 3 5/2	.102	−.038	.496	.199	−.058	.441
3 1 3/2	−.052	.139	−.363	.477	.075	−.189
1 5 9/2	−.051	−.042	.553	.548	−.101	.743
2 3 7/2	.052	.417	−.259	.527	.368	−.297
1 5 11/2	−.001	.830	.267	−.298	.869	.264
2 1 1/2	.849	.024	−.128	.013	0	0
2 1 3/2	.401	−.121	.120	−.108	−.061	.054
1 3 5/2	−.286	.025	−.185	−.112	.041	−.150
1 3 7/2	−.098	−.224	.023	−.014	−.187	.025
1 1 1/2	.063	.000	−.015	.002	0	0
1 1 3/2	.048	−.008	.018	−.021	−.005	.011

$\Omega = 5/2$	$\Omega = 7/2$	$\Omega = 9/2$	$\Omega = 11/2$
Energy	−7.244	−5.507	−3.619	−1.737
$Nn_z\Lambda$	532	523	514	505
1 9 19/2	.041	.032	.021	.010
1 7 13/2	−.063	−.068	−.061	−.044
1 7 15/2	.203	.175	.131	.076
2 3 5/2	−.042	0	0	0
1 5 9/2	−.134	−.137	−.106	0
2 3 7/2	.278	.163	0	0
1 5 11/2	.916	.956	.984	.996
1 3 5/2	.030	0	0	0
1 3 7/2	−.128	−.067	0	0

TABLE A.9. A = 165, Z = 0, RO = 1.26, VO = 44.8, $\varkappa$ = 0.43, α = 1.67.
Basis Wave Functions

$+E$	$N+1$	L	J	A	$B1$	C	B	Nn
+10.69	1	8	8.5	6.4238	5.0276	5.1469	4.0257	0.5496
+3.99	1	6	5.5	5.5633	4.1374	4.3081	3.8102	0.5505
+0.67	2	4	4.5	5.5190	3.1474	3.8151	3.5741	0.3399
−4.75	1	6	6.5	6.0123	4.3356	4.6330	4.6230	0.5676
−11.53	2	2	1.5	4.5375	2.3098	2.9694	3.7228	0.3571
−11.64	3	0	0.5	3.7063	1.3084	2.1766	3.2596	0.1683
−13.83	2	2	2.5	4.6955	2.3072	2.9890	3.8896	0.3519
−14.35	1	4	3.5	5.1385	3.4279	3.7295	4.2689	0.5547
−18.80	1	4	4.5	5.5020	3.4891	3.8637	4.6235	0.5416
−28.20	2	0	0.5	3.4675	1.1886	1.8349	3.2825	0.3311
−29.50	1	2	1.5	4.5604	2.4676	2.8302	4.0542	0.5009
−30.97	1	2	2.5	4.7767	2.4740	2.8602	4.1995	0.4854
−40.63	1	0	0.5	3.3216	1.0705	1.4212	2.9797	0.3809

TABLE A.10. A = 165, Z = 0, RO = 1.26, VO = 44.8, $\varkappa$ = 0.43, α = 1.67.
Basis Wave Functions

$+E$	$N+1$	L	J	A	$B1$	C	B	Nn
+13.91	1	7	6.5	5.7730	4.3772	4.4250	3.0999	0.5029
+2.82	1	7	7.5	6.2262	4.7162	4.9314	4.4419	0.5675
−2.91	3	1	0.5	4.2959	1.8456	2.7151	3.1218	0.1622
−2.98	2	3	2.5	4.9225	2.7437	3.3799	3.5258	0.3508
−4.13	3	1	1.5	4.3581	1.8425	2.7233	3.2684	0.1656
−5.51	1	5	4.5	5.3577	3.8166	4.0597	4.1546	0.5624
−6.47	2	3	3.5	5.1259	2.7465	3.4306	3.8801	0.3526
−11.98	1	5	5.5	5.7753	3.9312	4.2833	4.6742	0.5588
−19.95	2	1	0.5	4.0785	1.8063	2.4623	3.6253	0.3488
−21.13	2	1	1.5	4.1776	1.8026	2.4690	3.7018	0.3436
−22.39	1	3	2.5	4.8819	2.9863	3.3237	4.2313	0.5342
−25.15	1	3	3.5	5.1782	3.0107	3.3999	4.4688	0.5180
−35.57	1	1	0.5	4.0999	1.8550	2.2182	3.6859	0.4529
−36.17	1	1	1.5	4.2320	1.8554	2.2333	3.7611	0.4424

TABLE A.11. A = 165N

β_{20}	.280	.280	.280	.280	.280	.280
β_{40}	.020	.020	.020	.020	.020	.020
Energy	−11.776	−8.384	−7.575	−8.041	−7.170	−10.545
$Nn_z\Lambda$	411	400	660	402	651	402
a	−.542	.160	6.628	0	0	0
1 8 17/2	−.005	0	.201	.002	.199	−.005
1 6 11/2	−.104	−.077	−.015	−.088	−.039	.067
2 4 9/2	.076	−.069	.417	.066	.395	.093
1 6 13/2	−.044	.009	.860	.002	.874	−.042
2 2 3/2	.673	.519	.007	.921	−.034	−.0
3 −0 1/2	−.365	.766	.020	0	0	0
2 2 5/2	.470	−.280	−.059	.240	−.048	.939
1 4 7/2	−.377	−.194	.001	−.252	.017	.260
1 4 9/2	−.175	.078	−.206	−.082	−.190	−.159
2 −0 1/2	.011	−.076	.001	0	0	0
1 2 3/2	.014	.047	.001	.096	−.004	0
1 2 5/2	.035	−.047	.005	.045	.005	.102
1 −0 1/2	.003	.017	−.000	0	0	0

	Ω = 5/2	Ω = 7/2		Ω = 9/2	Ω = 11/2
Energy	−6.381	−10.403	−5.250	−3.825	−2.100
$Nn_z\Lambda$	642	404	633	624	615
1 8 17/2	.193	.003	.183	.164	.135
1 6 11/2	−.068	.120	−.089	−.100	−.090
2 4 9/2	.351	−.031	.277	.178	0
1 6 13/2	.899	.026	.930	.961	.987
2 2 5/2	−.020	0	0	0	0
1 4 7/2	.013	.981	.014	0	0
1 4 9/2	−.164	.150	−.127	−.083	0
1 2 5/2	.005	0	0	0	0

TABLE A.12. A = 165N

β_{20}	.280	.280	.280	.280	.280	.280
β_{40}	.020	.020	.020	.020	.020	.020
	$\Omega = 1/2$				$\Omega = 3/2$	
Energy	−9.634	−8.405	−5.193	−2.634	−8.158	−6.698
$Nn_z\Lambda$	541	530	521	510	532	521
a	.518	.549	.369	−.218	0	0
1 9 19/2	.012	−.013	.016	.018	.013	−.016
1 7 13/2	.095	.137	.108	−.096	.132	.128
1 7 15/2	.083	−.085	.087	.087	.082	−.095
3 1 1/2	.310	−.030	−.582	.068	0	0
2 3 5/2	.467	.306	−.341	.531	.462	.069
3 1 3/2	−.451	.434	.220	.643	−.249	.346
1 5 9/2	.469	.610	.434	−.314	.680	.539
2 3 7/2	−.339	.479	−.499	−.411	−.374	.701
1 5 11/2	.293	−.258	.180	.093	.276	−.243
2 1 1/2	−.095	−.004	.078	−.034	0	0
2 1 3/2	.119	−.087	−.006	.041	.058	−.054
1 3 5/2	−.144	−.124	−.034	.029	−.137	−.069
1 3 7/2	.026	−.013	−.022	−.042	.023	.015
1 1 1/2	−.009	.001	.017	−.011	0	0
1 1 3/2	.018	−.016	.000	.009	.010	−.013

	$\Omega = 3/2$		$\Omega = 5/2$		$\Omega = 7/2$	
Energy	−2.213	−.398	−6.218	−4.616	−11.855	−3.687
$Nn_z\Lambda$	512	501	523	512	523	514
1 9 19/2	−.019	.015	.012	−.015	.018	.010
1 7 13/2	−.086	−.080	.143	.112	−.064	.132
1 7 15/2	−.092	.066	.076	−.089	.168	.066
2 3 5/2	.653	.586	.325	−.042	0	0
3 1 3/2	−.517	.732	0	0	0	0
1 5 9/2	−.327	−.236	.802	.472	−.136	.868
2 3 7/2	.409	−.194	−.395	.847	.193	−.426
1 5 11/2	−.111	.017	.249	−.180	.951	.207
2 1 3/2	−.017	.109	0	0	0	0
1 3 5/2	.042	.046	−.085	−.036	0	0
1 3 7/2	.048	−.029	.014	.062	−.083	−.014
1 1 3/2	−.000	.026	0	0	0	0

	$\Omega = 7/2$	$\Omega = 9/2$		$\Omega = 11/2$
Energy	−2.297	−10.214	−.356	−8.034
$Nn_z\Lambda$	503	514	505	505
1 9 19/2	−.010	.015	.005	.009
1 7 13/2	.091	−.063	.112	−.050
1 7 15/2	−.061	.146	.035	.105
1 5 9/2	.443	−.117	.986	0
2 3 7/2	.877	0	0	0
1 5 11/2	−.087	.980	.120	.993
1 3 7/2	.121	0	0	0

TABLE A.13. A = 165, Z = 67, RO = 1.25, VO = 59.2, $\varkappa$ = 0.355, α = 1.63. Basis Wave Functions

$+E$	$N+1$	L	J	A	B_1	C	B	Nn
+30.94	1	8	7.5	5.8358	4.6489	4.6100	3.4589	0.5347
+16.65	1	8	8.5	6.2531	5.1019	5.2461	4.4739	0.5928
+12.25	2	4	3.5	5.1611	3.1768	3.7779	3.1606	0.3430
+9.54	1	6	5.5	5.4592	4.2177	4.3997	4.1850	0.5871
+7.27	2	4	4.5	5.3818	3.2115	3.8909	3.9110	0.3662
+0.32	1	6	6.5	5.8778	4.4106	4.7047	4.8457	0.5956
−5.59	3	0	0.5	3.6883	1.3174	2.2085	3.4124	0.1739
−5.80	2	2	1.5	4.4959	2.3490	3.0310	3.9104	0.3716
−8.22	2	2	2.5	4.6500	2.3497	3.0566	4.0650	0.3659
−9.50	1	4	3.5	5.0785	3.5100	3.8192	4.4664	0.5784
−14.23	1	4	4.5	5.4140	3.5985	3.9718	4.7963	0.5675
−22.99	2	0	0.5	3.5282	1.1999	1.8870	3.4496	0.3363
−24.90	1	2	1.5	4.5758	2.5679	2.9543	4.2481	0.5208
−26.55	1	2	2.5	4.7862	2.6069	3.0205	4.4042	0.5099
−35.73	1	0	0.5	3.6592	1.1603	1.6157	3.3996	0.3862

TABLE A.14. A = 165, Z = 67, RO = 1.25, VO = 59.2, $\varkappa$ = 0.355, α = 1.63.
Basis Wave Functions

+E	N+1	L	J	A	B_1	C	B	Nn
+20.09	1	7	6.5	5.6387	4.4901	4.5810	3.6006	0.5567
+14.66	2	5	5.5	5.7176	3.5782	4.2113	3.2978	0.3379
+8.29	1	7	7.5	6.0738	4.7770	5.0032	4.7323	0.5995
+4.09	3	1	0.5	4.2188	1.8650	2.7537	3.3629	0.1724
+3.31	2	3	2.5	4.8373	2.7917	3.4496	3.8033	0.3726
+2.65	3	1	1.5	4.2864	1.8619	2.7626	3.4817	0.1726
−0.37	1	5	4.5	5.2767	3.8938	4.1510	4.4031	0.5902
−0.49	2	3	3.5	5.0372	2.8029	3.5069	4.0945	0.3712
−7.20	1	5	5.5	5.6605	4.0193	4.3671	4.8624	0.5851
−14.55	2	1	0.5	4.0824	1.8351	2.5198	3.7910	0.3589
−15.76	2	1	1.5	4.1780	1.8355	2.5355	3.8648	0.3542
−17.72	1	3	2.5	4.8530	3.0729	3.4247	4.4154	0.5554
−20.71	1	3	3.5	5.1304	3.1361	3.5327	4.6499	0.5436
−30.92	1	1	0.5	4.2039	1.9652	2.3764	3.9341	0.4705
−31.61	1	1	1.5	4.3401	1.9856	2.4128	4.0260	0.4629

TABLE A.15. A = 165P

β_{20}	.280	.280	.280	.280	.280	.280
β_{40}	.020	.020	.020	.020	.020	.020
	Ω = 1/2		Ω = 3/2			
Energy	−9.919	−6.223	−2.933	−2.029	−11.077	−7.654
$Nn_z\Lambda$	420	411	400	660	422	411
a	1.827	−.735	6.649	.391	0	0
1 10 21/2	−.001	−.001	.035	.003	.001	−.001
1 8 15/2	.011	−.015	−.011	−.011	.020	.013
1 8 17/2	−.012	−.008	.228	.017	.007	−.011
2 4 7/2	−.003	.084	−.013	.104	.082	−.049
1 6 11/2	.089	−.113	−.018	−.067	.184	.092
2 4 9/2	.085	.086	.401	−.072	−.023	.121
1 6 13/2	−.091	−.055	.852	.073	.060	−.082
3 0 1/2	.483	−.303	−.023	.795	0	0
2 2 3/2	−.148	.695	−.017	.448	.338	−.192
2 2 5/2	.701	.460	−.039	−.295	−.173	.864
1 4 7/2	.333	−.389	.015	−.184	.858	.322
1 4 9/2	−.332	−.174	−.240	.075	.248	−.281
2 0 1/2	−.082	.016	−.004	.086	0	0
1 2 3/2	−.005	.014	−.002	.050	−.110	−.010
1 2 5/2	−.034	.035	.011	−.056	.030	.027
1 0 1/2	−.020	.005	−.002	.025	0	0
	Ω = 3/2		Ω = 5/2			Ω = 7/2
Energy	−2.526	−1.916	−8.524	−4.504	−1.705	−5.220
$Nn_z\Lambda$	402	651	413	402	642	404
1 10 21/2	.035	−.002	.001	−.001	.033	.000
1 8 15/2	−.032	−.011	.018	.009	−.049	.012
1 8 17/2	.226	−.011	.006	−.008	.222	.004
2 4 7/2	−.024	.123	−.003	−.076	−.031	−.101
1 6 11/2	−.061	−.080	.172	.061	−.092	.129
2 4 9/2	.381	.059	−.037	.125	.339	−.031
1 6 13/2	.864	−.050	.052	−.055	.886	.031
2 2 3/2	.018	.901	0	0	0	0
2 2 5/2	−.036	.274	−.182	.938	−.029	0
1 4 7/2	.014	−.255	.939	.218	.021	.974
1 4 9/2	−.223	−.075	.227	−.175	−.191	.148
1 2 3/2	.002	.106	0	0	0	0
1 2 5/2	.009	.054	.023	.115	.005	0

	Ω = 7/2	Ω = 9/2
Energy	−.470	−10.914
$Nn_z\Lambda$	633	404
1 10 21/2	.030	.001
1 8 15/2	−.062	−.008
1 8 17/2	.213	.010
2 4 7/2	−.024	0
1 6 11/2	−.114	−.058
2 4 9/2	.273	−.123
1 6 13/2	.916	.116
1 4 7/2	.015	0
1 4 9/2	−.151	.984

TABLE A.16. A = 165P

β_{20}	.280	.280	.280	.280	.280	.280
β_{40}	.020	.020	.020	.020	.020	.020
	Ω =1/2			Ω =3/2		
Energy	−10.273	−4.463	−3.111	−9.677	−3.144	−1.168
$Nn_z\Lambda$	550	541	530	541	532	521
a	−5.547	2.452	−1.259	0	0	0
1 9 19/2	.031	.010	−.017	.030	.011	−.016
1 7 13/2	−0.14	.147	.120	−.039	.171	.115
2 5 11/2	.137	−.017	.062	.115	−.022	.099
1 7 15/2	.218	.064	−.105	.217	.070	−.102
3 1 1/2	−.022	.252	−.123	0	0	0
2 3 5/2	−.023	.503	.138	−.045	.442	−.032
3 1 3/2	.105	−.304	.519	.058	−.170	.370
1 5 9/2	−.034	.642	.472	−.088	.773	.407
2 3 7/2	.426	−.224	.555	.386	−.243	.750
1 5 11/2	.826	.209	−.328	.857	.229	−.303
2 1 1/2	.029	−.095	.031	0	0	0
2 1 3/2	−.052	.104	−.137	−.017	.052	−.077
1 3 5/2	.012	−.196	−.088	.028	−.167	−.046
1 3 7/2	−.227	.024	−.025	−.198	.027	.008
1 1 1/2	.003	−.009	.006	0	0	0
1 1 3/2	.002	.018	−.028	.004	.009	−.021

	Ω =5/2		Ω =7/2	Ω =9/2	Ω =11/2
Energy	−8.604	−1.102	−7.138	−5.248	−2.770
$Nn_z\Lambda$	532	523	523	514	505
1 9 19/2	.027	.011	.023	.017	.010
1 7 13/2	−.060	.176	−.070	−.069	−.054
2 5 11/2	.073	−.030	.015	−.049	−.111
1 7 15/2	.210	.069	.193	.163	.115
2 3 5/2	−.035	.301	0	0	0
1 5 9/2	−.128	.862	−.143	−.123	0
2 3 7/2	.307	.259	.198	0	0
1 5 11/2	.901	.226	.942	.975	.986
1 3 5/2	.019	−.102	0	0	0
1 3 7/2	−.152	.023	−.098	0	0

TABLE A.17. A = 173, Z = 0, RO = 1.26, VO = 44.8, $\varkappa$ = 0.42, α = 1.67.
Basis Wave Functions

$+E$	$N+1$	L	J	A	$B1$	C	B	Nn
+9.60	1	8	8.5	6.4913	5.0465	5.1848	4.1798	0.5535
+2.59	1	6	5.5	5.6344	4.1557	4.3458	3.9529	0.5532
−0.12	2	4	4.5	5.5662	3.1452	3.8219	3.6942	0.3420
−5.62	1	6	6.5	6.0810	4.3377	4.6510	4.6957	0.5650
−12.38	2	2	1.5	4.5954	2.3058	2.9723	3.7811	0.3548
−12.39	3	0	0.5	3.7483	1.3058	2.1794	3.3005	0.1675
−14.55	2	2	2.5	4.7513	2.3043	2.9908	3.9388	0.3494
−15.30	1	4	3.5	5.2146	3.4353	3.7480	4.3376	0.5508
−19.43	1	4	4.5	5.5693	3.4872	3.8668	4.6717	0.5368
−28.66	2	0	0.5	3.5161	1.1845	1.8353	3.3047	0.3274
−29.99	1	2	1.5	4.6311	2.4664	2.8310	4.0934	0.4945
−31.35	1	2	2.5	4.8417	2.4740	2.8675	4.2325	0.4805
−40.77	1	0	0.5	3.3794	1.0656	1.4191	2.9979	0.3744

TABLE A.18. A = 173, Z = 0, RO = 1.26, VO = 44.8, $\varkappa$ = 0.42, α = 1.67.
Basis Wave Functions

$+E$	$N+1$	L	J	A	$B1$	C	B	Nn
+12.33	1	7	6.5	5.8370	4.4096	4.4886	3.1600	0.5052
+1.84	1	7	7.5	6.2936	4.7064	4.9484	4.5355	0.5660
—3.67	3	1	0.5	4.3353	1.8427	2.7178	3.2126	0.1630
—3.93	2	3	2.5	4.9769	2.7426	3.3909	3.6257	0.3515
—4.87	3	1	1.5	4.3969	1.8402	2.7235	3.3419	0.1639
—6.69	1	5	4.5	5.4329	3.8244	4.0830	4.2448	0.5602
—7.25	2	3	3.5	5.1784	2.7449	3.4358	3.9470	0.3516
—12.73	1	5	5.5	5.8425	3.9264	4.2851	4.7337	0.5544
—20.63	2	1	0.5	4.1350	1.8046	2.4630	3.6642	0.3454
—21.73	2	1	1.5	4.2298	1.8003	2.4705	3.7354	0.3405
—23.09	1	3	2.5	4.9576	2.9801	3.3290	4.2854	0.5281
—25.65	1	3	3.5	5.2450	3.0105	3.4035	4.5109	0.5130
—35.88	1	1	0.5	4.1689	1.8518	2.2210	3.7160	0.4464
—36.43	1	1	1.5	4.2948	1.8554	2.2351	3.7869	0.4369

TABLE A.19. A = 173N

β_{20}	.260	.260	.260	.260	.260	.260
β_{40}	—.020	—.020	—.020	—.020	—.020	—.020
	$\Omega = 1/2$			$\Omega = 3/2$		
Energy	—9.296	—7.899	—.338	—9.058	—7.680	—0.062
$Nn_z\Lambda$	400	660	651	402	651	642
a	.259	6.659	5.329	0	0	0
1 8 17/2	.011	.176	—.165	—.010	.177	—.159
1 6 11/2	—.091	—.010	—.016	—.104	—.037	—.025
2 4 9/2	—.066	.404	.898	.059	.385	.908
1 6 13/2	.073	.877	—.374	—.061	.887	—.356
2 2 3/2	.502	—.010	.002	.914	.011	—.039
3 0 1/2	.767	—.019	.050	0	0	0
2 2 5/2	—.297	.011	—.150	.251	.008	—.139
1 4 7/2	—.190	.003	.004	—.255	—.003	.018
1 4 9/2	.083	—.187	.019	—.083	—.180	.026
2 0 1/2	.074	—.005	.010	0	0	0
1 2 3/2	.045	—.001	.001	.094	.003	—.008
1 2 5/2	—.049	.016	—.030	.046	.014	—.027
1 0 1/2	.017	—.002	.002	0	0	0
	$\Omega = 5/2$		$\Omega = 7/2$		$\Omega = 9/2$	$\Omega = 11/2$
Energy	—11.409	—7.213	—11.583	—6.441	—5.253	—3.483
$Nn_z\Lambda$	402	642	404	633	624	615
1 8 17/2	—.009	.179	.005	.179	.175	.161
1 6 11/2	.076	—.059	.134	—.083	—.098	—.095
2 4 9/2	.104	.347	—.033	.286	.198	0
1 6 13/2	—.081	.903	.046	.927	.954	.982
2 2 5/2	.937	.012	0	0	0	0
1 4 7/2	.241	.002	.977	—.000	0	0
1 4 9/2	—.176	—.168	.158	—.144	—.106	0
1 2 5/2	.100	.012	0	0	0	0

	$\Omega = 13/2$
Energy	—.865
$Nn_z\Lambda$	606
1 8 17/2	.125
1 6 13/2	.992

TABLE A.20. A = 173N

β_{20}	.260	.260	.260	.260	.260	.260
β_{40}	—.020	—.020	—.020	—.020	—.020	—.020
	Ω =1/2					Ω =3/2
Energy	—9.934	—9.240	—6.397	—3.872	—.390	—9.122
$Nn_z\Lambda$	541	530	521	510	501	532
a	.557	.614	.552	—.239	.625	0
1 9 19/2	—.006	—.007	—.012	.019	.052	.007
1 7 13/2	—.088	.122	—.102	—.102	.078	.122
1 7 15/2	—.078	—.084	—.097	.119	.234	.079
3 1 1/2	—.271	—.026	.609	.025	.722	0
2 3 5/2	—.445	.306	.380	.546	—.484	.462
3 1 3/2	.457	.434	—.229	.631	.340	—.244
1 5 9/2	—.503	.618	—.409	—.304	.167	.703
2 3 7/2	.399	.489	.456	—.414	—.151	—.367
1 5 11/2	—.242	—.227	—.163	.102	.002	.231
2 1 1/2	.067	.001	—.095	—.033	.095	0
2 1 3/2	—.110	—.093	.011	.030	.054	.058
1 3 5/2	.131	—.117	.021	.022	—.043	—.139
1 3 7/2	—.030	—.020	.015	—.039	—.025	.026
1 1 1/2	.005	.003	—.021	—.011	.021	0
1 1 3/2	—.018	—.017	.001	.007	.013	.009
	Ω =3/2			Ω =5/2		Ω =7/2
Energy	—7.933	—3.518	—1.162	—7.649	—5.922	—5.266
$Nn_z\Lambda$	521	512	501	523	512	514
1 9 19/2	—.011	—.019	.030	.008	—.015	.010
1 7 13/2	.117	—.102	—.087	.142	.108	.148
1 7 15/2	—.109	—.121	.147	.082	—.124	.081
2 3 5/2	.059	.718	.505	.033	—.073	0
3 1 3/2	.369	—.423	.775	0	0	0
1 5 9/2	.520	—.346	—.198	.830	.423	.920
2 3 7/2	.705	.380	—.241	—.339	.862	—.296
1 5 11/2	—.241	—.112	.025	.220	—.203	.192
2 1 3/2	—.069	—.001	.111	0	0	0
1 3 5/2	—.064	.037	.040	—.098	—.030	0
1 3 7/2	.002	.041	—.036	.021	.049	.006
1 1 3/2	—.017	.003	.027	0	0	0

	Ω =7/2	Ω =9/2		Ω =11/2
Energy	—3.184	—11.445	—1.783	—8.867
$Nn_z\Lambda$	503	514	505	505
1 9 19/2	—.018	.010	.009	.009
1 7 13/2	0.85	—.065	.128	—.057
1 7 15/2	—.120	.165	.063	.138
1 5 9/2	.318	—.125	.982	0
2 3 7/2	.920	0	0	0
1 5 11/2	—.122	.976	.124	.989
1 3 7/2	.123	0	0	0

TABLE A.21. A = 173, Z = 71, RO = 1.25, VO = 59.2, $\varkappa$ = 0.32, α = 1.59. Basis Wave Functions

$+E$	$N+1$	L	J	A	$B1$	C	B	Nn
+29.15	1	8	7.5	5.9392	4.6606	4.6455	3.3820	0.5231
+16.74	1	8	8.5	6.3181	5.0518	5.2013	4.4832	0.5835
+11.57	2	4	3.5	5.2368	3.1794	3.7913	3.3911	0.3495
+9.70	3	2	2.5	4.8620	2.3152	3.2195	3.0383	0.1566
+8.56	1	6	5.5	5.5577	4.2267	4.4195	4.2783	0.5823
+7.19	2	4	4.5	5.4384	3.2056	3.8867	3.9608	0.3639
+0.58	1	6	6.5	5.9334	4.3962	4.6816	4.8518	0.5884
—5.60	3	0	0.5	3.7406	1.3140	2.2126	3.4399	0.1722
—6.00	2	2	1.5	4.5682	2.3460	3.0328	3.9532	0.3673
—8.09	2	2	2.5	4.7060	2.3510	3.0619	4.0869	0.3626
—9.74	1	4	3.5	5.1674	3.5181	3.8295	4.5118	0.5711
—13.84	1	4	4.5	5.4674	3.5958	3.9654	4.8003	0.5616
—22.57	2	0	0.5	3.5820	1.1977	1.8934	3.4642	0.3323
—24.56	1	2	1.5	4.6524	2.5792	2.9648	4.2714	0.5144
—25.99	1	2	2.5	4.8411	2.6039	3.0191	4.4105	0.5041
—34.97	1	0	0.5	3.7247	1.1672	1.6287	3.4161	0.3818

TABLE A.22. A = 173, Z = 71, RO = 1.25, VO = 59.2, $\varkappa$ = 0.32, α = 1.59.
Basis Wave Functions

$+E$	$N+1$	L	J	A	$B1$	C	B	Nn
+18.70	1	7	6.5	5.7413	4.4802	4.5967	3.8083	0.5587
+14.55	2	5	5.5	5.7717	3.5721	4.2052	3.3339	0.3361
+8.48	1	7	7.5	6.1320	4.7353	4.9660	4.7381	0 5908
+3.79	3	1	0.5	4.2765	1.8627	2.7549	3.4245	0.1715
+2.82	2	3	2.5	4.9134	2.7883	3.4522	3.8752	0.3696
+2.54	3	1	1.5	4.3389	1.8603	2.7664	3.5268	0.1716
−0.47	2	3	3.5	5.0937	2.8009	3.5058	4.1251	0.3680
−0.96	1	5	4.5	5.3702	3.8921	4.1582	4.4645	0.5829
−6.88	1	5	5.5	5.7145	4.0127	4.3476	4.8692	0.5783
−14.42	2	1	0.5	4.1467	1.8348	2.5280	3.8163	0.3547
−15.48	2	1	1.5	4.2328	1.8351	2.5397	3.8813	0.3504
−17.64	1	3	2.5	4.9351	3.0772	3.4346	4.4469	0.5482
−20.24	1	3	3.5	5.1841	3.1338	3.5264	4.6549	0.5375
−30.36	1	1	0.5	4.2760	1.9693	2.3845	3.9523	0.4640
−30.96	1	1	1.5	4.4006	1.9865	2.4189	4.0384	0.4574

TABLE A.23. A = 173P

β_{20}	.260	.260	.260	.260	.260	.260
β_{10}	−0.20	−.020	−.020	−.020	−.020	−.020
	Ω = 1/2				Ω = 3/2	
Energy	−9.995	−6.761	−2.333	−2.110	−11.420	−8.006
$Nn_z\Lambda$	420	411	400	660	422	411
a	2.017	−.775	1.828	5.236	0	0
1 10 21/2	.001	.000	.004	.008	−.001	.001
1 8 15/2	.005	−.011	−.014	−.002	.008	.009
1 8 17/2	−.008	−.011	.098	.165	.004	−.012
2 4 7/2	−.006	.076	.094	−.056	.085	−.044
3 2 5/2	.057	.001	.062	.080	−.004	.018
1 6 11/2	.069	−.120	−.082	.020	.173	.094
2 4 9/2	.072	.072	.098	.414	−.012	.106
1 6 13/2	−.107	−.091	.451	.730	.060	−.121
3 0 1/2	.517	−.279	.701	−.367	0	0
2 2 3/2	−.191	.715	.387	−.186	.350	−.220
2 2 5/2	.710	.450	−.283	.143	−.153	.861
1 4 7/2	.253	−.377	−.162	.081	.869	.302
1 4 9/2	−.304	−.175	−.012	−.240	.206	−.285
2 0 1/2	−.094	.021	.073	−.041	0	0
1 2 3/2	.008	.003	.044	−.021	−.122	−.005
1 2 5/2	−.043	.025	−.044	.041	.029	.012
1 0 1/2	−.023	.006	.022	−.013	0	0

	Ω = 3/2		Ω = 5/2			Ω = 7/2
Energy	−2.399	−1.904	−9.201	−4.607	−1.408	−5.756
$Nn_z\Lambda$	402	651	413	402	642	404
1 10 21/2	−.002	.010	−.000	−.000	.012	.000
1 8 15/2	−.008	−.026	.011	.011	−.040	.011
1 8 17/2	−.040	.192	.006	−.019	.200	.007
2 4 7/2	.135	.000	.007	−.077	−.029	−.101
3 2 5/2	−.023	.076	.015	−.044	.042	0
1 6 11/2	−.091	−.067	.176	.075	−.082	.144
2 4 9/2	.017	.400	−.026	.122	.355	−.030
1 6 13/2	−.192	.847	.071	−.120	.883	.055
2 2 3/2	.878	.138	0	0	0	0
2 2 5/2	.284	.051	−.166	.931	.033	0
1 4 7/2	−.258	−.032	.940	.206	.011	.969
1 4 9/2	−.057	−.224	.225	−.185	−.202	.160
1 2 3/2	.102	.017	0	0	0	0
1 2 5/2	.051	.024	.027	.113	.017	0

	Ω = 7/2	Ω = 9/2
Energy	−.569	−10.594
$Nn_z\Lambda$	633	404
1 10 21/2	.014	−.000
1 8 15/2	−.055	−.008
1 8 17/2	.205	.011
2 4 7/2	−.018	0
1 6 11/2	−.110	−.065
2 4 9/2	.287	−.117
1 6 13/2	.911	.147
1 4 7/2	−.001	0
1 4 9/2	−.172	.980

TABLE A.24. A = 173P

β_{20}	.260	.260	.260	.260	.260	.260
β_{40}	—.020	—.020	—.020	—.020	—.020	—.020
	Ω =1/2			Ω =3/2		
Energy	—9.262	—4.157	—3.078	—9.011	—3.501	—1.645
$Nn_z\Lambda$	550	541	530	541	532	521
a	—5.631	3.708	—2.404	0	0	0
1 9 19/2	.005	—.003	—.011	.006	.006	—.014
1 7 13/2	—.010	—.155	.077	—.029	.164	.098
2 5 11/2	.117	.007	.050	.102	—.010	.078
1 7 15/2	.187	—.038	—.120	.189	.061	—.130
3 1 1/2	—.011	—.186	—.158	0	0	0
2 3 5/2	—.007	—.501	.036	—.029	.441	—.072
3 1 3/2	.063	.189	.581	.038	—.142	.407
2 3 7/2	.407	.144	.619	.380	—.193	.760
1 5 9/2	—.025	—.759	.318	—.070	.810	.344
1 5 11/2	.861	—.109	—.314	.875	.170	—.299
2 1 1/2	.019	.051	.042	0	0	0
2 1 3/2	.015	—.059	—.157	.022	.042	—.099
1 3 5/2	—.002	.193	—.045	.011	—.171	—.033
1 3 7/2	—.196	—.017	—.036	—.188	.025	—.007
1 1 1/2	.004	.001	.007	0	0	0
1 1 3/2	.011	—.010	—.033	.011	.006	—.026

	Ω =5/2		Ω =7/2	Ω =9/2	Ω =11/2
Energy	—8.428	—2.013	—7.335	—5.483	—2.511
$Nn_z\Lambda$	532	523	523	514	505
1 9 19/2	.008	.008	.011	0.13	.012
1 7 13/2	—.050	.175	—.066	—.073	—.061
2 5 11/2	.073	—.016	.029	—.033	—.106
1 7 15/2	.194	.075	.195	.187	.151
2 3 5/2	—.026	.309	0	0	0
2 3 7/2	.318	—.206	.222	0	0
1 5 9/2	—.118	.878	—.145	—.137	0
1 5 11/2	.901	.198	.933	.969	.981
1 3 5/2	.006	—.119	0	0	0
1 3 7/2	—.164	.026	—.123	0	0

TABLE A.25. A = 181, Z = 0, RO = 1.26, VO = 43.4, $\varkappa$ = 0.40, α = 1.67.
Basis Wave Functions

$+E$	$N+1$	L	J	A	$B1$	C	B	Nn
+9.77	1	8	8.5	6.5570	5.0263	5.1719	4.1390	0.5434
+2.18	1	6	5.5	5.7372	4.1666	4.3651	4.0035	0.5471
+0.08	2	4	4.5	5.6424	3.1445	3.8212	3.6800	0.3368
—5.18	1	6	6.5	6.1609	4.3211	4.6391	4.6916	0.5564
—11.98	3	0	0.5	3.8074	1.3015	2.1800	3.3059	0.1650
—12.07	2	2	1.5	4.6736	2.3031	2.9750	3.7963	0.3495
—14.02	2	2	2.5	4.8195	2.3018	2.9927	3.9401	0.3446
—15.01	1	4	3.5	5.3100	3.4355	3.7590	4.3614	0.5425
—18.71	1	4	4.5	5.6469	3.4872	3.8745	4.6745	0.5300
—27.79	2	0	0.5	3.5767	1.1823	1.8373	3.3102	0.3222
—29.15	1	2	1.5	4.7180	2.4692	2.8386	4.1089	0.4867
—30.37	1	2	2.5	4.9194	2.4684	2.8660	4.2423	0.4728
—39.52	1	0	0.5	3.4411	1.0660	1.4212	2.9992	0.3680

TABLE A.26. A = 181, Z = 0, RO = 1.26, VO = 43.4, $\varkappa$ = 0.40, α = 1.67.
Basis Wave Functions

$+E$	$N+1$	L	J	A	$B1$	C	B	Nn
+11.57	1	7	6.5	5.9402	4.4319	4.5233	3.2068	0.5017
+2.14	1	7	7.5	6.3765	4.6918	4.9385	4.5224	0.5572
—3.55	3	1	0.5	4.4029	1.8400	2.7183	3.2219	0.1607
—3.90	2	3	2.5	5.0613	2.7404	3.3953	3.6495	0.3468
—4.64	3	1	1.5	4.4623	1.8376	2.7250	3.3432	0.1615
—6.73	1	5	4.5	5.5327	3.8186	4.0982	4.2784	0.5523
—6.89	2	3	3.5	5.2510	2.7427	3.4388	3.9472	0.3468
—12.15	1	5	5.5	5.9208	3.9193	4.2836	4.7339	0.5468
—20.06	2	1	0.5	4.2081	1.8005	2.4673	3.6765	0.3401
—21.03	2	1	1.5	4.2965	1.7964	2.4718	3.7401	0.3354
—22.52	1	3	2.5	5.0492	2.9806	3.3381	4.3053	0.5200
—24.81	1	3	3.5	5.3230	3.0079	3.4038	4.5185	0.5056
—34.83	1	1	0.5	4.2497	1.8521	2.2245	3.7284	0.4387
—35.32	1	1	1.5	4.3698	1.8509	2.2331	3.7959	0.4292

TABLE A.27. A = 181N

β_{20}	.240	.240	.240	.240	.240	.240
β_{40}	—.030	—.030	—.030	—.030	—.030	—.030
	$\Omega = 1/2$			$\Omega = 3/2$		$\Omega = 5/2$
Energy	—9.231	—7.138	—.203	—9.108	—6.989	—11.192
$Nn_z\Lambda$	400	660	651	402	651	402
a	.323	6.689	5.297	0	0	0
1 8 17/2	.009	.101	—.156	—.008	.164	—.008
1 6 11/2	—.086	—.010	—.020	—.100	—.035	.071
2 4 9/2	—.067	.387	.907	.059	.370	.101
1 6 13/2	.069	.891	—.358	—.059	.898	—.082
3 0 1/2	.775	—.015	.051	0	0	0
2 2 3/2	.490	—.007	.001	.915	.009	0
2 2 5/2	—.305	.023	—.141	.257	.018	.942
1 4 7/2	—.182	.001	.004	—.250	—.004	.223
1 4 9/2	.087	—.169	.014	—.085	—.166	—.180
2 0 1/2	.069	—.004	.010	0	0	0
1 2 3/2	.042	—.001	.001	.087	.002	0
1 2 5/2	—.047	.016	—.028	.043	.014	.093
1 0 1/2	.016	—.001	.002	0	0	0
$\Omega = 5/2$		$\Omega = 7/2$		$\Omega = 9/2$	$\Omega = 11/2$	$\Omega = 13/2$
Energy	—6.646	—11.712	—6.025	—4.989	—3.345	—.813
$Nn_z\Lambda$	642	404	633	624	615	606
1 8 17/2	.167	.004	.169	.168	.158	.125
1 6 11/2	—.056	.130	—.080	—.097	—.096	0
2 4 9/2	.337	—.031	.281	.197	0	0
1 6 13/2	.911	.045	.931	.955	.983	.992
2 2 5/2	.017	0	0	0	0	0
1 4 7/2	—.000	.977	—.001	0	0	0
1 4 9/2	—.159	.159	—.140	—.105	0	0
1 2 5/2	.012	0	0	0	0	0

TABLE A.28. A = 181N

β_{20}	.240	.240	.240	.240	.240	.240
β_{40}	—.030	—.030	—.030	—.030	—.030	—.030
	$\Omega = 1/2$					$\Omega = 3/2$
Energy	—9.368	—8.856	—6.255	—3.924	—.562	—8.857
$Nn_z\Lambda$	541	530	521	510	501	532
a	2.020	—.761	.659	—.287	.828	0
1 9 19/2	—.003	—.005	—.008	.014	.029	.004
1 7 13/2	—.104	.094	—.093	—.096	.076	.123
1 7 15/2	—.058	—.090	—.087	.109	.153	.064
3 1 1/2	—.233	—.082	.618	—.002	.736	0
2 3 5/2	—.475	.201	.422	.550	—.479	.454
3 1 3/2	.357	.513	—.230	.635	.361	—.206
1 5 9/2	—.642	.514	—.385	—.289	.161	.760
2 3 7/2	.327	.571	.435	—.418	—.170	—.310
1 5 11/2	—.175	—.248	—.154	.108	.025	.191
2 1 1/2	.051	.015	—.096	—.030	.090	0
2 1 3/2	—.081	—.109	.012	.024	.054	.048
1 3 5/2	.139	—.082	.011	.017	—.041	—.137
1 3 7/2	—.025	—.027	.012	—.036	—.028	.025
1 1 1/2	.003	.004	—.021	—.010	.020	0
1 1 3/2	—.013	—.020	.001	.006	.013	.007
	$\Omega = 3/2$			$\Omega = 5/2$		
Energy	—7.720	—3.653	—1.285	—7.661	—5.855	—.227
$Nn_z\Lambda$	521	512	501	523	512	503
1 9 19/2	—.008	—.014	.021	.006	—.012	—.028
1 7 13/2	.098	—.100	—.080	.139	.094	—.084
1 7 15/2	—.109	—.106	.124	.071	—.122	—.151
2 3 5/2	.008	.746	.476	.323	—.099	.929
3 1 3/2	.392	—.390	.797	0	0	0
1 5 9/2	.454	—.342	—.181	.859	.375	—.240
2 3 7/2	.740	.371	—.260	—.290	.882	.186
1 5 11/2	—.251	—.114	.039	.199	—.215	—.038
2 1 3/2	—.075	.003	.106	0	0	0
1 3 5/2	—.047	.031	.036	—.097	—.022	.108
1 3 7/2	—.005	.036	—.037	.023	.041	.039
1 1 3/2	—.018	.004	.026	0	0	0
	$\Omega = 7/2$		$\Omega = 9/2$		$\Omega = 11/2$	
Energy	—5.545	—3.202	—11.078	—2.345	—8.614	
$Nn_z\Lambda$	514	503	514	505	505	
1 9 19/2	.007	—.015	.007	.007	.008	
1 7 13/2	.145	.075	—.062	.125	—.054	
1 7 15/2	.073	—.119	.160	.058	.136	
1 5 9/2	.937	.270	—.126	.982	0	
2 3 7/2	—.248	.936	0	0	0	
1 5 11/2	.183	—.135	.977	.126	.989	
1 3 7/2	.012	.116	0	0	0	

TABLE A.29. A = 181, Z = 73, RO = 1.24, VO = 59.8, $\varkappa$ = 0.33, α = 1.67. Basis Wave Functions

$+E$	$N+l$	L	J	A	$B1$	C	B	Nn
+28.50	1	8	7.5	5.9136	4.7723	4.7994	3.4372	0.5393
+15.56	1	8	8.5	6.3411	5.1282	5.3220	4.6709	0.5978
+11.22	2	4	3.5	5.2348	3.1932	3.8284	3.5410	0.3582
+9.52	3	2	2.5	4.8602	2.3169	3.2303	3.1949	0.1609
+7.62	1	6	5.5	5.5726	4.2715	4.4907	4.4029	0.5920
+6.62	2	4	4.5	5.4545	3.2171	3.9221	4.0708	0.3685
—0.51	1	6	6.5	5.9737	4.4436	4.7621	4.9762	0.5952
—6.16	3	0	0.5	3.7625	1.3128	2.2153	3.4902	0.1724
—6.62	2	2	1.5	4.5951	2.3499	3.0486	4.0211	0.3684
—8.77	2	2	2.5	4.7420	2.3533	3.0759	4.1596	0.3630
—10.63	1	4	3.5	5.2064	3.5505	3.8812	4.6062	0.5751
—14.74	1	4	4.5	5.5222	3.6181	4.0136	4.9044	0.5635
—23.15	2	0	0.5	3.6300	1.1972	1.8988	3.5193	0.3302
—25.24	1	2	1.5	4.7148	2.5914	2.9971	4.3600	0.5136
—26.65	1	2	2.5	4.9123	2.6285	3.0608	4.5045	0.5039
—35.36	1	0	0.5	3.8340	1.1818	1.6638	3.5222	0.3784

TABLE A.30. A = 181, Z = 73, RO = 1.24, VO = 59.8, $\varkappa$ = 0.33, α = 1.67.
Basis Wave Function

$+E$	$N+l$	L	J	A	$B1$	C	B	Nn
+17.83	1	7	6.5	5.7396	4.5633	4.6982	4.0062	0.5769
+14.16	2	5	5.5	5.7721	3.5894	4.2529	3.4779	0.3446
+7.32	1	7	7.5	6.1649	4.8061	5.0628	4.8849	0.6008
+3.41	3	1	0.5	4.2863	1.8629	2.7631	3.4945	0.1729
+2.27	2	3	2.5	4.9281	2.7971	3.4747	3.9579	0.3729
+2.08	3	1	1.5	4.3529	1.8611	2.7719	3.5961	0.1727
−1.13	2	3	3.5	5.1204	2.8070	3.5278	4.2103	0.3701
−1.89	1	5	4.5	5.3974	3.9303	4.2195	4.5676	0.5894
−7.87	1	5	5.5	5.7611	4.0433	4.4152	4.9770	0.5827
−15.06	2	1	0.5	4.1841	1.8363	2.5382	3.8769	0.3542
−16.13	2	1	1.5	4.2751	1.8361	2.5473	3.9444	0.3494
−18.43	1	3	2.5	4.9845	3.1059	3.4773	4.5349	0.5501
−21.03	1	3	3.5	5.2453	3.1581	3.5713	4.7514	0.5385
−30.89	1	1	0.5	4.3520	1.9840	2.4154	4.0407	0.4621
−31.49	1	1	1.5	4.4814	2.0026	2.4517	4.1292	0.4555

TABLE A.31. A = 181P

β_{20}	.240	.240	.240	.240	.240	.240
β_{40}	−.030	−.030	−.030	−.030	−.030	−.030
		Ω = 1/2			Ω = 3/2	
Energy	−10.563	−7.544	−3.169	−2.754	−8.851	−3.285
$Nn_z\Lambda$	420	411	400	660	411	402
a	2.199	−.851	1.158	5.969	0	0
1 10 21/2	.002	.001	−.001	−.001	.002	0
1 8 15/2	.003	−.009	−.012	−.003	.007	−.008
1 8 17/2	−.006	−.009	.065	.163	−.011	−.036
2 4 7/2	−.009	.075	.102	−.039	−.042	.136
3 2 5/2	.061	−.003	.057	.061	.018	−.031
1 6 11/2	.053	−.113	−.081	.010	.087	−.090
2 4 9/2	.071	.067	.030	.399	.102	.022
1 6 13/2	−.109	−.090	.341	.812	−.124	−.189
3 0 1/2	.507	−.299	.751	−.256	0	0
2 2 3/2	−.201	.736	.412	−.126	−.222	.882
2 2 5/2	.747	.428	−.291	.121	.871	.277
1 4 7/2	.187	−.359	−.171	.052	.287	−.255
1 4 9/2	−.273	−.160	.027	−.219	−.271	−.057
2 0 1/2	−.091	.023	.073	−.029	0	0
1 2 3/2	.015	−.005	.044	−.014	−.000	.096
1 2 5/2	−.046	.022	−.047	.035	.005	.049
1 0 1/2	−.023	.007	.023	−.010	0	0
	Ω = 3/2		Ω = 5/2		Ω = 7/2	
Energy	−2.641	−10.221	−5.555	−2.315	−6.954	−1.671
$Nn_z\Lambda$	651	413	402	642	404	633
1 10 21/2	.001	−.001	.001	.003	.000	.007
1 8 15/2	−.022	.007	.010	−.035	.009	−.050
1 8 17/2	.176	.005	−.018	.186	.006	.195
2 4 7/2	.007	.008	−.076	−.023	−.103	−.013
3 2 5/2	.057	.013	−.059	.031	0	0
1 6 11/2	−.058	.169	.072	−.072	.139	−.101
2 4 9/2	.378	−.026	.117	.339	−.030	.277
1 6 13/2	.867	.069	−.128	.896	.055	.919
2 2 3/2	.131	0	0	0	0	0
2 2 5/2	.067	−.168	.933	.049	0	0
1 4 7/2	−.035	.945	.204	.007	.971	−.004
1 4 9/2	−.207	.211	−.180	−.193	.153	−.168
1 2 3/2	.017		0	0	0	0
1 2 5/2	.025	.028	.106	.018	0	0

	Ω = 9/2	
Energy	−11.750	−.496
$Nn_z\Lambda$	404	624
1 10 21/2	−.001	.010
1 8 15/2	−.007	−.061
1 8 17/2	.009	.199
1 6 11/2	−.063	−.115
2 4 9/2	−.116	.198
1 6 13/2	.147	.942
1 4 9/2	.980	−.127

TABLE A.32. A = 181P

β_{20}	.240	.240	.240	.240	.240	.240
β_{40}	—.030	—.030	—.030	—.030	—.030	—.030
	Ω = 1/2				Ω = 3/2	
Energy	—9.822	—4.644	—3.565	—.546	—9.703	—4.225
$Nn_z\Lambda$	550	541	530	521	541	532
a	—5.701	4.279	—3.006	.969	0	0
1 9 19/2	—.006	.001	—.009	—.010	—.004	.004
1 7 13/2	—.008	.158	.049	—.108	—.024	.159
2 5 11/2	.106	—.004	.053	.051	.094	—.009
1 7 15/2	.170	.022	—.122	—.088	.174	.052
3 1 1/2	—.004	.127	—.151	.607	0	0
2 3 5/2	—.000	.468	—.020	.512	—.017	.421
3 1 3/2	.033	—.104	.579	—.224	.022	—.120
2 3 7/2	.374	—.089	.684	.378	.356	—.178
1 5 9/2	—.019	.826	.199	—.344	—.058	.837
1 5 11/2	.887	.058	—.291	—.143	.893	.136
2 1 1/2	.012	—.029	.038	—.121	0	0
2 1 3/2	.039	.020	—.155	.021	.033	.035
1 3 5/2	—.006	—.182	—.019	—.005	.004	—.164
1 3 7/2	—.173	.012	—.043	.012	—.173	.026
1 1 1/2	.003	.001	.006	—.030	0	0
1 1 3/2	.013	.005	—.034	.003	.012	.005
	Ω = 3/2		Ω = 5/2		Ω = 7/2	
Energy	—2.419	—9.318	—2.983	—.181	—8.417	—.539
$Nn_z\Lambda$	521	532	523	512	523	514
1 9 19/2	—.012	—.000	.006	—.017	.005	.010
1 7 13/2	.086	—.043	.169	.095	—.060	.174
2 5 11/2	.076	.070	—.016	.105	.029	—.024
1 7 15/2	—.132	.181	.070	—.141	.188	.079
2 3 5/2	—.085	—.019	.300	—.135	0	0
3 1 3/2	.404	0	0	0	0	0
2 3 7/2	.783	.306	—.201	.895	.219	—.185
1 5 9/2	.306	—.106	.889	.287	—.137	.947
1 5 11/2	—.283	.911	.178	—.238	.938	.180
2 1 3/2	—.100	0	0	0	0	0
1 3 5/2	—.022	.002	—.115	—.014	0	0
1 3 7/2	—.016	—.158	.028	.040	—.122	.020
1 1 3/2	—.027	0	0	0	0	0
	Ω = 9/2	Ω = 11/2				
Energy	—6.698	—3.809				
$Nn_z\Lambda$	514	505				
1 9 19/2	.009	.011				
1 7 13/2	—.069	—.059				
2 5 11/2	—.031	—.110				
1 7 15/2	.185	.153				
1 5 9/2	—.132	0				
1 5 11/2	.971	.980				

APPENDIX

We begin with the tables of the basis neutron wave functions $\varphi^{\Omega}_{n\,lj}$ satisfying Eq. (2.20). The expression for φ^{Ω}_{nlj} includes the spherical spinor

$$Y^{\Omega}_{lj}=\sum_{\mu}(l1/2\Omega-\mu\mu\,|\,j\Omega)\,Y_{l\Omega-\mu}\chi_{1/2\mu}. \qquad \text{(A.1)}$$

In Eq. (A.1) we have used the definition of the Clebsch–Gordan coefficients given in ref. 39. The radial part of φ^{Ω}_{nlj} is approximated highly accurately by

$$R_{nlj}(r)=(N_n/r)\,(A/C)^{1/2}\,H_n\,[S(r)]\exp[-S^2(r)/2], \qquad \text{(A.2)}$$

where n gives the number of nodes of $R_{nlj}(r)$. For example, we have n = 0 for the 1s, 1p, 1d, 1f, 1g, ... states.

Quantum number l is the eigenvalue of the angular-momentum operator; we have j = $l \pm 1/2$, and N_n is a normalization constant. The phase of $R_{nlj}(r)$ is chosen so that we have $R_{nlj}(r) \to (-1)^n r^l$ as $r \to 0$. The r dependence of the correction function S(r) which satisfies the equation

$$\int_{-\sqrt{E}}^{S}(E-\sigma^2)^{1/2}\,d\sigma=\int_{r_1}^{r}p(\xi)\,d\xi, \qquad \text{(A.3)}$$

is given approximately by

$$S(r)=\begin{cases}B\ln(r/A), & r\geqslant A;\\ B1\ln(r/A)1 & r\leqslant A.\end{cases} \qquad \text{(A.4)}$$

The parameters B, B1, and A are calculated by requiring that the exact and approximate functions S(r), given by Eqs. (A.3) and (A.4), respectively, be equal.

The parameters B, B1, C, A (in fermis) and the normalization constant N_n are given in Tables A.1, A.2, A.9, A.10, A.17, A.18, A.25, and A.26 (neutron scheme), and A.5, A.6, A.13, A.14, A.22, A.29, and A.30 (proton scheme). Where necessary, numerical solutions of the Schrödinger equation with the spherical Woods–Saxon potential can be used as the radial part of wave function φ^{Ω}_{nlj}. In this case the mixing coefficients a^{Ω}_{nlj} are essentially unaffected, so use can still be made of the a^{Ω}_{nlj} values given in Tables A.3, A.4, A.7, A.8, A.11, A.12, A.15, A.16, A.19, A.20, A.24, A.28, A.31, and A.32. In most problems, however, the necessary accuracy can be achieved with our functions.

Each of Tables A.3, A.4, A.7, A.11, A.12, A.15, A.16, A.19, A.20, A.23, A.24, A.27, A.28, A.31, and A.32 is headed by the mass number A defining the subrange and

a "P" or "N" to show whether the proton or neutron scheme is shown. Next come the β_{20}, β_{40}, and Ω values; the Ω values are followed by the energies E (in MeV). Tables of the mixing coefficients for states of identical parity are arranged in order of increasing projection of Ω and energy. For each state we show the set of mixing coefficients corresponding to the basis functions shown in the first three columns of the table. For example, the symbols "1 8 17/2" in Table A.3 show that (n + 1) is 1, l is 8, and j is 17/2, i.e., this is the $1K_{17/2}$ basis state. Furthermore, each state is characterized by asymptotic quantum numbers $Nn_z\Lambda$. Where a level pseudocrossing occurs, it is taken into account in the identification of states. For the states with $\Omega = 1/2$ we show the single-particle values of the decoupling parameter a.

[1]V. G. Solov'ev, Theory of Compound Nuclei [in Russian], Nauka, Moscow (1971).
[2]S. G. Nilsson, Mat. Fys. Medd. Dan. Vid. Selsk., 29, No. 16 (1965).
[3]C. Gustafson et al., Ark. Fys., 36, 613 (1967).
[4]P. É. Nemirovskii and V. A. Chepurnov, Yad. Fiz., 3, 998 (1966) [Sov. J. Nucl. Phys., 3, 730 (1966)].
[5]F. A. Gareev, S. P. Ivanova, and B. N. Kalinkin, Izv. Akad. Nauk SSSR, Ser. Fiz., 33, 1690 (1968) [Bull. Acad. Sci. USSR, Phys. Ser., 33 (1968)].
[6]V. G. Solov'ev (Soloviev), Atomic Energy Rev., 3, No. 2, 117 (1965).
[7]A. A. Korneichuk et al., Yad. Fiz., 9, 750 (1969) [Sov. J. Nucl. Phys., 9, 436 (1969)]; L. A. Malov, V. G. Solov'ev, and U. M. Fainer, Dokl. Akad. Nauk SSSR, 186, 299 (1969) [Sov. Phys. – Dokl., 14, 461 (1969)]; L. A. Malov, V. G. Solov'ev, and S. I. Fedotov, Dokl. Akad. Nauk SSSR, 189, 987 (1969) [Sov. Phys. – Dokl., 14, 1186 (1970)].
[8]A. L. Komov, L. A. Malov, and V. G. Solov'ev, Izv. Akad. Nauk SSSR, Ser. Fiz., 35, 1550 (1971) [Bull. Acad. Sci. USSR, Phys. Ser., 35 (1971)].
[9]V. G. Solov'ev (Soloviev) and P. Vogel, Nucl. Phys., A92, 449 (1967); V. G. Solov'ev, P. Vogel, and H. Jungclaussen, Izv. Akad. Nauk SSSR, Ser. Fiz., 31, 518 (1967) [Bull. Acad. Sci. USSR, Phys. Ser., 31 (1967)].
[10]A. Faessler and R. Sheline, Phys. Rev., 148, 1003 (1966); P. Ropper, Z. Phys., 195, 316 (1966); E. Rost, Phys. Rev., 154, 994 (1967); G. P. Ford, D. C. Hoffman, and E. Rost, Preprint LA-4329, UC-34, Phys., TID 4500 (1970); V. V. Pashkevich and V. M. Strutinskii, Yad. Fiz., 9, 56 (1969) [Sov. J. Nucl. Phys., 9, 35 (1969)]; B. L. Anderson, Nucl. Phys., A112, 443 (1968); J. H. Vogeler, Nucl. Phys., A133, 289 (1969); B. L. Anderson, B. B. Back, and J. M. Bang, Nucl. Phys., A147, 33 (1970); G. Ehrling and S. Wahlborn, Phys. Lett., B34, 369 (1971); J. P. Boisson and R. Riepenbring, Nucl. Phys., A168, 385 (1971); E. O. Fiset, J. R. Nix, and M. Bolsterli, Report LA-4735-MS, US-34 (1971).
[11]B. N. Kalinkin, Ya. Grabovskii, and F. A. Gareev, Acta Phys. Pol., 30, 999 (1966); F. A. Gareev, S. P. Ivanova, and B. N. Kalinkin, Acta Phys. Pol., 32, 461 (1967).
[12]F. A. Gareev, S. P. Ivanova, and B. N. Kalinkin, Acta Phys. Pol., 33, 135 (1968).
[13]F. A. Gareev and S. P. Ivanova, JINR Report R4-5221, 1970.
[14]F. A. Gareev et al., JINR Preprint R4-3607, 1967; F. A. Gareev, S. P. Ivanova, and N. Yu. Shirikova, JINR Report R4-5457, 1970.
[15]F. A. Gareev, S. P. Ivanova, and M. I. Chernei, Yad. Fiz., 9, 308 (1969) [Sov. J. Nucl. Phys., 9, 182 (1969)]; J. H. Wiebicke and H. Schulz, JINR Preprint No. 4-4210, Dubna, 1969.
[16]F. A. Gareev et al., Yad. Fiz., 8, 305 (1968) [Sov. J. Nucl. Phys., 8, 176 (1969)]; Phys. Lett., B27, 117 (1968).
[17]F. A. Gareev, S. P. Ivanova, and V. V. Pashkevich, Yad. Fiz., 11, 1200 (1970) [Sov. J. Nucl. Phys., 11, 667 (1970)]; D. L. Hendrie et al., Phys. Lett., B26, 127 (1968); I. L. Lamm, Nucl. Phys., A125, 504 (1969); B. Nilsson, Nucl. Phys., A129, 445 (1969); S. G. Nilsson, Preprint UCRL-18355, Berkeley, California, 1968.
[18]D. A. Arsen'ev et al., Izv. Akad. Nauk SSSR, Ser. Fiz., 32, 866 (1968); P. Vogel, Phys. Lett., B25, 65 (1967).
[19]F. A. Gareev et al., Nucl. Phys., A171, 194 (1971).
[20]N. I. Pyatov and M. I. Chernei, JINR Preprint R4-4366, Dubna, 1970; M. K. Chernei, M. I. Baznat, and N. I. Pyatov, Izv. Akad. Nauk SSSR, Ser. Fiz., 36, 789 (1972); G. Winter et al., Nucl. Phys., A176, 609 (1971).
[21]V. G. Solov'ev (Soloviev), Phys. Lett., 16, 308 (1965).
[22]L. A. Malov, V. G. Solov'ev, and U. M. Fainer, Izv. Akad. Nauk SSSR, Ser. Fiz., 33, 1244 (1969); V. G. Solov'ev and U. M. Fainer, Izv. Akad. Nauk SSSR, Ser. Fiz., 36, 698 (1972).
[23]L. A. Malov, V. G. Solov'ev, and S. I. Fedotov, Izv. Akad. Nauk SSSR, Ser. Fiz., 35, 747 (1971); V. G. Solov'ev and S. I. Fedotov, Izv. Akad. Nauk SSSR, Ser. Fiz., 36, 706 (1972).
[24]V. G. Solov'ev (Soloviev), Phys. Lett., 21, 311 (1965).
[25]D. A. Arsen'ev et al., JINR Preprint R4-6345, Dubna, 1972.
[26]V. M. Strutinskii (Strutinsky), Nucl. Phys., A95, 420 (1967); 122, 1 (1968).
[27]M. E. Bunker and C. W. Reich, Rev. Mod. Phys., 43, 348 (1971).
[28]C. M. Reich and M. E. Bunker, IAEA Panel on the Future of Nuclear Structure Studies, Dubna, 1968, IAEA, Vienna (1969), p. 119; R. K. Sheline, IAEA Panel on the Future of Nuclear Structure Studies, Dubna, 1968, IAEA, Vienna (1969), p. 71.
[29]O. Tjøm and B. Elbek, Mat. Fys. Medd. Dan. Vid. Selsk., 36, No. 8 (1967); T. Grotdal, K. Nybø, and B. Elbek, Mat. Fys. Medd. Dan. Vid. Selsk., 37, No. 12 (1970).
[30]F. A. Gareev, S. P. Ivanova, and N. Yu. Shirikova, JINR Preprint R4-4259, 1969.
[31]B. L. Andersen, B. B. Back, and J. M. Bang, Nucl. Phys., A147, 33 (1970); B. L. Andersen, Nucl. Phys., A112, 443 (1968); 162, 208 (1971).
[32]I. Kaneström, P. O. Tjøm, and J. Bang, Nucl. Phys., A164, 664 (1971).
[33]S. Kisuno and M. Sakagami, Preprint, Osaka University, Japan, 1970.
[34]V. G. Solov'ev (Soloviev), IAEA Panel on the Future of Nuclear Studies, Dubna, 1968, IAEA, Vienna (1969), p. 101.
[35]F. A. Gareev, V. G. Solov'ev, and S. I. Fedotov, Yad. Fiz., 14, 1165 (1971) [Sov. J. Nucl. Phys., 14, 649 (1972)].
[36]W. Oglo, S. Wahlborn, R. Piepenbring, and S. Fredriksson, Rev. Mod. Phys., 43, 424 (1971).
[37]M. S. Bennett, R. K. Sheline, and Y. Shida, Nucl. Phys., A171, 113 (1971); L. Funke et al., JINR, D6-4783, 143, Dubna, 1971; Ts. Vylov et al., JINR, D6-5783, 137, Dubna, 1971; G. Winter et al., Nucl. Phys., A176, 609 (1971); G. Mauron, J. Kern, and O. Huber, Nucl. Phys., A181, 489 (1972); I. L. Wood and D. S. Bernner, Nucl. Phys., A185, 58 (1972).
[38]K. Ya. Gromov et al., Fiz. El. Chast. Atom. Yad., 1, 524 (1971) [Sov. J. Particles Nucl., 1, 159 (1972)].
[39]E. U. Condon and G. H. Shortley, Theory of Atomic Spectra, Cambridge Univ. Press, London (1949).